Research Project Number TPF-5(193) Supplement #74
NDOT Sponsoring Agency Code RHE-03

ALTERNATIVE DESIGN OF LOW-TENSION CABLE BARRIER ADJACENT TO STEEP SLOPES

Submitted by

Robert W. Bielenberg, M.S.M.E.
Research Associate Engineer

Cody Stolle, Ph.D.
Research Assistant Professor

Dylan T. Meyer
Former Undergraduate Research Assistant

Elisa Vasquez, B.S.M.E.
Graduate Research Assistant

Ronald K. Faller, Ph.D., P.E.
Research Associate Professor
MwRSF Director

John D. Reid, Ph.D.
Professor

MIDWEST ROADSIDE SAFETY FACILITY
Nebraska Transportation Center
University of Nebraska-Lincoln

Main Office
Prem S. Paul Research Center at Whittier School
Room 130, 2200 Vine Street
Lincoln, Nebraska 68583-0853
(402) 472-0965

Outdoor Test Site
4630 N.W. 36th Street
Lincoln, Nebraska 68524

Submitted to

NEBRASKA DEPARTMENT OF TRANSPORTATION
1500 Nebraska Highway 2
Lincoln, Nebraska 68502

MwRSF Research Report No. TRP-03-334-21

April 27, 2021

TECHNICAL REPORT DOCUMENTATION PAGE

1. Report No. TRP-03-334-21	**2. Government Accession No.**	**3. Recipient's Catalog No.**
4. Title and Subtitle Alternative Design of Low-Tension Cable Barrier Adjacent to Steep Slopes		**5. Report Date** April 27, 2021
		6. Performing Organization Code
7. Author(s) Bielenberg, R.W., Stolle, C.S., Meyer, D.T., Vasquez, E., Faller, R.K., and Reid, J.D.		**8. Performing Organization Report No.** TRP-03-334-21
9. Performing Organization Name and Address Midwest Roadside Safety Facility (MwRSF) Nebraska Transportation Center University of Nebraska-Lincoln Main Office: Prem S. Paul Research Center at Whittier School Room 130, 2200 Vine Street Lincoln, Nebraska 68583-0853	Outdoor Test Site: 4630 N.W. 36th Street Lincoln, Nebraska 68524	**10. Work Unit No.**
		11. Contract
12. Sponsoring Agency Name and Address Nebraska Department of Transportation 1500 Nebraska Highway 2 Lincoln, Nebraska 68502		**13. Type of Report and Period Covered** Final Report: 2014 – 2021
		14. Sponsoring Agency Code TPF-5(193) Supplement #74

15. Supplementary Notes

Prepared in cooperation with U.S. Department of Transportation, Federal Highway Administration

16. Abstract

In the early 2000s, MwRSF conducted full-scale crash testing on low-tension cable barrier systems installed adjacent to 1.5H:1V slopes. A design was successfully tested according to NCHRP Report 350 criteria, but the tested and approved configuration utilized a 4-ft (1.2 m) post spacing and a 4-ft (1.2 m) offset from the slope break point (SBP). Therefore, NDOT funded this research study to investigate if revisions to the low-tension cable barrier system could be identified which were likely to satisfy MASH requirements and which would be more cost-effective.

This research study was conducted to investigate alternative low-tension cable barrier designs and configurations which would be likely to satisfy MASH TL-3 impact conditions and which would improve cost-effectiveness and/or usability for NDOT. Test nos. LTCB-1 through LTCB-5 were conducted on S3x5.7 steel posts at varying offset distances from a 1.8H:1V slope. Test no. LTCB-6 was conducted to evaluate the propensity for S3x5.7 posts to penetrate a small car test vehicle's floor pan, and tearing was observed. Subsequent component tests of an HSS3x2x⅛ tubular post alternative in development for use with high-tension cable median barrier systems was found to provide acceptable performance while mitigating floor pan tearing.

Computer simulations were performed to investigate alternative barrier configurations. Various combinations of post spacing, barrier offset, and cable heights were evaluated. It was determined that systems with 3-ft (0.9-m) offset from the slope with 4-ft (1.2-m) post spacing, or 4-ft (1.2-m) offset from the slope with 6-ft (1.8-m) post spacing, may perform acceptably according to MASH TL-3 test designation no. 3-11.

17. Key Words Highway Safety, Crash Test, Roadside Appurtenances, Compliance Test, Cable, Cable Guardrail, Slopes, LS-DYNA	**18. Distribution Statement** No restrictions. This document is available through the National Technical Information Service. 5285 Port Royal Road Springfield, VA 22161

19. Security Classification (of this report) Unclassified	**20. Security Classification (of this page)** Unclassified	**21. No. of Pages** 124	**22. Price**

Form DOT F 1700.7 (8-72) Reproduction of completed page authorized

DISCLAIMER STATEMENT

This material is based upon work supported by the Federal Highway Administration, U.S. Department of Transportation and the Nebraska Department of Transportation under TPF-5(193) Supplement #74. The contents of this report reflect the views and opinions of the authors who are responsible for the facts and the accuracy of the data presented herein. The contents do not necessarily reflect the official views or policies of the University of Nebraska-Lincoln, Nebraska Department of Transportation, nor the Federal Highway Administration, U.S. Department of Transportation. This report does not constitute a standard, specification, or regulation. Trade or manufacturers' names, which may appear in this report, are cited only because they are considered essential to the objectives of the report. The United States government and the State of Nebraska do not endorse products or manufacturers.

UNCERTAINTY OF MEASUREMENT STATEMENT

The Midwest Roadside Safety Facility (MwRSF) has determined the uncertainty of measurements for several parameters involved in standard full-scale crash testing and non-standard testing of roadside safety features. Information regarding the uncertainty of measurements for critical parameters is available upon request by the sponsor and the Federal Highway Administration. The tests contained within were non-certified component tests conducted for research and development purposes only and are outside the scope of MwRSF's A2LA Accreditation.

ACKNOWLEDGEMENTS

The authors wish to acknowledge several sources that contributed to this project: (1) the Nebraska Department of Transportation, and (2) MwRSF personnel for conducting the bogie and component tests.

Acknowledgement is also given to the following individuals who contributed to the completion of this research project.

Midwest Roadside Safety Facility
K.A. Lechtenberg, M.S.M.E., Research Engineer
S.K. Rosenbaugh, M.S.C.E., Research Engineer
J.D. Rasmussen, Ph.D., P.E., Former Research Associate Professor
J.S. Steelman, Ph.D., P.E., Associate Professor
M. Pajouh, Ph.D., P.E., Research Assistant Professor
A.T. Russell, B.S.B.A., Testing and Maintenance Technician II
E.W. Krier, B.S., Construction and Testing Technician II
S.M. Tighe, Construction and Testing Technician I
D.S. Charroin, Construction and Testing Technician I
R.M. Novak, Construction and Testing Technician I
T.C. Donahoo, Construction and Testing Technician I
J.T. Jones, Construction and Testing Technician I
J.E. Kohtz, B.S.M.E., Former CAD Technician
E.L. Urbank, B.A., Research Communication Specialist
Z.Z. Jabr, Engineering Technician
J.R. Revell, Research Communication Specialist Assistant
Undergraduate and Graduate Research Assistants

Nebraska Department of Roads
Phil TenHulzen, P.E., Design Standards Engineer
Jim Knott, P.E., State Roadway Design Engineer
Jodi Gibson, Former Research Coordinator

Federal Highway Administration
John Perry, P.E., Nebraska Division Office
Danny Briggs, Nebraska Division Office

TABLE OF CONTENTS

LIST OF FIGURES

LIST OF TABLES

1 INTRODUCTION

1.1 Background

Three-cable guardrail systems are commonly used to protect motorists from roadside slopes. However, concerns arise when the barrier must be placed in close proximity to a steep slope. Previously, the Midwest States Pooled Fund Program funded a research project to investigate the performance of a low-tension cable barrier adjacent to slopes as steep as 1.5H:1V. Researchers at the Midwest Roadside Safety Facility (MwRSF) conducted test no. CS-1 with a three-quarter ton pickup truck on a standard, three-cable guardrail offset 12 in. (305 mm) from the slope break point (SBP) of a 1.5H:1V slope [1]. The system consisted of 63-in. (1,600-mm) long, S3x5.7 posts spaced 16 ft (4.9 m) on center. During the 2000P crash test conducted according to The National Cooperative Highway Research Program (NCHRP) Report 350 Test Level 3 (TL-3) safety performance criteria [2], the posts rotated without much soil resistance, resulting in the vehicle becoming completely airborne and encroaching onto the steep slope. This caused the vehicle to roll over the cables and come to rest at the bottom of the embankment. The standard, three-cable guardrail system offset 12 in. (305 mm) from the slope break point of a 1.5H:1V slope performed unsatisfactorily according to the NCHRP Report 350 TL-3 safety performance criteria.

A second full-scale crash test, test no. CS-2, was conducted using a reduced post spacing of 4 ft. (1.2 m) and an increased barrier offset from the slope breakpoint of 4 ft (1.2 m) [3]. Implementation of these changes resulted in the safe redirection of a 2000P vehicle according to TL-3 of NCHRP Report 350, but was not without drawbacks. The closely spaced posts used in the modified system can be difficult to install, and the cost of the system made it non-cost effective as compared to available W-beam guardrail systems adjacent to steep slopes. Thus, a need existed to reconsider the design of low-tension cable barrier adjacent to steep slopes to alleviate these issues. Additionally, the design needed to consider the updated roadside hardware evaluation criteria for cable barriers for TL-3 of the *Manual for Assessing Safety Hardware, Second Edition* (MASH) [4-5].

1.2 Objective

The objective of this study was to review the design of the low-tension cable barrier adjacent to steep slopes and determine improved design configurations that could increase post spacing and reduce the offset of the barrier from the slope while meeting MASH TL-3. If design modifications for improving the cable barrier adjacent to slopes were developed in this research, full-scale crash testing according to the TL-3 evaluation criteria published in MASH would be used to evaluate the system in a subsequent effort.

1.3 Scope

The research effort was split into two phases. The Phase I effort detailed herein consisted of the review of design modifications, design and analysis of improvements to the low-tension, three-cable barrier system adjacent to steep slopes, dynamic component testing of posts adjacent to slopes, and completion of design details for later use in a full-scale crash testing program.

2 LITERATURE REVIEW

2.1 Evaluation Criteria

Testing and evaluation criteria for cable barriers are set forth in MASH [4]. For cable barrier systems meeting TL-3, full-scale crash tests are required involving both an 1100C small passenger car and a 2270P pickup truck. Additionally, this most recent update to the MASH criteria specified standardized test conditions for cable barriers included a 1500A sedan test for barriers.

2.2 Relevant Low-Tension Cable Barrier Research

In 2001, MwRSF conducted a full-scale crash test of a standard three-cable guardrail system installed at the slope break point of a 1.5H:1V slope [1] under NCHRP Report 350 TL-3 criteria. The system consisted of four major components: (1) wire rope; (2) posts; (3) spring compensating cable end assemblies; and (4) end anchorage assemblies. Three ¾-in. (19-mm) diameter 3x7 wire ropes were supported by S3x5.7 posts, spaced 16 ft (4.9 m) apart on center with an embedment depth of 30 in. (762 mm) and a welded soil plate. The cable barrier was offset 1 ft (305 mm) from the slope break point of a 20-ft (6.1-m) wide 1.5H:1V slope. During test CS-1, the 4,484-lb (2,034-kg) 2000P pickup truck impacted the three-cable guardrail system at a speed of 61 mph (98.1 km/h) and at an angle of 26.2 degrees. During impact, the S3x5.7 posts rotated through the SBP, protruding through the slope, and the top cable slid beneath the rear tires causing rollover. Therefore, test no. CS-1 was determined to be unacceptable according to the TL-3 safety performance criteria in NCHRP Report 350.

The barrier system was redesigned after test no. CS-1 [3]. The post spacing was reduced to 4 ft (1,291 mm) on center and the posts were shifted forward to an offset of 4 ft (1,291 mm) from the slope break point of the 1.5H:1V slope. A second full-scale crash test, test no. CS-2, consisted of a 4,487 lb (2,035 kg) 2000P pickup truck impacting the barrier system at a velocity and angle of 61.1 mph (100 km/h) and 23.6 degrees, respectively. The barrier captured and redirected the test vehicle, and results were determined to be satisfactory according to the TL-3 safety performance criteria in NCHRP Report 350. Although the modified system performed acceptably, the redesigned barrier increased the complexity and cost of installation and was no longer cost-competitive with other systems such as W-beam guardrail installed adjacent to steep slopes.

Low-tension cable barrier systems have also been shown to satisfy the safety performance requirements of MASH test no. 3-11. The New York State DOT generic, low-tension, three-cable barrier system was tested to evaluate the safety performance of the barrier system installed on a curve. The barrier was subjected to three full-scale crash tests and evaluated according to TL-3 impact safety standards from MASH using a modified test designation no. 3-11. The impact angle was 20 degrees instead of 25 degrees and the impact point was targeted as 70 ft (21.3 m) downstream from the anchor. The top cable height was 27 in. (686 mm) with a 6-in. (15.2 mm) cable spacing, and the curve radius was 360 ft (110 m) [6].

For test no. NYCC-1, the 2270P vehicle impacted the system at an angle of 19.9 degrees relative to the tangent of the curve and at a speed of 61.6 mph (99.1 km/h) [6]. The vehicle was satisfactorily contained and redirected. No excessive deformations or penetrations to the occupant compartment occurred, and the recorded vehicle accelerations did not violate the OIV or ORA limits established in MASH. Therefore, test no. NYCC-1 was deemed a successful test according to the modified MASH test designation no. 3-11 safety evaluation criteria.

The radius of the barrier system for test no. NYCC-2 was increased to 440 ft (134 m), but all other components and dimensions remained the same. In test no. NYCC-2, the 2270P vehicle impacted the system at an angle of 22.1 degrees relative to the tangent of the curve and at a speed of 61.7 mph (99.3 km/h) [6]. The vehicle overrode the barrier system as the top cable did not release quick enough to capture the bumper of the vehicle. The vehicle was penetrated behind the system for approximately 150 ft (45 m) before striking an embankment, which caused it to roll over. Test no. NYCC-2 was deemed unsuccessful according to the modified MASH test designation no. 3-11 safety evaluation criteria because the vehicle was not contained by the barrier. Following the results of test no. NYCC-2, it was thought that the cable mounting heights were too low to capture taller vehicles (e.g., 2270P vehicle). Thus, it was decided to raise the entire system 2 in. (51 mm) to achieve a top cable height of 29 in. (737 mm).

In test no. NYCC-3, the 2270P vehicle impacted the system with revised cable heights at an angle of 21.6 degrees relative to the tangent of the curve and at a speed of 63.1 mph (101.6 km/h). The vehicle was satisfactorily contained and redirected [6]. No excessive deformations or penetrations to the occupant compartment occurred, and the recorded vehicle accelerations did not violate the OIV or ORA limits established in MASH. Therefore, test no. NYCC-3 was deemed a successful test according to the modified MASH test designation no. 3-11 safety evaluation criteria, and a top mounting height of at least 29 in. was recommended.

2.3 Relevant Cable Barrier Post Research

In 2007, MwRSF used dynamic component testing to explore various cost-control methods to reduce the need for expensive post assemblies utilizing soil plates for cable barriers. A total of ten bogie tests were conducted on S3x5.7 posts, with lengths from 70 to 90 in. (1,778 to 2,286 mm) and an embedment from 36 to 54 in. (914 to 1,372 mm). A steel frame surrogate vehicle impacted the posts at a height of 27 in. (683 mm) and at approximately 13 mph (20.9 km/h) at an angle of 90 degrees to the strong axis [7]. The objectives of the research project were to (1) determine the post-soil behavior for steel posts used in cable median barrier systems; (2) determine post length and embedment depth for which the post does not need soil plate such that it bends at the groundline; and (3) investigate the strength and energy dissipation capabilities of S3x5.7 posts embedded in compacted soil. After analyzing and comparing the results, it was recommended to use an S3x5.7 post with a length of 78 in. (1,981 mm) and a 42-in. (1,067-mm) embedment depth.

MwRSF researchers also conducted a research study to develop a new post section for a nonproprietary, high-tension cable median barrier that improved the safety and performance of the barrier system [8]. The design of the nonproprietary, high-tension cable median barrier system had progressed through a series of crash tests that identified flaws in the system related to vehicle capture during testing in a V-ditch and deformations of the occupant compartment during sedan testing on level terrain. These concerns led the researchers to revisit performance of the basic design elements of the barrier system. Three design problems stood out that needed to be addressed to improve the system and meet the TL-3 test requirements for cable median barrier found in MASH. First, full-scale testing had shown that the current design of the cable median barrier had difficultly capturing vehicles when the barrier was placed down the slope. Second, full-scale testing indicated that the current cable barrier system design could cause A-pillar crush in small cars and sedans. Finally, review of the behavior of the cable-to-post attachments in the current design found that the current attachment behavior was not optimized. Review of the full-scale test results suggested that two factors contributing to the A-pillar crush were the lateral, or strong-axis, strength of the post and the release forces of the cable to post attachment.

In order to improve the A-pillar crush, a research effort was undertaken to lower the lateral, or strong-axis, strength of the support post. It was believed that a post with lower strong-axis capacity would result in lower forces imparted to the A-pillar and reduced A-pillar damage. Lowering the lateral capacity of the post would also allow for yielding and deflection of the post at lower loads, which was hoped to improve energy absorption as compared to the current post design.

The design and dynamic component testing in that study led to the development of a new steel post section formed from folded or rolled steel sheet, dubbed the Midwest Weak Post (MWP). This post had advantages over standard post sections in that it was tuned to provide desired strong and weak axis capacities while using less material than the standard S-section post it was replacing. In addition, the new post section could be rolled from sheet steel, which makes it economical to fabricate.

Full-scale testing of a nonproprietary, four-cable median barrier design using the MWP post indicated some additional problems, including unexpected buckling of the post at cable-to-post attachments and floorboard tearing of small car vehicles [9-10]. Floorboard tearing violates MASH requirements to maintain the integrity of the occupant compartment. Dynamic component testing was conducted with a bogie vehicle equipped with a simulated floorboard [11]. The testing evaluated a series of two posts spaced 8 ft (2.4 m) apart and offset by 4¼ in. (108 mm) in. using a floorboard-equipped bogie impacting at 25 mph (40 km/h). The baseline testing conducted on the MWPs resulted in tearing and creasing of the simulated floorboard. Two tests were also conducted on S3x5.7 posts, which is the standard low-tension cable guardrail post. The S3x5.7 post caused twice as many tears the MWP, and the tears seemed to be larger than those observed from the MWP. This testing confirmed that this problem was not specific for the MWP and can occur with other deformable posts with free/exposed edges.

In order to improve the performance of the nonproprietary, four-cable median barrier, MwRSF researchers undertook a research effort to develop a new closed section weak post design [12]. Several post design criteria were identified and included (1) reduction of the longitudinal (weak-axis) capacity in order to mitigate the potential for snag concerns and vehicle floor pan tearing, (2) maintain the lateral (strong-axis) capacity similar to the MWP post in order to provide sufficient strength and energy dissipation during vehicle redirection, (3) provide a geometry without free edges to mitigate vehicle floor pan tearing and allow attachment of the cable-to-post attachment brackets developed previously, and (4) utilize an alternative section that could reduce the costs of post fabrication. After a review of currently available, closed, structural steel sections, variations of closed-section posts including HSS3x2x⅛, MT 3x2x11-gauge, and MT 4x2x14-gauge were selected for further investigation. Post weakening was accomplished by adding holes of different sizes and patterns at the ground line. In order to evaluate the new post section, a total of 20 dynamic component tests were conducted on the strong and weak axes of the posts. Based on these component tests, an HSS3x2x⅛ post with two ¾-in. (19-mm) diameter holes was chosen for the post section as it met the design criteria for strong and weak axis post strength, as shown in Figure 1. Additional dynamic component testing was conducted on the HSS3x2x⅛ post with two ¾-in. (19-mm) diameter holes to evaluate potential floorboard tearing, and the new post section showed no potential for floorboard tearing. This tubular post section developed for the nonproprietary, four-cable median barrier was included herein as it was eventually used as part of this research effort.

Figure 1. Tubular Post for Nonproprietary, Four-Cable Median Barrier

3 DESIGN CRITERIA AND INITIAL DESIGN CONCEPT

At the onset of the research effort, the MwRSF researchers met with Nebraska Department of Transportation (NDOT) representatives to discuss the design criteria and initial design concepts for the revised low-tension cable barrier adjacent to steep slopes. The following design criteria were established for the revised system.

1. The system must meet MASH TL-3 safety requirements.

2. The barrier system was to be developed for use adjacent to a 1.8H:1V slope. Preliminary discussions on the barrier design and review of the previous full-scale crash testing under NCHRP Report 350 suggested that the barrier deflections might increase significantly under MASH TL-3. As such it was suggested to potentially consider slopes of 2H:1V or flatter. However, NDOT noted that they needed to consider steeper slopes than 2H:1V and compromised on the use of a 1.8H:1V slope for the development of the revised cable barrier.

3. It was desired that the revised design utilize wider post spacing and reduced lateral barrier offset from the slope to improve the overall cost of the system. The preferred offset was 2 ft (610 mm) or less.

4. It was desired that the system utilize the same basic components to the existing, low-tension cable barrier system used by NDOT. Modifications were allowed if needed to improve performance.

Development of the revised system was to begin with the basic setup and layout of the original NDOT low-tension cable barrier design shown in Figure 2. The system would then be modified to improve performance as necessary. Potential modifications that could improve performance included, increasing the cable mounting heights, modification of the post type/section, lateral post offset from the slope, post spacing, increased number of cables, and increased cable tension. The use of additional cables and increased cable tension were not as desired. Increasing the number of cables was expected to add complexity and cost to the system, and increased cable tension has shown minimal benefit in terms of reducing barrier deflection. Additionally, these modifications would require modification of NDOT’s current low-tension cable barrier anchorage and end terminal design. Thus, design modifications focused primarily on post spacing, barrier offset, and cable mounting heights.

The initial design proposed for the system consisted of a modified version of the original NDOT low-tension cable barrier, as shown in Figure 3. The original barrier design was modified to increase the cable mounting heights to 34 in. (864 mm), 28 in. (711 mm), and 22 in. (559 mm). This increased the top cable height by 4 in. (102 mm) over the original design and increased the vertical cable spacing from 3 in. (76 mm) to 6 in. (152 mm). Increased cable heights and vertical spacing have been previously applied to cable median barriers in sloped ditches to improve vehicle capture and stability. Small car capture cable heights have been shown to be effective in ranges of 20 in. to 34 in. (508 mm to 864 mm) above grade, while pickup truck capture cable heights have been shown to be effective in the 22 in. to 38 in. (559 mm to 965 mm) range. The cable height range chosen for the revised low-tension cable barrier was selected to maintain vehicle capture within those ranges while improving vehicle capture and stability as the vehicle was redirected and partially traversing the slope.

The S3x5.7 post section with the soil plate was retained for the proposed low-tension cable barrier. It was hoped that retention of the soil plate on the post would aid in development of the post at reduced offsets to a steep slope. The initial post spacing was increased to 8 ft (2,438 mm) and the lateral barrier offset to the slope was proposed to be 1 ft to 2 ft (305 mm to 610 mm) in order to reduce the cost of the system. The researchers believed that proper performance of the cable barrier would require that the combination of post offset and embedment be capable of fully developing the flexural capacity of the post section to limit barrier deflection over the slope and maintain vehicle capture during redirection. In order to evaluate the potential for the reduced lateral offset, dynamic component testing of the posts adjacent to a steep slope was proposed to evaluate potential minimum offsets for the posts adjacent to a steep slope. The data was also utilized to aid in development of LS-DYNA computer simulation models for analysis of the proposed barrier system performance. Additional details on the dynamic component testing of the posts are provided in subsequent sections.

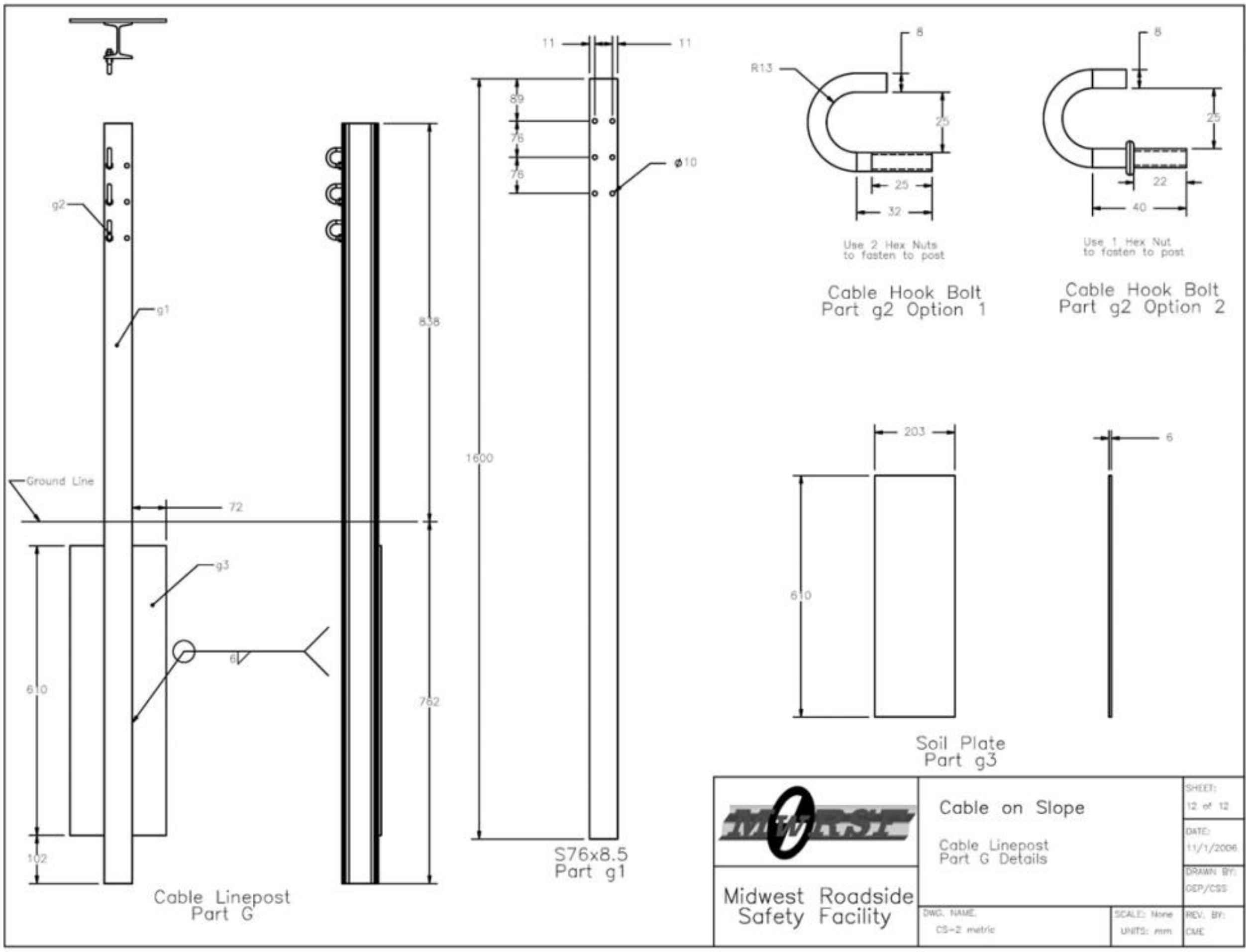

Figure 2. Original NDOT Low-Tension Cable Barrier Design Adjacent to Slope

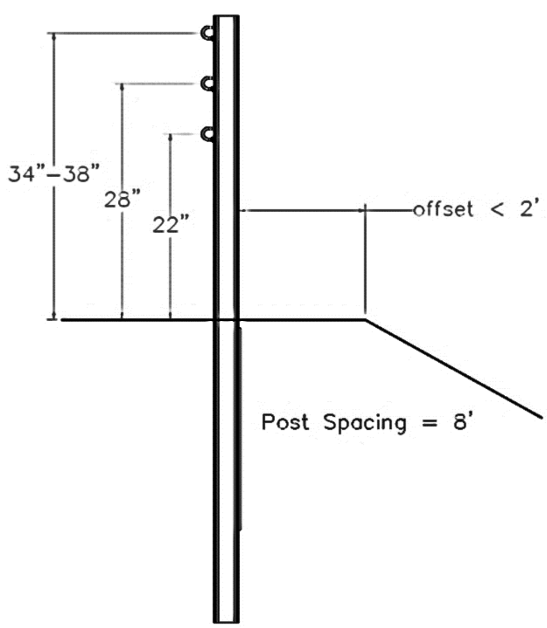

Figure 3. Initial Proposed Design for Low-Tension Cable Barrier Design Adjacent to Slope

4 COMPONENT TESTING CONDITIONS

4.1 Purpose

The first step in developing the design modifications for a low-tension cable barrier system adjacent to steep slopes was to conduct bogie testing on the system posts to determine their performance at reduced offsets to steep slopes and determine a minimum offset for adequate post performance. The tests reported herein were conducted to determine properties of posts on level terrain and near steep slopes of up to 1.8H:1V. Additionally, one test was conducted to investigate the potential for the posts to lacerate and penetrate the floorboard of small car vehicles. All dynamic tests were conducted at the MwRSF Proving Grounds in Lincoln, Nebraska.

4.2 Equipment and Instrumentation

Equipment and instrumentation utilized to collect and record data during the dynamic bogie tests included a bogie vehicle, an accelerometer, a retroreflective speed trap, high-speed and standard-speed digital video cameras, and still cameras.

4.2.1 Bogie Vehicles

Two rigid-frame bogies were used to impact the posts. Both bogies used for testing utilized a variable height, detachable impact head. The bogie head was constructed of 8-in. (203-mm) diameter, ½-in. (13-mm) thick standard steel pipe, with ¾-in. (19-mm) neoprene belting wrapped around the pipe to prevent local damage to the post from the impact. In test nos. LTCB-1 through LTCB-6 and test nos. CTPS-1 and CTPS-2, the impact head was bolted to the bogie vehicle, creating a rigid frame with an impact height of 22 in. (559 mm). The bogie used in test nos. LTCB-1 through LTCB-5, CTPS-1, and CTPS-2 with the impact head is shown in Figure 4, and the bogie with impact head used in test no. LTCB-6 is shown in Figure 5. The weight of the bogie used in test nos. LTCB-1 through LTCB-5 with the addition of the mountable impact head and accelerometers was 1,868 lb (847 kg), the weight of the bogie used in test no. LTCB-6 was 2,548 lb (1,156 kg), and the weight of the bogie used in test nos. CTPS-1 and CTPS-2 was 1,872 lb (849 kg).

Figure 4. Rigid-Frame Bogie No. 3, Test Nos. LTCB-1 through LTCB-5, CTPS-1, and CTPS-2

Figure 5. Rigid-Frame Bogie No. 4, Test No. LTCB-6

In test nos. LTCB-1 through LTCB-5, CTPS-1, and CTPS-2, a pickup truck with a reverse-cable tow system was used to propel the bogie to a target impact speed of 20 mph (32 km/h). In test no. LTCB-6, a pickup truck with a reverse-cable tow system was used to propel the bogie to a target impact speed of 25 mph (40 km/h). When the bogie approached the end of the guidance system, it was released from the tow cable, allowing it to be free rolling when it impacted the post. A radio-controlled braking system was installed on the bogie allowing it to be brought safely to rest after the test.

4.2.2 Accelerometers

One SLICE 6DX accelerometer system (SLICE-2) was mounted on the bogie vehicle near the center of gravity to measure the acceleration in the longitudinal, lateral, and vertical directions. However, only the longitudinal acceleration was processed and reported.

The SLICE 6DX (SLICE-2) was a modular data acquisition system manufactured by Diversified Technical Systems, Inc. of Seal Beach, California. The acceleration sensor was mounted inside the body of a custom-built SLICE 6DX event data recorder and recorded data at 10,000 Hz to the onboard microprocessor. The SLICE 6DX was configured with 7 GB of non-volatile flash memory, a range of ±500 g's, a sample rate of 10,000 Hz, and a 1,650 Hz (CFC 1000) anti-aliasing filter. The "SLICEWare" computer software program and a customized Microsoft Excel worksheet were used to analyze and plot the accelerometer data.

4.2.3 Retroreflective Optic Speed Trap

The retroreflective optic speed trap was used to determine the speed of the bogie vehicle before impact. Four retroreflective targets, spaced at approximately 18-in. (457-mm) intervals, were applied to the side of the vehicle for test nos. LTCB-1 through LTCB-5. For test no. LTCB-6 and test nos. CTPS-1 and CTPS-2, five retroreflective targets, spaced at approximately 18-in. (457-mm) intervals were applied to the side of the vehicle. When the emitted beam of light was reflected by the targets and returned to the Emitter/Receiver, a signal was sent to the data acquisition computer, recording at 10,000 Hz, as well as the external LED box activating the LED flashes. The speed was then calculated using the spacing between the retroreflective targets and the time between the signals. LED lights and high-speed digital video analysis are only used as a backup in the event that vehicle speeds cannot be determined from the electronic data.

4.2.4 Digital Photography

One AOS high-speed digital video camera and two GoPro digital video cameras were used to document test nos. LTCB-1 through LTCB-5, CTPS-1, and CTPS-2, and one AOS high speed digital video camera and seven GoPro digital video cameras were used to document test no. LTCB-6. The AOS high-speed camera had a frame rate of 500 frames per second and the GoPro video cameras had frame rates of 120 and 240 frames per second. In test nos. LTCB-1 through LTCB-5, CTPS-1, and CTPS-2, the cameras were placed laterally from the post, with a view perpendicular to the bogie's direction of travel as well as diagonally from the post. In test no. LTCB-6 the GoPro digital cameras were placed in the same locations as test nos. LTCB-1 through LTCB-5 with an additional three GoPro cameras onboard the bogie vehicle and two located adjacent to each post to provide detailed views of the posts while the test was being conducted. A Nikon D3100 digital still camera was also used to document pre- and post-test conditions for all tests.

4.3 End of Test Determination

When the impact head initially contacts the test article, the force exerted by the surrogate test vehicle is directly perpendicular. However, as the post rotates, the surrogate test vehicle's orientation and path moves further from perpendicular. This introduces two sources of error: (1) the contact force between the impact head and the post has a vertical component and (2) the impact head slides upward along the test article. Therefore, only the initial portion of the accelerometer trace should be used since variations in the data become significant as the system rotates and the surrogate test vehicle overrides the system. Additionally, guidelines were established to define the end of test time using the high-speed video of the impact. The first occurrence of either of the following events was used to determine the end of the test: (1) the test article fractures; or (2) the surrogate vehicle overrides or loses contact with the test article.

4.4 Data Processing

The electronic accelerometer data obtained in dynamic testing was filtered using the SAE Class 60 Butterworth filter conforming to the SAE J211/1 specifications [13]. The pertinent acceleration signal was extracted from the bulk of the data signals. The processed acceleration data was then multiplied by the mass of the bogie to get the impact force using Newton's Second Law. Next, the acceleration trace was integrated to find the change in velocity versus time. Initial velocity of the bogie, calculated from the pressure tape switch data, was then used to determine the bogie velocity. Next, the calculated velocity trace was integrated to find the bogie's displacement. This displacement is also the displacement of the post. Combining the previous results, a force vs. deflection curve was plotted for each test. Finally, integration of the force vs. deflection curve provided the energy vs. deflection curve for each test.

5 COMPONENT TESTING OF S3x5.7 POSTS

5.1 Scope

A series of dynamic component tests or bogie tests were conducted on S3x5.7 steel posts to determine the potential minimum offset for the revised, low-tension cable barrier adjacent to steep slopes. Two tests were conducted on posts installed on level terrain in order to serve as a baseline for the force vs. deflection and energy dissipation of the standard low-tension cable barrier post. Three additional tests were conducted at reduced lateral offsets to a 1.8H:1V slope. Lateral offsets of 24 in. (610 mm), 12 in. (305 mm), and 6 in. (152 mm), were evaluated and compared with the level terrain tests. It was desired that the posts installed at the reduced offsets perform similarly to the level terrain posts.

Five bogie tests were conducted on 63-in. (1,600-mm) long, S3x5.7 steel posts with an embedment depth of 30 in. (762 mm) and a 24-in. long by 8-in. wide x ¼-in. thick (610-mm. long by 203-mm wide x 6.4-mm thick) soil plate located 4 in. (102 mm) from the base of the post. This was the same post section, embedment, and soil plate used in the original low-tension cable barrier adjacent to slope design. In test nos. LTCB-1 through LTCB-5, the target impact conditions were an impact speed of 20 mph (32.2 km/h) and an angle of 90 degrees, creating a classical "head-on" impact and strong axis bending. The posts were impacted 22 in. (559 mm) above the groundline The test matrix is shown in Table 1, and the test setups are shown in Figures 6 through 8. Note that for test nos. LTCB-1 and LTCB-2, the soil plate was oriented on the back side of the post similar to a standard cable barrier installation. For test nos. LTCB-3 through LTCB-5, the soil plate location was flipped to the front face of the post to provide slightly more soil between the plate and the slope break point and increase soil resistance. Material specifications and certificates of conformity for the S3x5.7 steel posts are shown in Appendix A.

Table 1. Test Matrix for Test Nos. LTCB-1 through LTCB-5

Test No.	Offset Distance in. (mm)	Soil Plate Dimension in. (mm)	Target Impact Conditions		
			Impact Velocity mph (km/h)	Impact Height in. (mm)	Impact Angle degrees
LTCB-1	N/A	8 x 24 x ¼ (203 x 610 x 6)	20.0 (32.2)	22 (559)	90
LTCB-2	N/A	8 x 24 x ¼ (203 x 610 x 6)	20.0 (32.2)	22 (559)	90
LTCB-3	24 (610)	8 x 24 x ¼ (203 x 610 x 6)	20.0 (32.2)	22 (559)	90
LTCB-4	12 (305)	8 x 24 x ¼ (203 x 610 x 6)	20.0 (32.2)	22 (559)	90
LTCB-5	6 (152)	8 x 24 x ¼ (203 x 610 x 6)	20.0 (32.2)	22 (559)	90

Test Nos.	Soil Plate Dimensions in. x in. x in. [mm x mm x mm]	Offset Distance in. [mm]	Bogie No.	Impact Speed mph [km/h]
1–2	8x24x1/4 [203x610x6] (Part a1)	NA	3	20 [32]

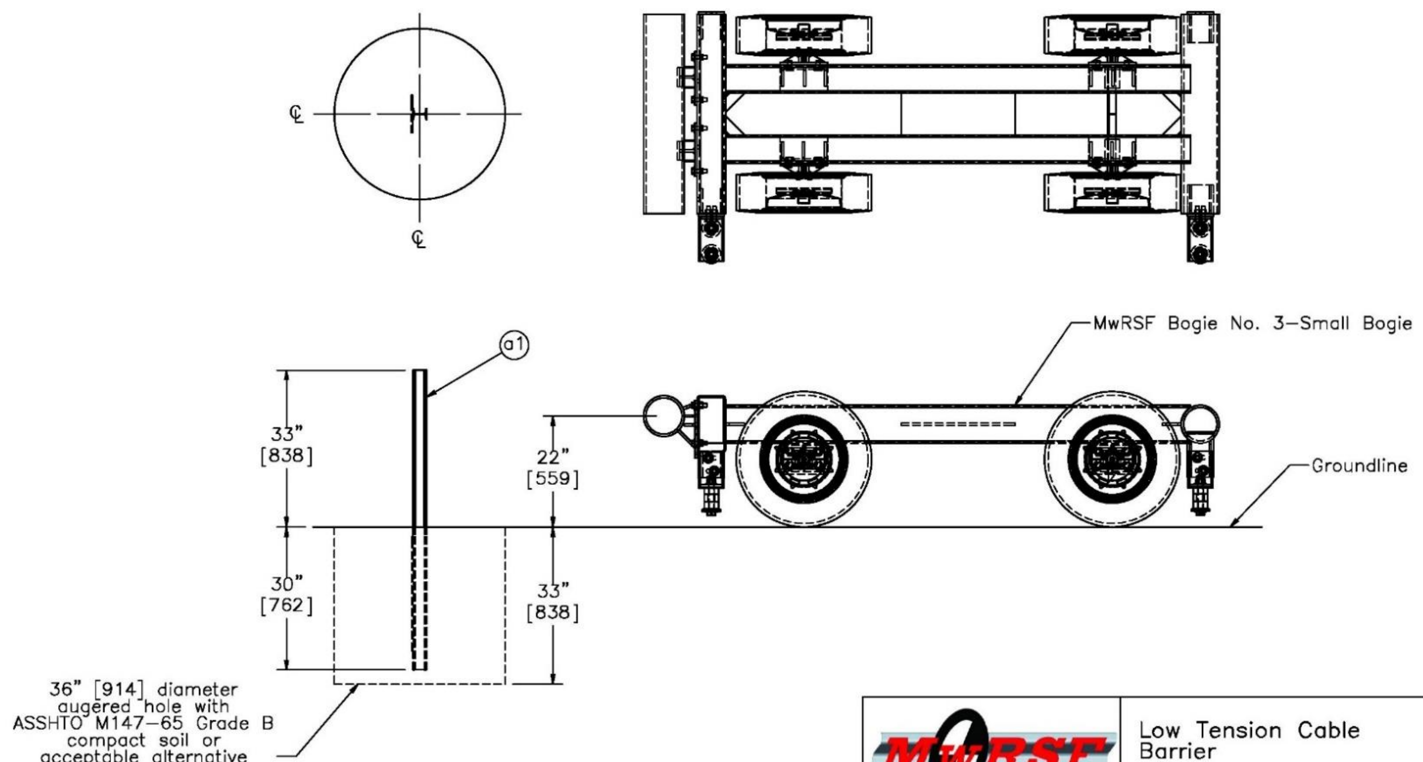

Notes: (1) Soil plate on back side of post.

Midwest Roadside Safety Facility	Low Tension Cable Barrier	SHEET: 1 of 4
		DATE: 3/31/2017
	Bogie Tests 1 & 2	DRAWN BY: ALL/TJD
	DWG. NAME. LTCB_Bogie_R12 / SCALE: 1:32 UNITS: Inches	REV. BY: SDB/SKR/KAL/RWB

Figure 6. Bogie Tests 1 and 2 Matrix and Setup, Test Nos. LTCB-1 and LTCB-2

Test Nos.	Soil Plate Dimensions in. x in. x in. [mm x mm x mm]	Offset Distance, D in. [mm]	Bogie No.	Impact Speed mph [km/h]
3	8x24x1/4 [203x610x6] (Part a1)	24 [610]	3	20 [32]
4	8x24x1/4 [203x610x6] (Part a1)	12 [305]	3	20 [32]
5	8x24x1/4 [203x610x6] (Part a1)	6 [152]	3	20 [32]

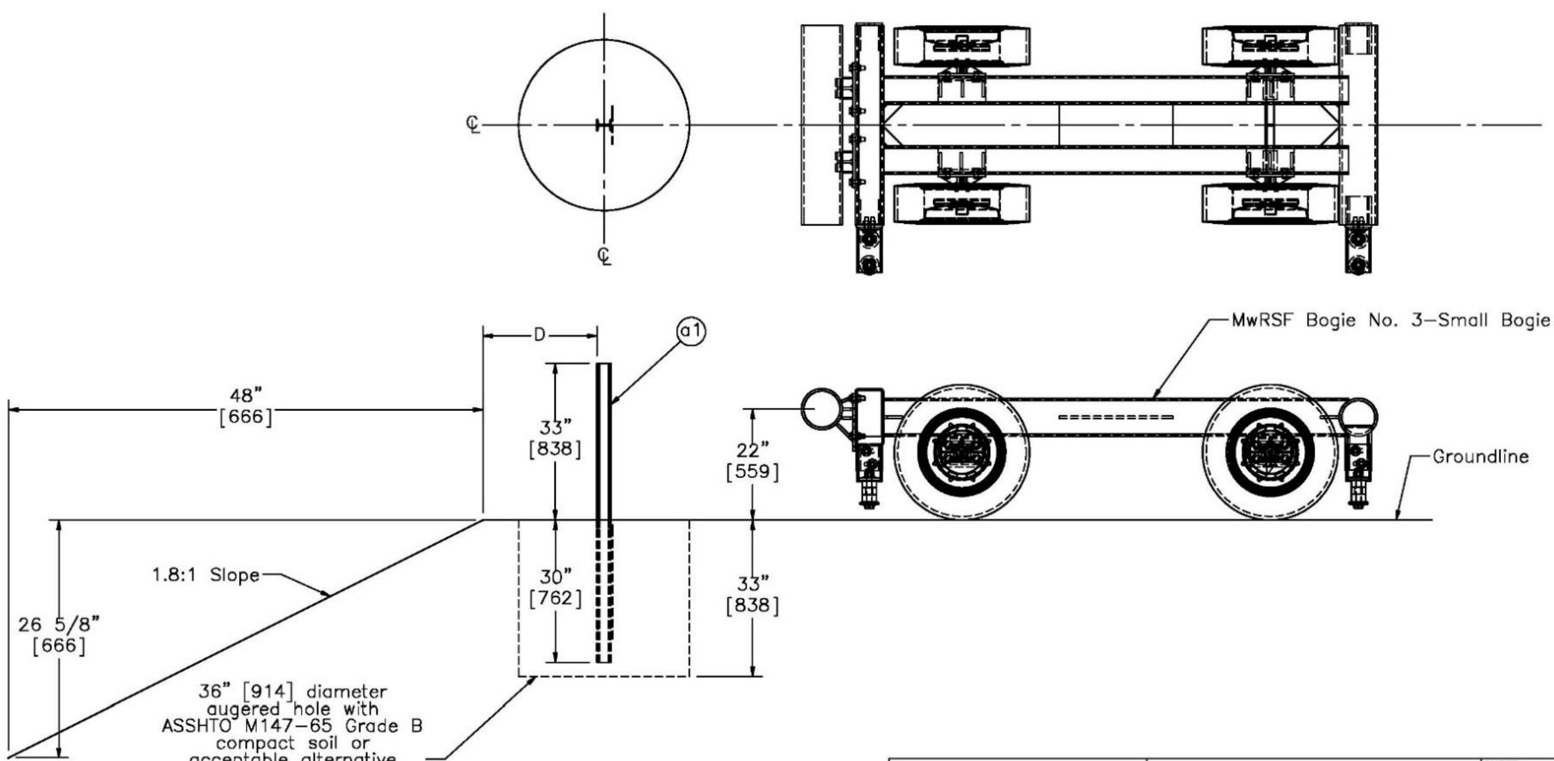

Note: (1) Soil plate on front side of post.

(2) Test 4 dependent upon results from Test 3.
–If successful, place post with standard soil plate at 12" [305] offset from slope breakpoint and oriented with soil plate on front of post.
–If unsuccessful, place post with larger soil plate at 24" [610] offset from slope breakpoint and oriented with soil plate on front of post.

MwRSF / Midwest Roadside Safety Facility	Low Tension Cable Barrier	SHEET: 2 of 4
		DATE: 3/31/2017
	Bogie Tests 3 through 5	DRAWN BY: ALL/TJD
	DWG. NAME. LTCB_Bogie_R12 / SCALE: 1:32 UNITS: Inches	REV. BY: SDB/SKR/KAL/RWB

Figure 7. Bogie Tests 3 through 5, Test Nos. LTCB-3 through LTCB-5

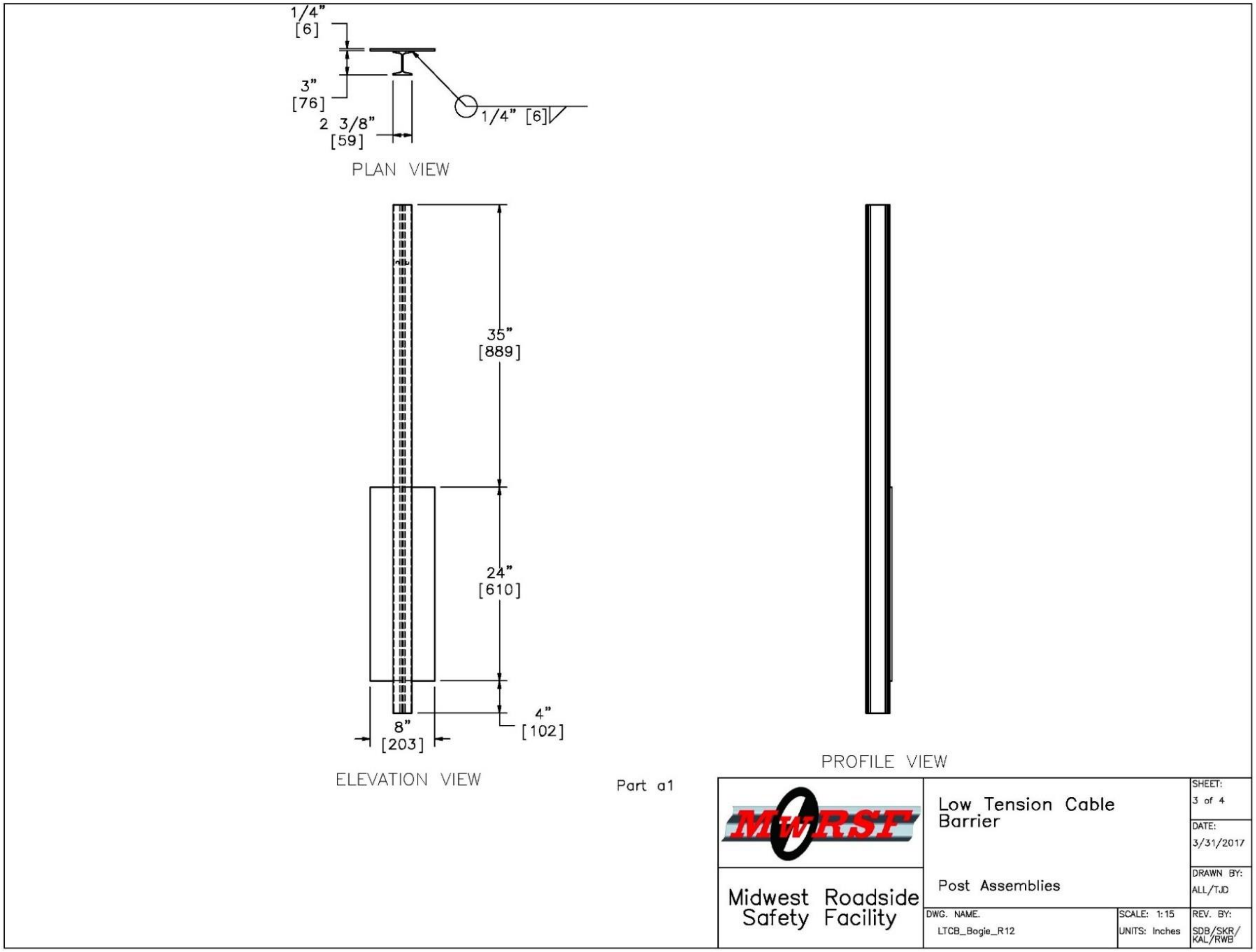

Figure 8. Post Assemblies, Test Nos. LTCB-1 through LTCB-5

5.2 Results

The accelerometer data for each test was processed in order to obtain acceleration, velocity, and deflection curves, as well as force vs. deflection and energy vs. deflection curves. Post deformation and soil displacement was compared for all of the tests as well. Test results for all transducers are provided in Appendix A. A summary of the bogie testing results is shown in Table 2.

5.2.1 Test No. LTCB-1

Test no. LTCB-1 was conducted on a 63-in. (1,600-mm) long, S3x5.7 steel post with an embedment depth of 30 in. (762 mm) and a 24-in. long by 8-in. wide x ¼-in. thick (610-mm. long by 203-mm wide x 6.4-mm thick) soil plate installed on the back face of the post and 4 in. (102 mm) from the base of the post. The post was installed on level terrain. During test no. LTCB-1, the bogie impacted the S3x5.7 post at a speed of 19.9 mph (32.0 km/h) causing strong-axis loading of the post. The post experienced significant rotation through the soil and yielded. The bogie overrode the top of the post at a displacement of 39.8 in. (1,011 mm).

Force-deflection and energy-deflection curves were created from the accelerometer data, as shown in Figure 9. The force rose to a peak of 7.0 kips (31.1 kN) at 3.0 in. (76.2 mm) of deflection. A total of 142.9 kip-in. (16.1 kJ) of energy was absorbed by the post before the bogie overrode the post at 39.8 in. (1,011 mm) of deflection. Time-sequential and post-impact photographs are shown in Figure 10.

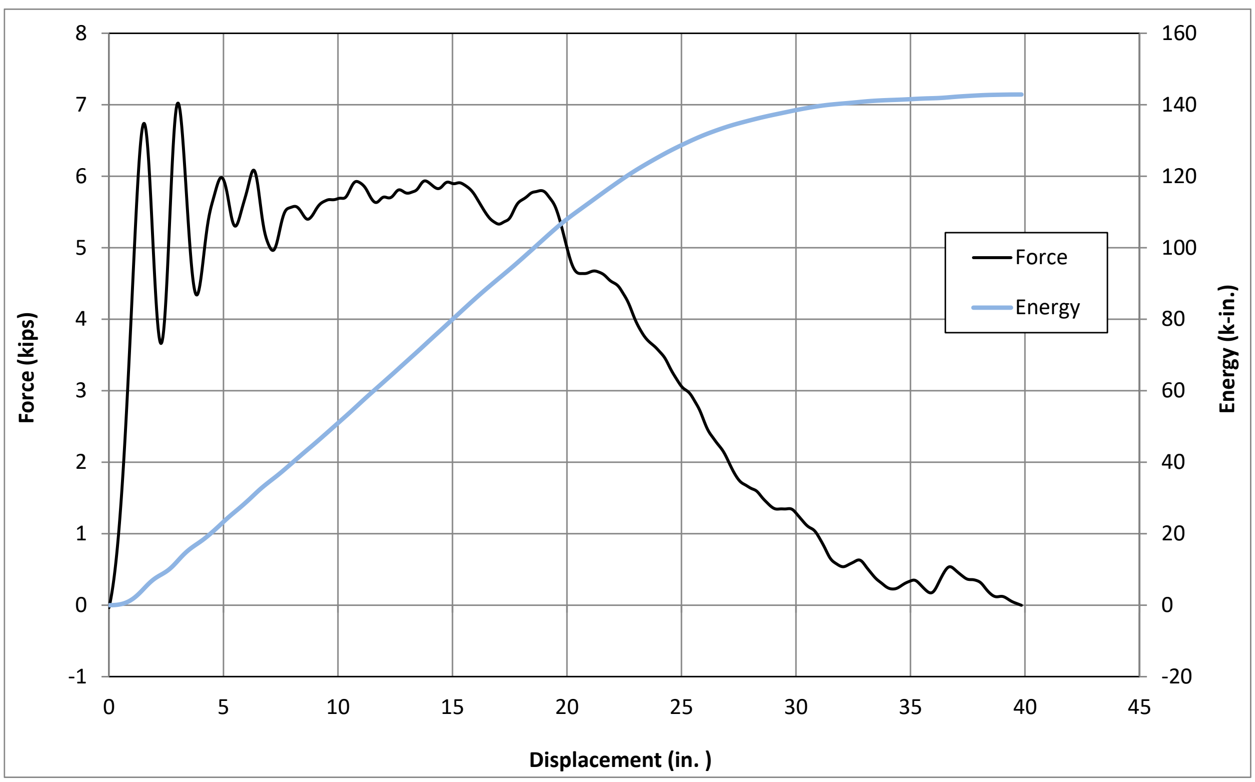

Figure 9. Force vs. Deflection and Energy vs. Deflection, Test No. LTCB-1

IMPACT

0.050 sec

0.100 sec

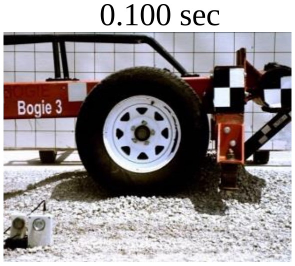

0.150 sec

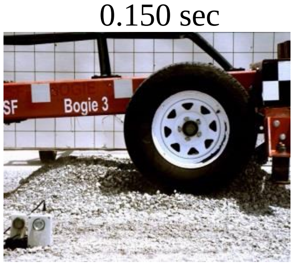

0.200 sec

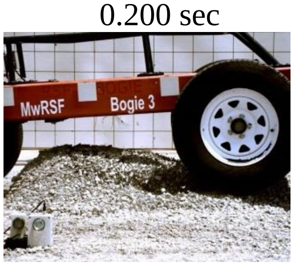

0.250 sec

Figure 10. Time-Sequential and Post-Impact Photographs, Test No. LTCB-1

5.2.2 Test No. LTCB-2

Test no. LTCB-2 was conducted on a 63-in. (1,600-mm) long, S3x5.7 steel post with an embedment depth of 30 in. (762 mm) and a 24-in. long by 8-in. wide x ¼-in. thick (610-mm. long by 203-mm wide x 6.4-mm thick) soil plate installed on the back face of the post and 4 in. (102 mm) from the base of the post. The post was installed on level terrain. During test no. LTCB-2, the bogie impacted the S3x5.7 steel post at a speed of 21.9 mph (35.2 km/h) causing strong axis loading of the post. The post rotated through the soil and yielded. The bogie overrode the top of the post at a displacement of 39.4 in. (1,001 mm).

Force-deflection and energy-deflection curves were created from the accelerometer data, as shown in Figure 11. The force rose to a peak of 7.6 kips (33.8 kN) at 2.0 in. (50.8 mm) of deflection. A total of 163.8 kip-in. (18.5 kJ) of energy was absorbed by the post before the bogie overrode the post at 39.4 in. (1,001 mm). Time-sequential and post-impact photographs are shown in Figure 12.

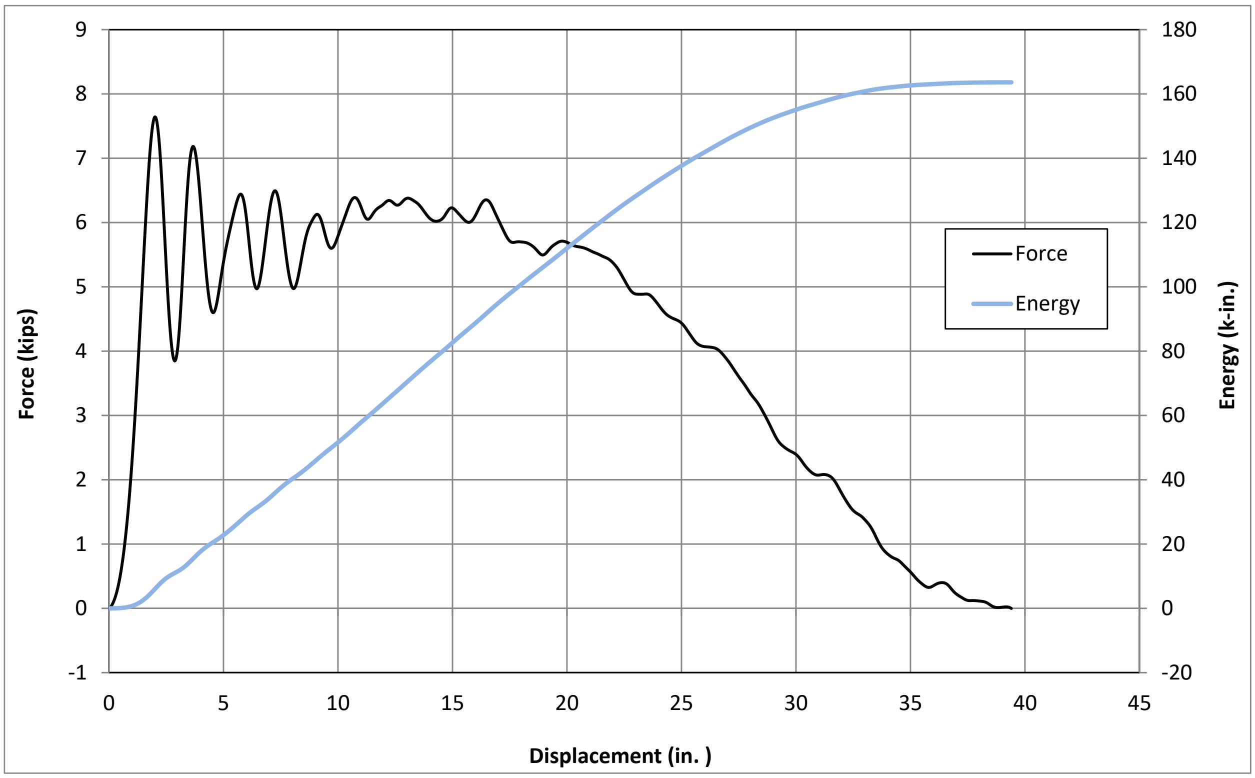

Figure 11. Force vs. Deflection and Energy vs. Deflection, Test No. LTCB-2

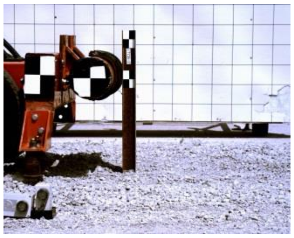

IMPACT

0.050 sec

0.100 sec

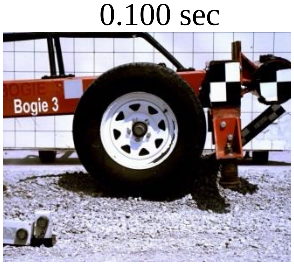

0.150 sec

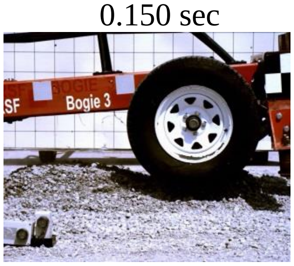

0.200 sec

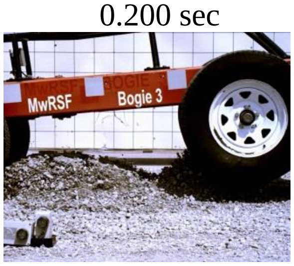

0.250 sec

Figure 12. Time Sequential and Post-Impact Photographs, Test No. LTCB-2

5.2.3 Test No. LTCB-3

Test no. LTCB-3 was conducted on a 63-in. (1,600-mm) long, S3x5.7 steel post with an embedment depth of 30 in. (762 mm). The post was offset 24-in. (610-mm) from a 1.8H:1V slope breakpoint. During test no. LTCB-3, the bogie impacted the S3x5.7 steel post at a speed of 20.9 mph (33.6 km/h) causing strong axis loading of the post. Upon impact, the post yielded, deflected backward, and underwent torsional buckling. The post had experienced minimal rotation through the soil. The bogie overrode the top of the post at a displacement of 39.4 in. (1,001 mm). The post contacted the bogie's undercarriage, causing the bogie to become airborne and land on the cement downstream of the slope.

Force-deflection and energy-deflection curves were created from the accelerometer data and are shown in Figure 13. The force rose to a peak of 7.6 kips (33.8 kN) at 1.8 in. (46 mm) of deflection. A total of 131.6 kip-in. (14.9 kJ) of energy was absorbed by the post before the bogie overrode the post at 39.4 in. (1,001 mm). Time-sequential and post-impact photographs are shown in Figure 14.

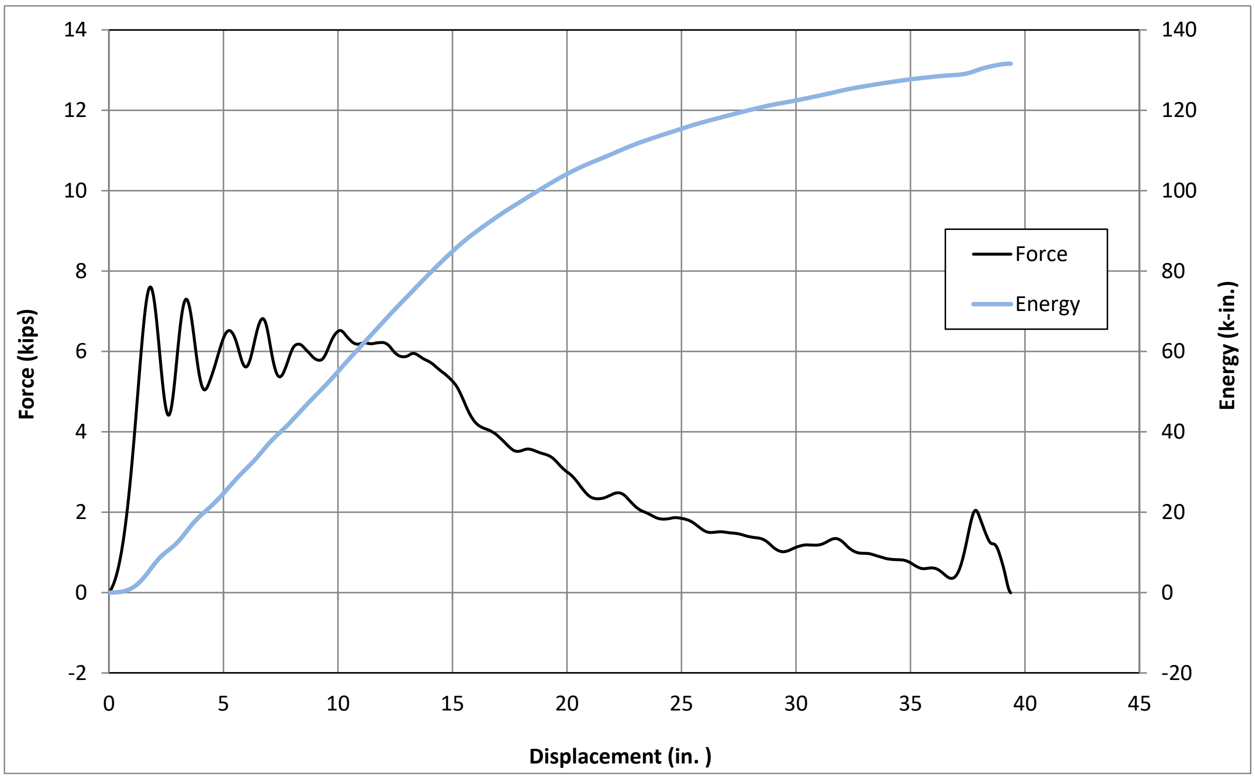

Figure 13. Force vs. Deflection and Energy vs. Deflection, Test No. LTCB-3

IMPACT

0.050 sec

0.100 sec

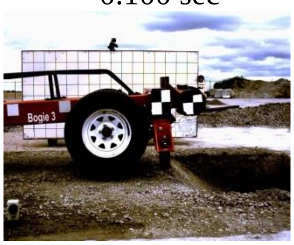

0.150 sec

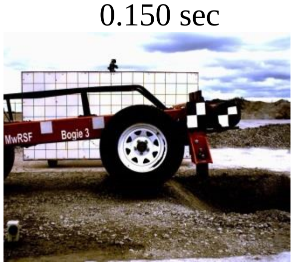

0.200 sec

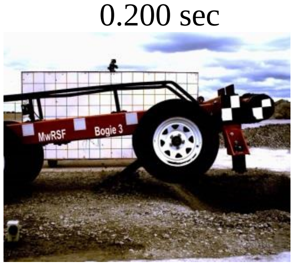

0.250 sec

Figure 14. Time-Sequential and Post-Impact Photographs, Test No. LTCB-3

5.2.4 Test No. LTCB-4

Test no. LTCB-4 was conducted on a 63-in. (1,600-mm) long, S3x5.7 steel post with an embedment depth of 30 in. (762 mm). The post was offset 12-in. (305-mm) from a 1.8H:1V slope breakpoint. During test no. LTCB-4, the bogie impacted the S3x5.7 steel post along its strong axis at a speed of 20.4 mph (32.8 km/h). Upon impact, the post rotated through the soil, yielded, and experienced torsional buckling as the bogie began to override the post. The bogie overrode the top of the post at a displacement of 36.5 in. (927 mm). The post contacted the bogie's undercarriage, causing the bogie to become airborne and land on the concrete downstream of the slope.

Force-deflection and energy-deflection curves were created from the accelerometer data, as shown in Figure 15. The force rose to a peak of 7.2 kips (32.0 kN) at 1.5 in. (38.1 mm) of deflection. A total of 127.4 kip-in. (14.4 kJ) of energy was absorbed by the post before the bogie overrode the post at 36.5 in. (927 mm). Time-sequential and post-impact photographs are shown in Figure 16.

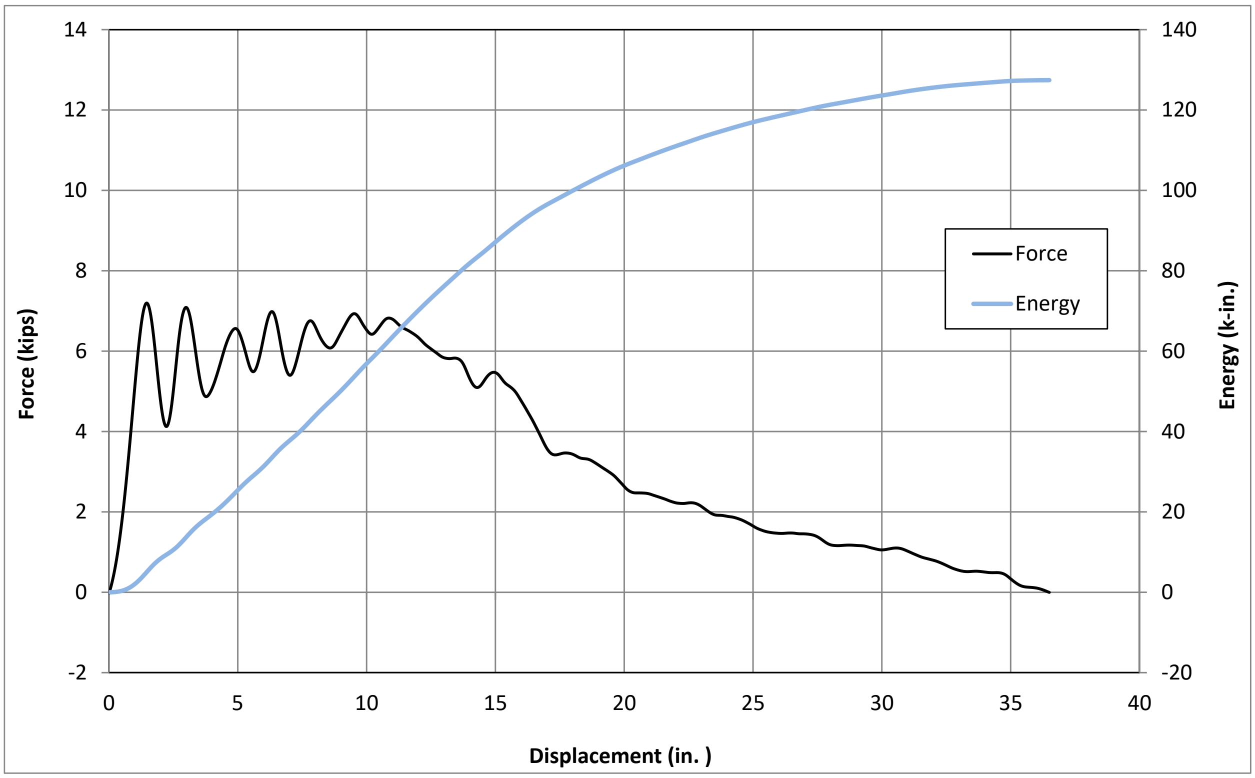

Figure 15. Force vs. Deflection and Energy vs. Deflection, Test No. LTCB-4

IMPACT

0.050 sec

0.100 sec

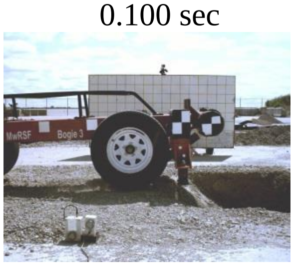

0.150 sec

0.200 sec

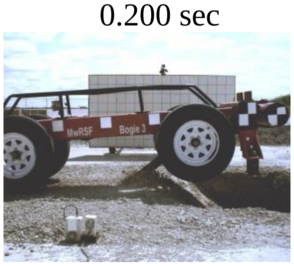

0.250 sec

Figure 16. Time-Sequential and Post-Impact Photographs, Test No. LTCB-4

5.2.5 Test No. LTCB-5

Test no. LTCB-5 was conducted on a 63-in. (1,600-mm) long, S3x5.7 steel post with an embedment depth of 30 in. (762 mm). The post was offset 6-in. (152-mm) from a 1.8H:1V slope breakpoint. During test no. LTCB-5 the bogie impacted the S3x5.7 steel post along its strong axis at a speed of 20.6 mph (33.2 km/h). The post rotated through the soil and experienced minor bending and deformation prior to the bogie overriding the top of the post at a displacement of 42.2 in. (1,072 mm). The bogie continued downstream after overriding the post and landed on the concrete downstream of the slope.

Force-deflection and energy-deflection curves were created from the accelerometer data, as are shown in Figure 17. The force rose to a peak of 7.3 kips (32.5 kN) at 1.6 in. (40.6 mm) of deflection. A total of 127.4 kip-in. (14.4 kJ) of energy was absorbed by the post before the bogie overrode the post at 42.2 in. (1,072 mm). Time-sequential and post-impact photographs are shown in Figure 18.

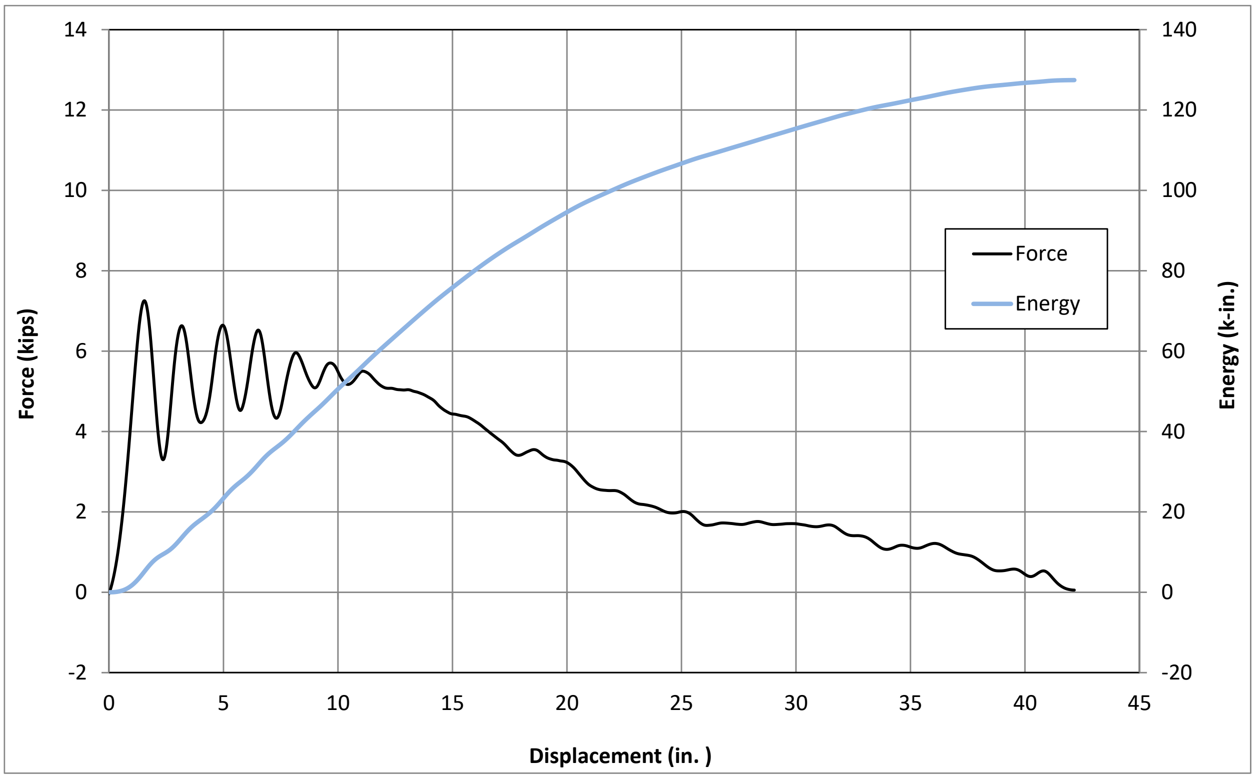

Figure 17. Force vs. Deflection and Energy vs. Deflection, Test No. LTCB-5

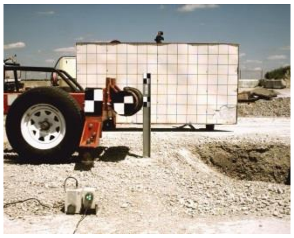

IMPACT

0.050 sec

0.100 sec

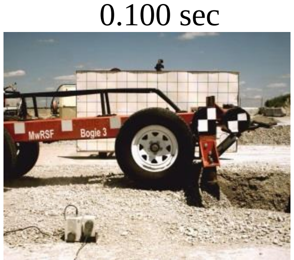

0.150 sec

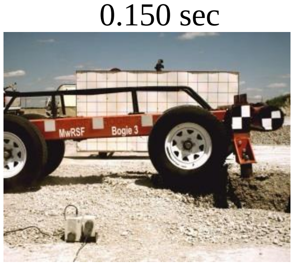

0.200 sec

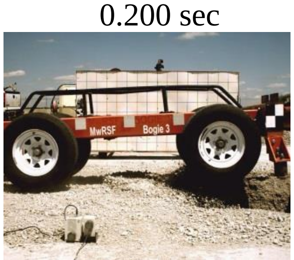

0.250 sec

Figure 18. Time-Sequential and Post-Impact Photographs, Test No. LTCB-5

5.3 Discussion

Five tests were conducted on 63-in. (1,600-mm) long, S3x5.7 steel posts with varying soil conditions ranging from level terrain to posts embedded adjacent to a 1.8H:1V slope with offsets of 24 in. (610 mm), 12 in. (305 mm), and 6 in. (152 mm). All five posts used for testing were impacted through the strong axis of the post at a height of 22 in. (559 mm) above the groundline. The test results are summarized in Table 2. Comparison graphs of force vs. deflection and energy vs. deflection are shown in Figures 19 and 20, respectively.

The posts exhibited varying amounts of bending and rotation through the soil and developed different force and energy levels. Test nos. LTCB-1 and LTCB-2 on level terrain served as the baseline for comparison. These two tests exhibited a combination of post rotation through the soil and post deformation and bending near ground line. Test nos. LTCB-1 and LTCB-2 displayed average forces of 5.33 kips (23.7 kN) and 5.50 kips (24.5 kN), respectively, at 15 in. (381 mm) of post deflection and average forces of 5.39 kips (24.0 kN) and 5.60 kips (24.9 kN), respectively, at 20 in. (508 mm) of post deflection. Energy through 15 in. (381 mm) and 20 in. (508 mm) of post deflection levels followed a similar trend.

Test nos. LTCB-3 and LTCB-4 performed very similarly to one another when evaluated at offsets of 24 in. (610 mm) and 12 in. (305 mm) from a 1.8H:1V slope, respectively. The posts in both tests went through limited displacement in the soil, bending of the post section near ground line, and torsional buckling of the post. Test nos. LTCB-3 and LTCB-3 displayed average forces of 5.65 kips (25.1 kN) and 5.80 kips (25.8 kN), respectively, at 15 in. (381 mm) of post deflection and average forces of 5.20 kips (23.1 kN) and 5.31 kips (23.6 kN), respectively, at 20 in. (508 mm) of post deflection. These average forces (and corresponding energy dissipation) were slightly higher than the baseline posts tested on level terrain at 15 in. (381 mm) of post deflection, but the average forces were slightly lower than the baseline posts at 20 in. (508 mm) of post deflection. Because rotation of the post in soil for these tests was limited, it was believed that the reduction of post resistive force at larger deflection was largely due to the torsional buckling of the post section. These results would indicate that the offsets of 24 in. (610 mm) and 12 in. (305 mm) from a 1.8H:1V slope evaluated in these tests were capable of fully developing the capacity of the S3x5.7 steel post section and could be considered as a potential option for the low-tension cable barrier adjacent to steep slopes.

Finally, test no. LTCB-5 evaluated the S3x5.7 post when installed 6 in. (152 mm) from the slope break point of a 1.8H:1V slope. In this test, the post rotated through the soil and disengaged a large section of the slope behind the post. Minor deformation and bending of the post were observed near groundline. Test no. LTCB-5 displayed an average force of 5.05 kips (22.5 kN) at 15 in. (381 mm) of post deflection and an average of 4.73 kips (21.0 kN) at 20 in. (508 mm) of post deflection. These average force levels were lower than the level terrain post tests and the two tests with larger post offsets from the 1.8H:1V slope. Energy dissipation of the post in test no. LTCB-5 was lower as well. While the post and slope offset configuration evaluated in test no. LTCB-5 still exhibited sufficient load to induce bending of the post, the proximity of the post to the steep slope produced increased soil displacement and reduced the force and energy developed by the post as compared to the other tested configurations. This suggested that a 6 in. (152 mm) offset from the 1.8H:1V slope may be at or past the limit for acceptable performance when applied to the low-tension cable barrier adjacent to slope as it may lead increased barrier deflections and loss of vehicle capture.

As noted previously, the researchers believed that adequate safety performance of the low-tension cable barrier adjacent to steep slopes would rely on developing the full plastic strength of the posts in the system to maintain vehicle capture and limit barrier deflections over the slope. After reviewing these post component tests, the researchers recommended a minimum post offset of 12 in. (305 mm) from a 1.8H:1V slope for the analysis of potential low-tension cable barrier adjacent configurations in order to maintain a consistent post response.

Table 2. Dynamic Component Testing Results, Test Nos. LTCB-1 through LTCB-5

Test No.	Post Description	Embedment Depth in. (mm)	Peak Force kips (kN)	Average Force kips (kN)				Energy kip-in. (kJ)					Maximum Deflection in. (mm)
				@ 5"	@ 10"	@ 15"	@ 20"	@ 5"	@ 10"	@ 15"	@ 20"	Total	
LTCB-1	S3x5.7	30 (762)	7.0 (31.1)	4.66 (20.7)	5.08 (22.6)	5.33 (23.7)	5.39 (24.0)	23.3 (2.63)	50.8 (5.74)	79.9 (9.03)	107.9 (12.2)	142.9 (16.1)	39.8 (1,011)
LTCB-2	S3x5.7	30 (762)	7.6 (33.8)	4.53 (20.2)	5.14 (22.9)	5.50 (24.5)	5.60 (24.9)	22.7 (2.56)	51.4 (5.81)	82.4 (9.31)	112.0 (12.7)	163.6 (18.5)	39.4 (1,001)
LTCB-3	S3x5.7	30 (762)	7.6 (33.8)	4.91 (21.8)	5.50 (24.5)	5.65 (25.1)	5.20 (23.1)	24.6 (2.78)	55.0 (6.21)	84.7 (9.57)	104.1 (11.8)	131.6 (14.9)	39.4 (1,001)
LTCB-4	S3x5.7	30 (762)	7.2 (32.0)	5.07 (22.6)	5.69 (25.3)	5.80 (25.8)	5.31 (23.6)	25.4 (2.87)	56.9 (6.43)	87.0 (9.83)	106.1 (12.0)	127.4 (14.4)	36.5 (927)
LTCB-5	S3x5.7	30 (762)	7.3 (32.5)	4.67 (20.8)	5.04 (22.4)	5.05 (22.5)	4.73 (21.0)	23.3 (2.63)	50.4 (5.69)	75.8 (8.56)	94.5 (10.7)	127.4 (14.4)	42.2 (1,072)

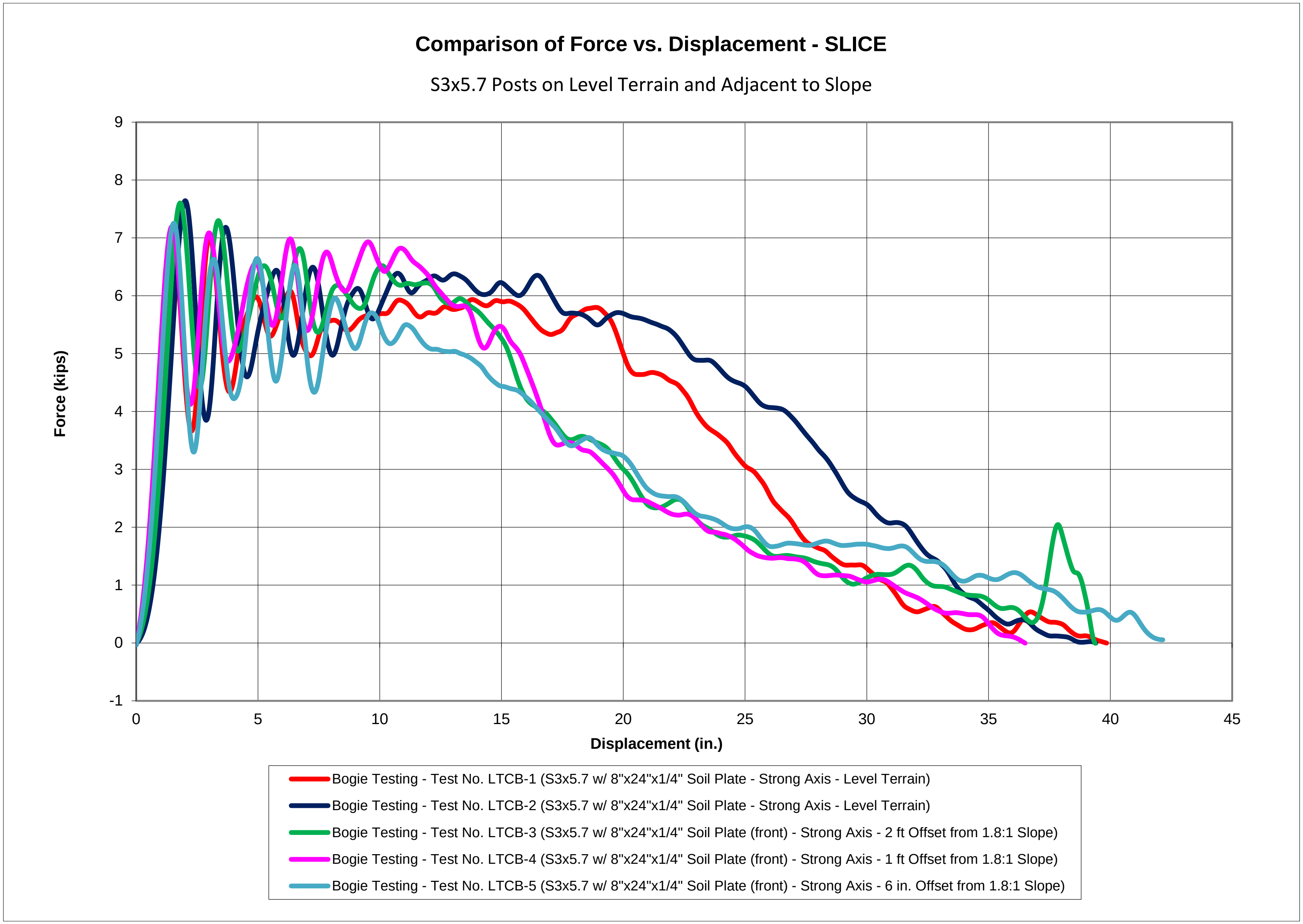

Figure 19. Force vs. Deflection Comparison, Test Nos. LTCB-1 through LTCB-5

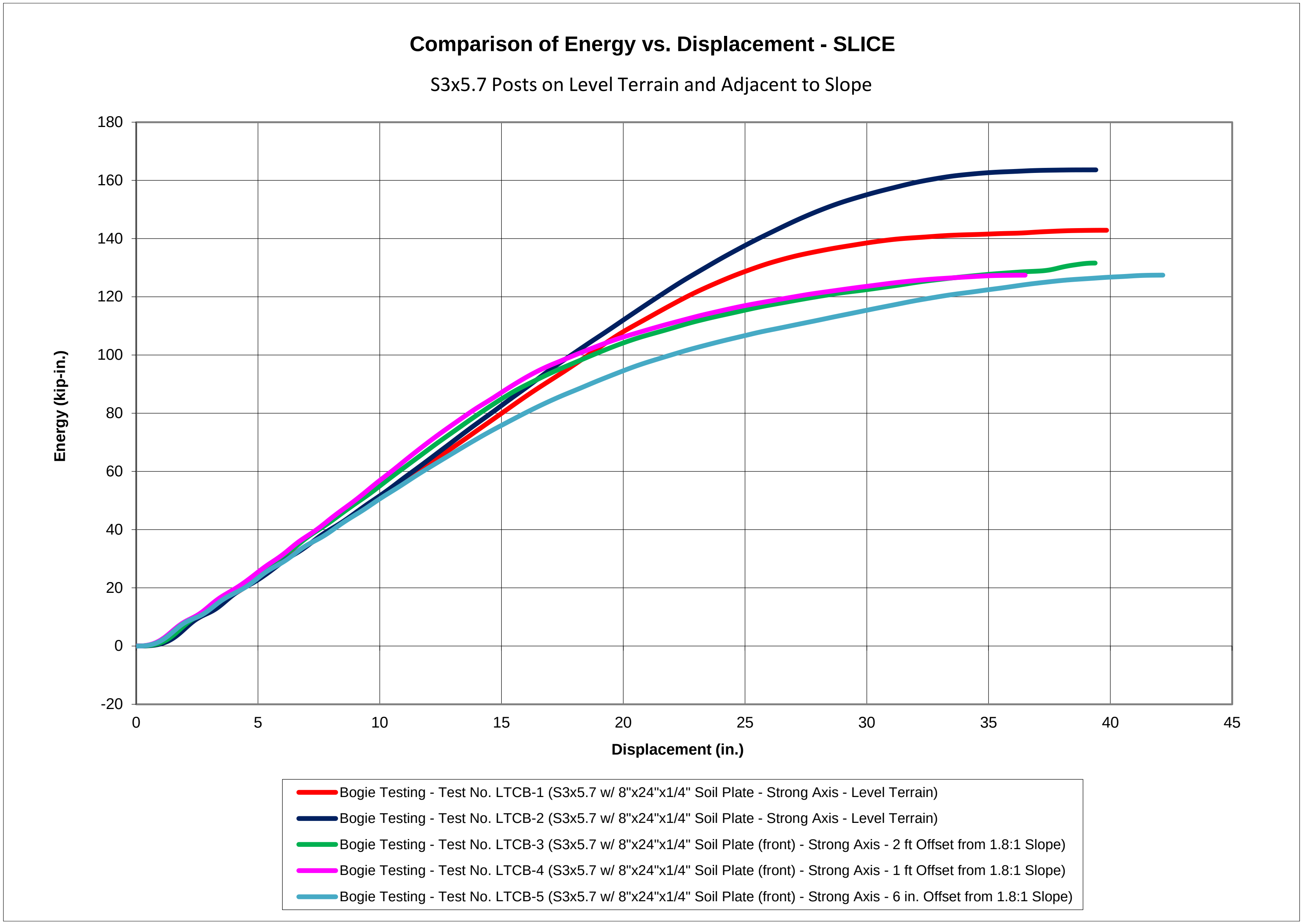

Figure 20. Energy vs. Deflection Comparison, Test Nos. LTCB-1 through LTCB-5

6 EVALUATION OF FLOORBOARD TEARING BY S3x5.7 POSTS

After completing the dynamic component testing of the S3x5.7 posts, the researchers reviewed full-scale crash testing of a nonproprietary, high-tension cable median barrier developed through the Midwest Pooled Fund Program [8-10]. The nonproprietary, high-tension cable median barrier was being tested and evaluated with the newly developed Midwest Weak Post (MWP) section. The full-scale crash testing of the system with the 1100C small car vehicle indicated that the flanges of the MWP post could lacerate and penetrate the floorboard of the vehicle as it overrode the weak axis of the posts, as shown in Figure 21. This floorboard penetration was deemed a failure of the full-scale crash test under MASH safety requirements. Based on the performance of the MWP post in the high-tension cable median barrier testing, there was concern that the flanges of the S3x5.7 post proposed for use in the low-tension cable barrier adjacent to steep slopes could produce similar floorboard laceration and penetration. In order to evaluate the potential for the S3x5.7 post to lacerate and penetrate the floorboard of the small car, dynamic component testing was undertaken that overrode the S3x5.7 posts with a specialized bogie vehicle with a simulated floorboard.

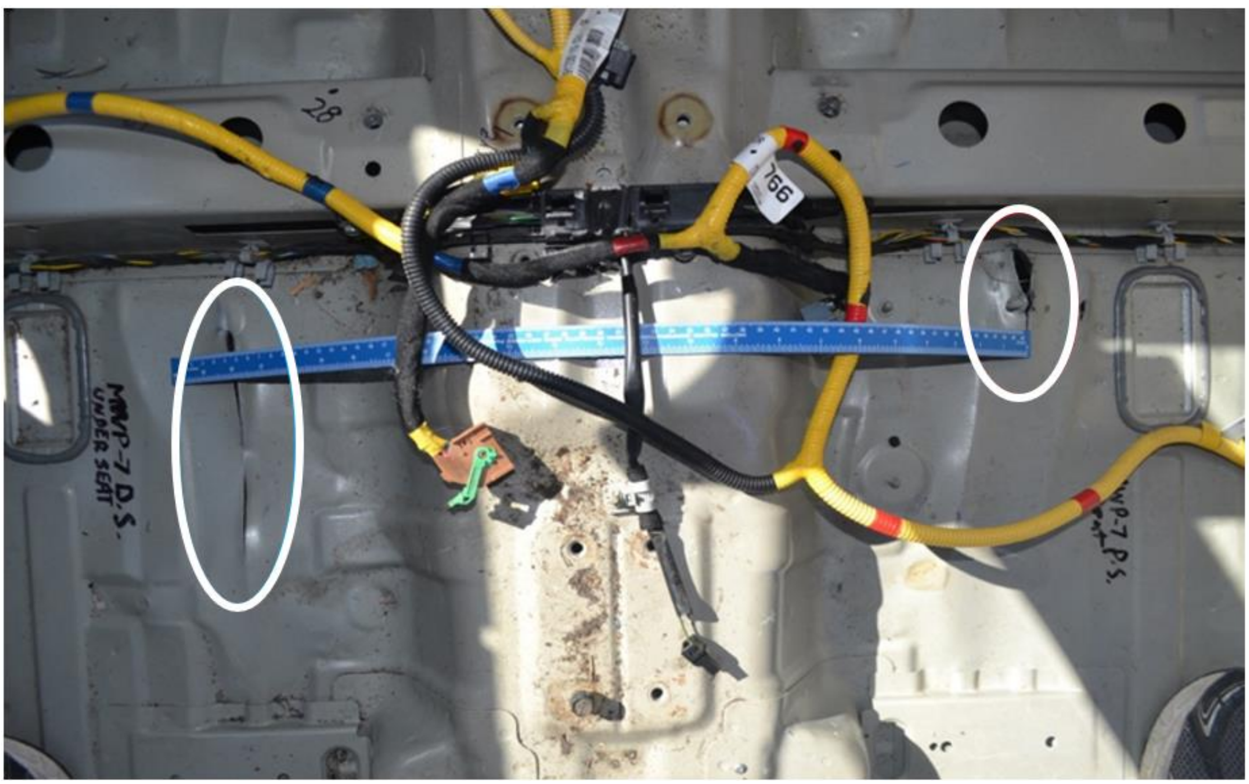

Figure 21. Floorboard Laceration and Penetration, Test No. MWP-7

To perform this testing, a specialized bogie vehicle with a simulated floorboard developed in a parallel study was used [11]. A rigid-frame bogie vehicle, equipped with a simulated small car floorboard, was used to impact the posts. The simulated floorboard consisted of a 120-in. x 23¾-in. (3,048-mm x 603-mm) sheet of 24-gauge (0.61-mm) ASTM A653 steel. The sheet steel was mounted to the bottom of an undercarriage frame at a height of 8 in. (203 mm), which matched the height of the Kia Rio floorboards from previous full-scale crash tests. The undercarriage frame was constructed from 3½-in. x 3½-in. x ⅜-in. (90-mm x 90-mm x 10-mm) steel tubes and was bolted to the inside of the bogie vehicle frame. The front beam of the undercarriage frame was positioned in front of the simulated floorboard and shifted downward 1¾ in. (44 mm). This vertical offset prevented the top of the post from snagging on the front edge of the sheet steel, and acted as a stiff cross member of the vehicle undercarriage (e.g., frame element, axle) that caused the post to bend down and spring back upward toward the floorboard as the bogie overrode the top of the post. A 1¾-in. (44-mm) square tube was bolted underneath and across the middle of the simulated floorboard to create a second location where the post would be pushed down and allowed to spring back upward.

In test no LTCB-6 two S3x5.7 posts similar to those evaluated in test nos. LTCB-1 through LTCB-5 were spaced 8 ft (2,438 mm) apart, impacted on their weak axis, and overridden by the modified bogie in order to determine if the S3x5.7 posts proposed for use in the low-tension cable barrier adjacent to steep slopes posed a potential for floorboard tearing. Details of the bogie testing setup for test no. LTCB-6 are provided in Table 3 and Figures 22 through 24 Photographs of the test setup are shown in Figure 25. Other details of the test documentation and setup were provided in Chapter 4.

Table 3. Test Matrix for Test No. LTCB-6

Test No.	Offset Distance in. (mm)	Soil Plate Dimension in. (mm)	Target Impact Conditions		
			Impact Velocity mph (km/h)	Impact Height in. (mm)	Impact Angle degrees
LTCB-6	N/A	8 x 24 x ¼ (203 x 610 x 6)	25.0 (40.2)	22 (559)	Weak Axis 0

Test Name	Impact Height	Bogie No.	Estimated Bogie Weight (lb)	Bogie Speed (mph)	Post Orientation (deg) (X)*	Post Specimen
LTCB–6	22" [558]	4 with floorpan	2400	25	0	S3x5.7 [S76x8.5] 63" [1600] Long Post with 8"x24"x1/4" [203x610x6] Soil Plate

*0° = weak axis, 90° = strong axis

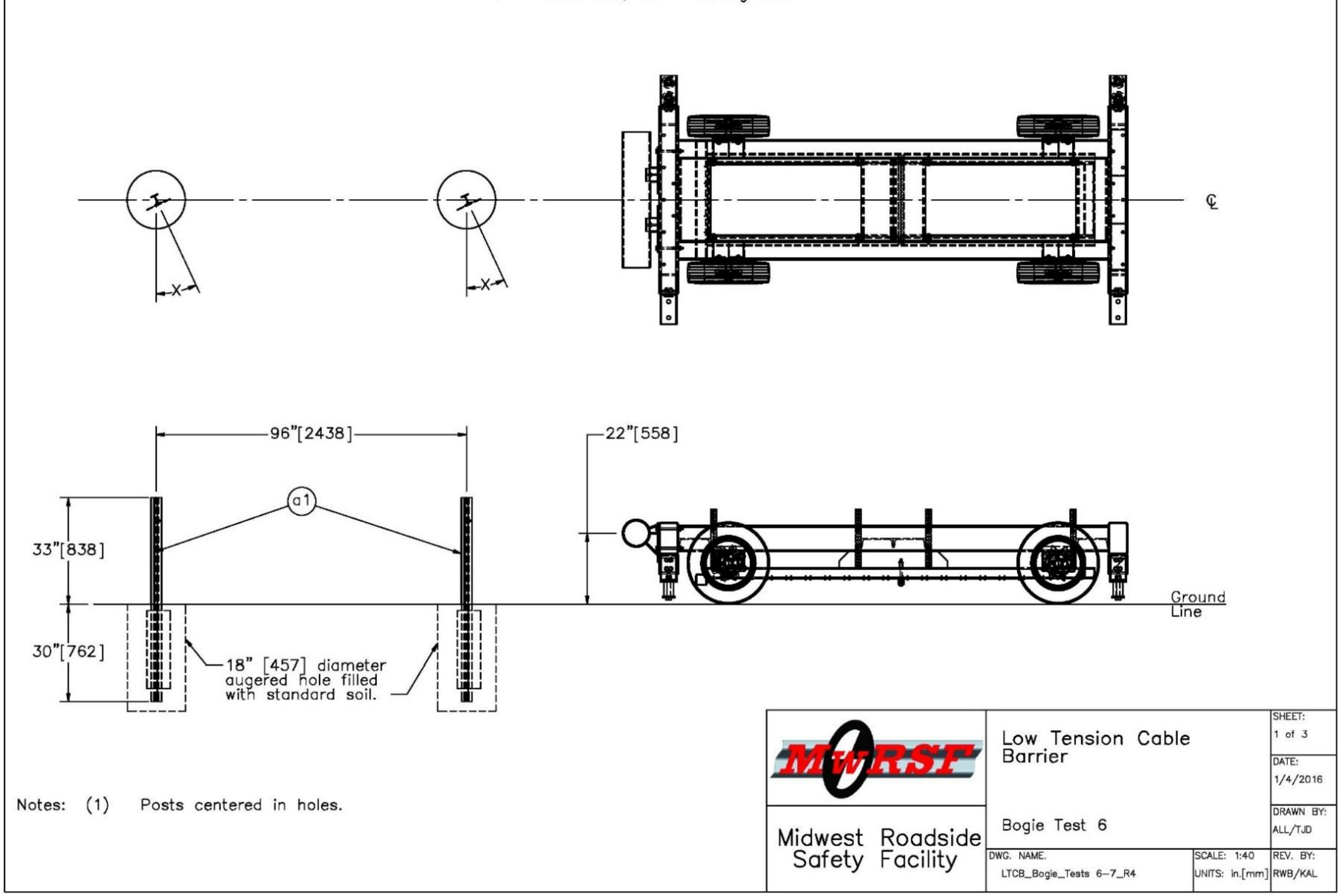

Figure 22. Test Setup, Test No. LBCT-6

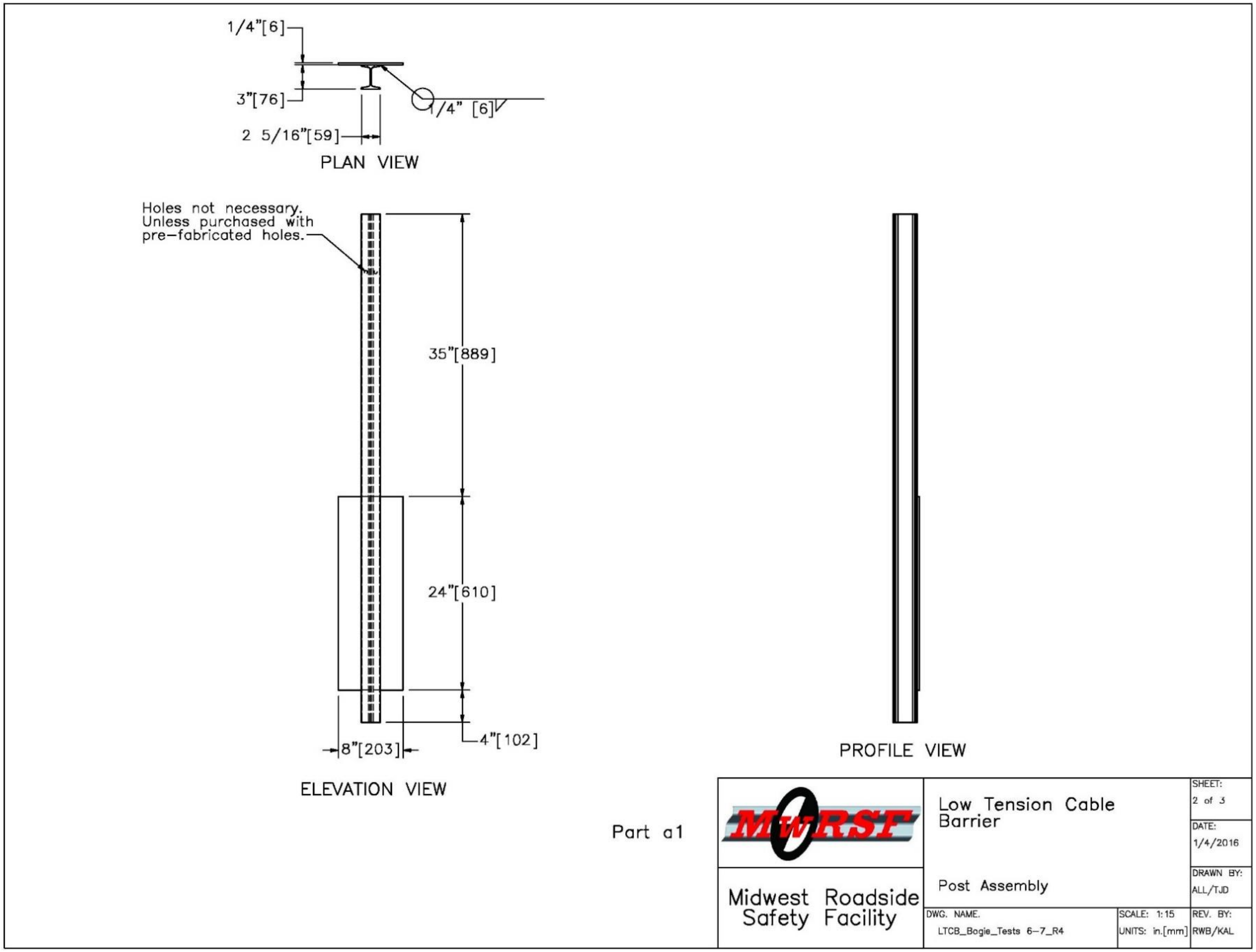

Figure 23. Test Setup, Test No. LBCT-6

Item No.	QTY.	Description	Material Spec	Hardware Guide
a1	2	S3x5.7 [S76x8.5] by 63" [1575] Long Steel Post with 8"x24"x1/4" [203x610x6] Soil Plate	ASTM A992, ASTM A572–Grade 50, ASTM A709–Grade 50	PSE01

Midwest Roadside Safety Facility	Low Tension Cable Barrier Bill of Materials	SHEET: 3 of 3 DATE: 1/4/2016 DRAWN BY: ALL/TJD
	DWG. NAME. LTCB_Bogie_Tests 6-7_R4	SCALE: 1:12 UNITS: in.[mm]
		REV. BY: RWB/KAL

Figure 24. Bill of Materials, Test No. LBCT-6

Figure 25. Bogie Test Setup, Test No. LTCB-6

6.1 Test No. LTCB-6

Test no. LTCB-6 was conducted on two 63-in. (1,600-mm) long, S3x5.7 steel posts spaced 8 ft (2,438 mm) apart with an embedment depth of 30 in. (762 mm). The two posts were impacted through their weak axis to investigate the propensity of floorboard tearing due to the free edge on the S3x5.7 post. During test no. LTCB-6, the bogie impacted the first S3x5.7 steel post at a speed of 25.8 mph (41.5 km/h). the impact of the bogie vehicle caused the post to yield and bend about its weak axis near the ground line. As the bogie overrode the first post, the post flanges and upper corners contacted and scraped across the simulated floorboard. The front of the bogie was lifted from the ground and remained airborne until impacting the second S3x5.7 steel post approximately 0.220 sec after the impact with the first post with a speed of 25.4 mph (40.9 km/h). The bogie vehicle impact caused the second post to yield and bend about its weak axis as well, and the flanges and corners of the second post contacted and scraped across the simulated floorboard as it was overridden by the bogie vehicle.

Force-deflection and energy-deflection curves were created from the accelerometer data and are shown in Figure 26. The force rose to a peak of 6.9 kips (30.7 kN) at 2.0 in. (50.8 mm) of deflection after impacting the first post. A total of 192.1 kip-in. (21.7 kJ) of energy was absorbed from both posts. Time-sequential and post-impact photographs are shown in Figure 27.

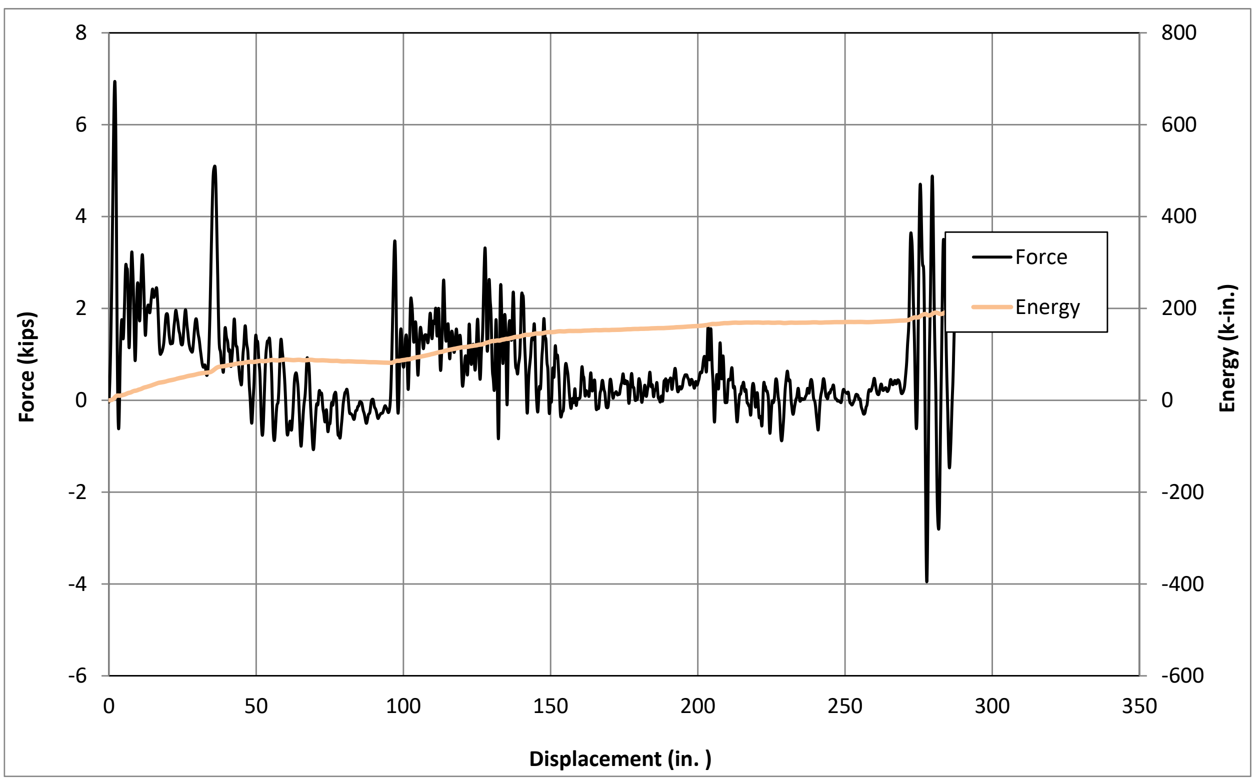

Figure 26. Force vs. Deflection and Energy vs. Deflection, Test No. LTCB-6

The condition of the simulated floorboard was reviewed following the bogie test. Both the front and rear sections of the simulated floorboard displayed tearing and heavy gouging due to contact with the post flanges, as shown in Figure 28. In the front section of the simulated floorboard, the contact with the first post produced a tear due to the right flange of the post and a deep groove in the simulated floorboard due to the left flange of the post. The second impacted post produced more tearing and gouging in the first section of the simulated floorboard with both post flanges creating tears upon initial contact. As the post continued to contact the simulated floorboard, deep grooves were observed in the simulated floorboard, and the right flange of the second post formed a long tear near the back of the first section of floorboard. The rear section of the simulated floorboard had four tears at the front of the simulated floorboard sections due to contact with both flanges of both posts. Deep grooves from all four post flanges were also observed down the entire length of the second section of the simulated floorboard.

IMPACT

0.100 sec

0.200 sec

0.300 sec

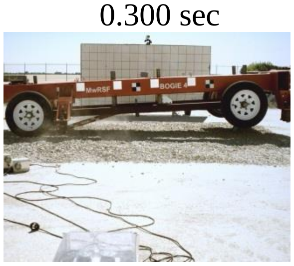

0.400 sec

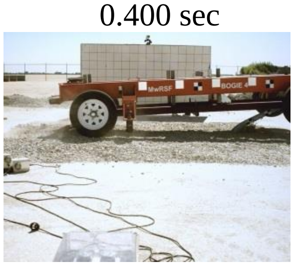

0.500 sec

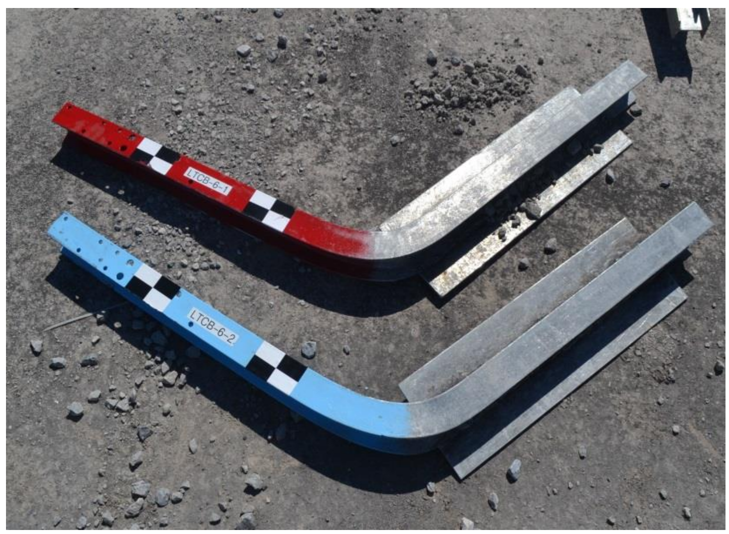

Figure 27. Time-Sequential and Post-Impact Photographs, Test No. LTCB-6

Figure 28. Floorboard Tearing Photographs, Test No. LTCB-6

6.2 Discussion

Based on results of test no. LTCB-6, concerns for the potential for floorboard tearing existed with the standard S3x5.7 post section. Several options were considered for further development of the low-tension cable barrier adjacent to steep slopes. One option was to continue to use the S3x5.7 post with the concession that there was a high potential that full-scale crash testing would be a failure under MASH TL-3 criteria due to floorboard tearing. This option was not desired as the concern that the barrier system would not meet MASH TL-3 was too high.

As such, an alternative post configuration was desired to avoid the propensity for floorboard penetration observed with the S3x5.7 posts initially proposed for use with the low-tension cable barrier adjacent to steep slopes. A second option was to modify the existing S3x5.7 post design to mitigate the potential for floorboard tearing. This could be done through weaking mechanisms, the use of a slip-base or breakaway base, or shielding of the post flanges. This option was also not desired due to the added complexity of these design changes and the time and cost involved to develop and evaluate such a post.

A third option was to utilize an alternative cable post design that had just been developed for use in high-tension cable median barrier. As noted previously, the parallel development of the nonproprietary, high-tension cable median barrier for the Midwest Pooled Fund Program faced a similar floorboard tearing and penetration issue and had developed a closed-section tubular post to address this issue [12]. An HSS3x2x⅛ post with two ¾-in. (19-mm) diameter holes at ground line was chosen for the post section as it met the design criteria for strong and weak axis post strength and showed the potential to mitigate floorboard tearing. This post section was named the Midwest Tube Post (MTP). Based on the performance of the MTP, it was decided to apply this closed-section tubular post design to the low-tension cable median barrier to steep slopes as well. In order to better evaluate the MTP for this application, additional dynamic component tests were conducted on this post at reduced offsets to a steep slope to determine a minimum offset from the slope break point where the post bending capacity could be fully developed similar to the previous component testing of the S3x5.7 post section. Additional testing to evaluate the potential for floorboard tearing was not necessary as that had been evaluated previously during its development for the high-tension cable median barrier system.

7 COMPONENT TESTING OF MIDWEST TUBE POST (MTP)

7.1 Tubular Post Testing Adjacent to 1.8H:1V Slope

A series of dynamic component tests were conducted on the MTP to evaluate its performance adjacent to a 1.8H:1V slope. The MTP consisted of an HSS3x2x⅛ post section with two ¾-in. (19-mm) thru holes in the weak axis. The purpose of the tests was to determine the minimum offset of the posts from the slope break point which would develop the full capacity of the post.

Test nos. CTPS-1 and CTPS-2 were conducted on the MTP for this study. The target impact speed was 20 mph (32 km/h) for both tests, and the impact was oriented along the strong axis of the post. Test no. CTPS-1 was conducted on a post located 12 in. (305 mm) from the slope break point of a 1.8H:1V slope. Test no. CTPS-2 was conducted on a post located 6 in. (152 mm) from the slope break point of a 1.8H:1V slope. Both posts had an embedment depth of 40 in. (1,016 mm) and did not incorporate a soil plate below grade. The decision was made to remove the soil plate to reduce the cost of the post, and the embedment depth was increased to compensate for the lack of the soil plate. The dynamic component test matrix is shown in Table 4. The test set-up for test nos. CTPS-1 and CTPS-2 is shown in Figure 2 through 3. Material specifications, mill certificates, and certificates of conformity for the post materials used in all tests are shown in Appendix A.

The accelerometer data for each test was processed in order to obtain acceleration, velocity, and deflection curves, as well as force vs. deflection and energy vs. deflection curves. The values described herein were calculated from the SLICE 1 and SLICE 2 data curves in order to provide common basis for comparing results from multiple tests.

Table 4. Dynamic Post Testing Matrix, Tests Nos. CTPS-1 and CTPS-2

Test No.	Post Type	Post Length in. (mm)	Post Embedment in. (mm)	Offset From Slope Break Point in. (mm)	Target Impact Conditions		
					Impact Velocity mph (km/h)	Impact Height in. (mm)	Impact Angle degrees
CTPS-1	MTP	78 (1,981)	40 (1,016)	12 (610)	20.0 (32.2)	22 (559)	90
CTPS-2	MTP	78 (1,981)	40 (1,016)	6 (305)	20.0 (32.2)	22 (559)	90

Test Nos.	Offset Distance, D in. [mm]	Bogie No.	Impact Speed mph [km/h]
CTPS-1	12 [305]	3	20 [32]

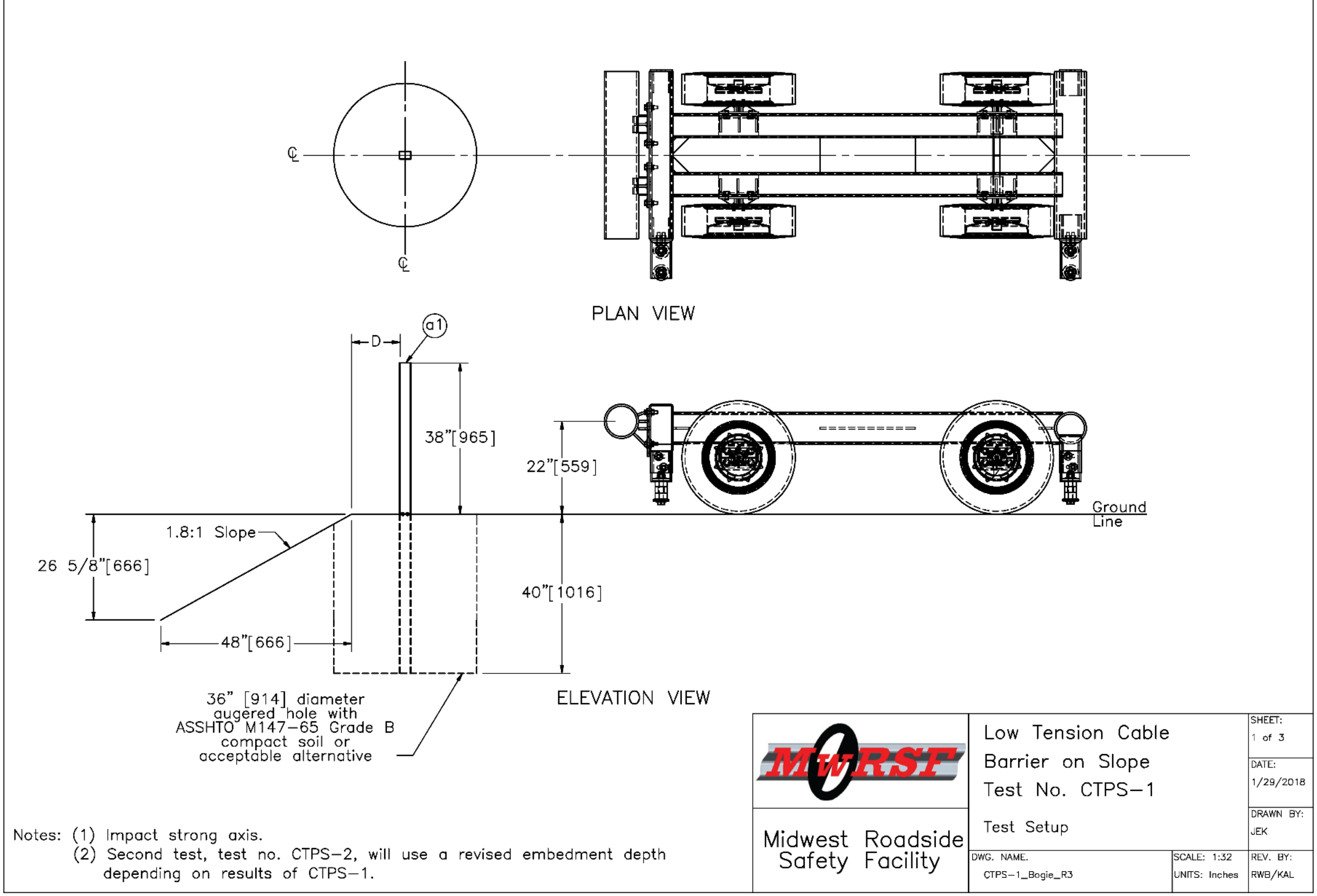

Figure 29. Test Setup, Test No. CTPS-1

Test Nos.	Offset Distance, D in. [mm]	Bogie No.	Impact Speed mph [km/h]
CTPS-2	6 [152]	3	20 [32]

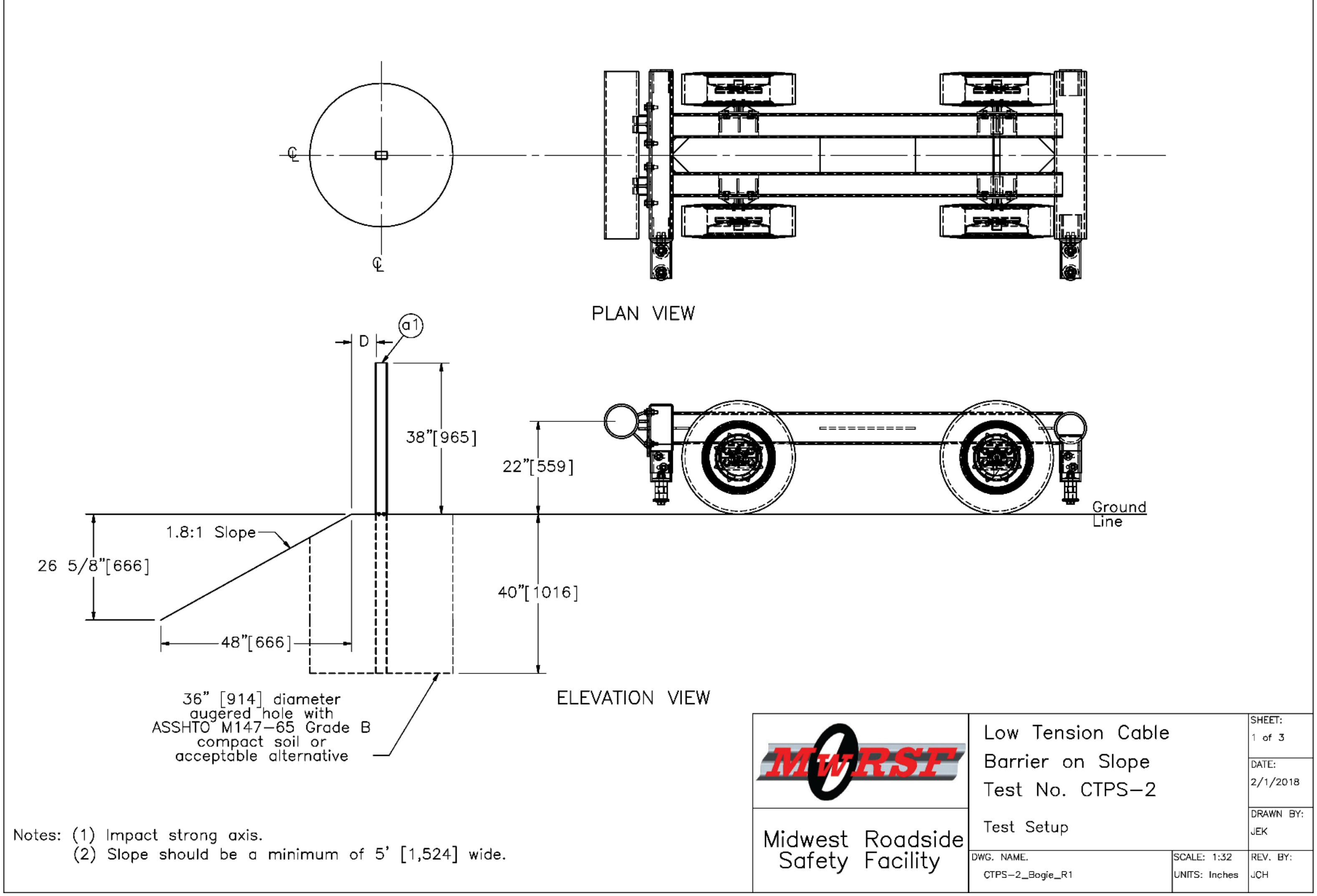

Figure 30. Test Setup, Test No. CTPS-2

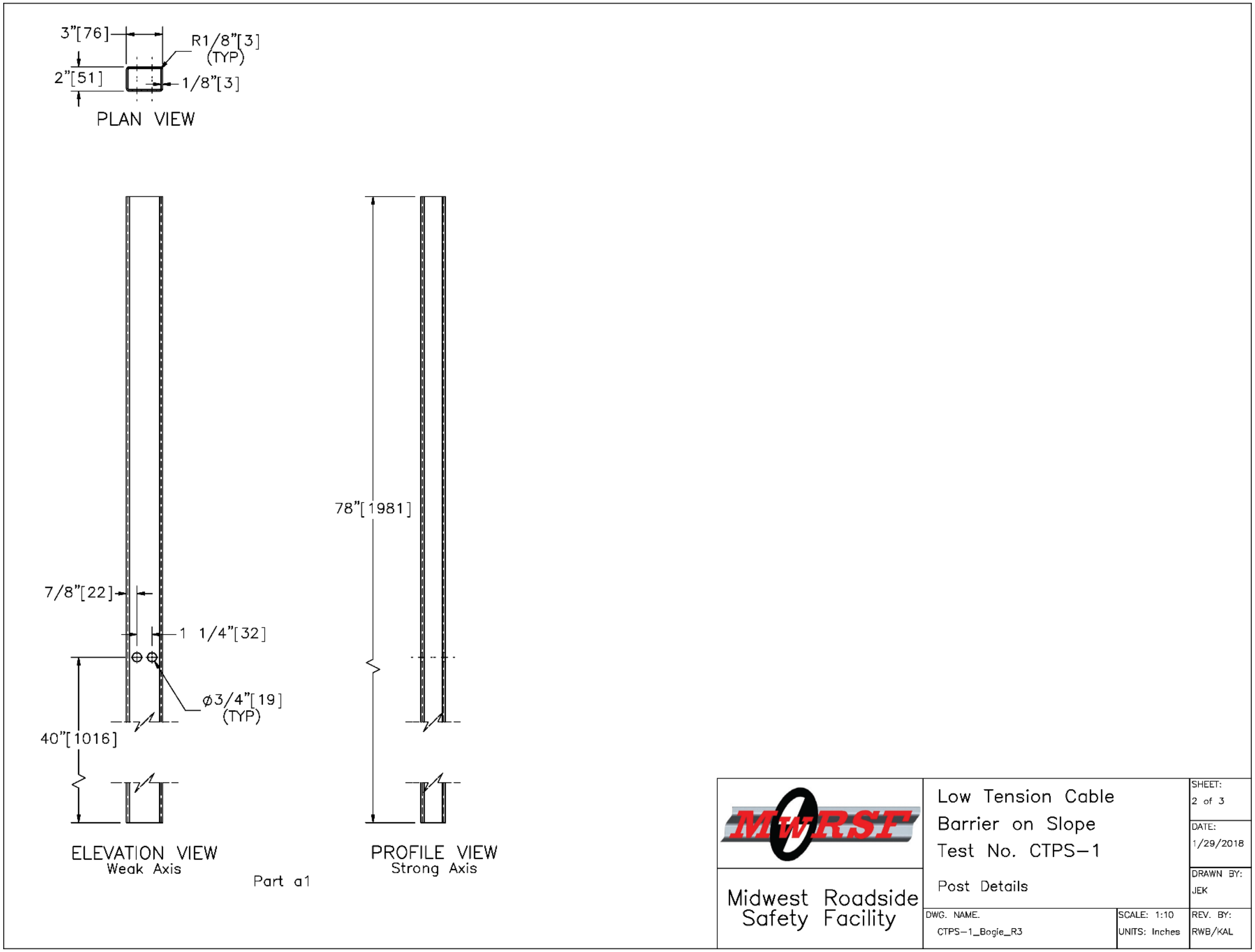

Figure 31. Post Details, Tests Nos. CTPS-1 and CTPS-2

7.2 Dynamic Testing Results

The accelerometer data for each test was processed to obtain acceleration, velocity, and deflection curves, as well as force vs. deflection and energy vs. deflection curves. The values described herein were calculated from the SLICE 2 data curves. Test results for all transducers are provided in Appendix C.

7.2.1 Test No. CTPS-1

During test no. CTPS-1, the bogie impacted the MTP along its strong axis at a speed of 23.2 mph (37.4 km/h). During the impact, the post had a small displacement in the soil followed by yielding and hinging of the post near ground line. The 1.8H:1V slope sustained little to no damage during the test as the post bent backward. The bogie overrode the top of the post at a displacement of 40 in. (1016 mm) as determined from the SLICE 1 data.

Force-deflection and energy-deflection curves were created from DTS accelerometer data, as shown in Figure 32. Initially, inertial effects resulted in a high peak force over the first few inches of deflection. Following the inertia force, a relatively steady force in the range of 3 to 4 kips (13.3 to 17.8 kN) was observed through 10 in. (254 mm) of deflection. As the impact continued, the force gradually decreased until the bogie overrode the post at a displacement of 40 in. (1016 mm). The energy absorbed by the post was 75 kip-in. (8.5 kJ) through 40 in. (1016 mm) of deflection. Pre-test and post-test photographs are shown in Figure 33.

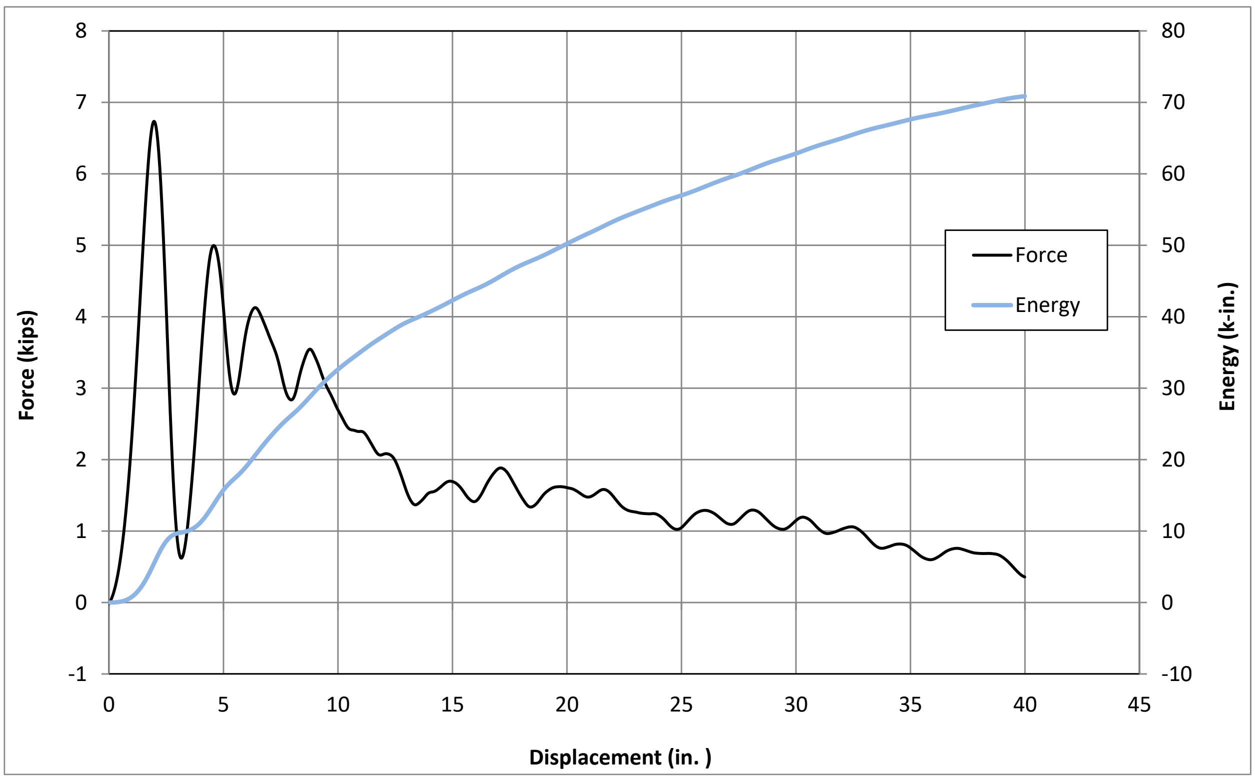

Figure 32. Force vs. Deflection and Energy vs. Deflection, Test No. CTPS-1

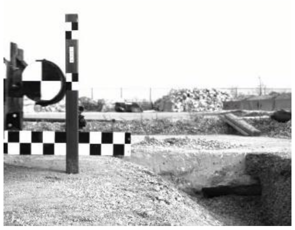

IMPACT

0.020 sec

0.040 sec

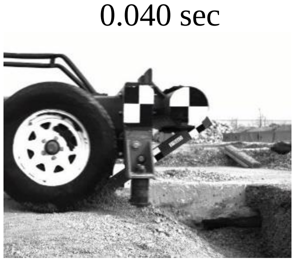

0.080 sec

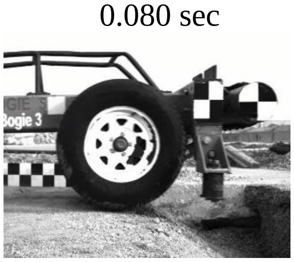

0.120 sec

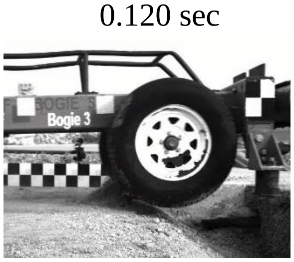

0.150 sec

Figure 33. Time-Sequential, Pretest and Post-Test Photographs, Test No. CTPS-1

7.2.2 Test No. CTPS-2

During test no. CTPS-2, the bogie impacted the MTP along its strong axis at a speed of 20.4 mph (32.9 km/h). During the impact, the post yielded and hinged below ground line. The 1.8H:1V slope sustained minimal damage as the post pushed the soil behind it down the slope. The bogie overrode the top of the post at a displacement of 44 in. (1,118 mm) as determined from the DTS data.

Force vs. deflection and energy vs. deflection curves created from the DTS accelerometer data are shown in Figure 34. Initially, inertial effects resulted in a high peak force over the first few inches of deflection. Following the inertia force, a relatively steady force of approximately 4 kips (17.8 kN) was observed through 11.5 in. (292 mm) of deflection. As the impact continued, the force gradually decreased until the bogie overrode the post at a displacement of 44 in. (1,118 mm). Sequential images from the test and pre-test and post-test photographs are shown in Figure 35.

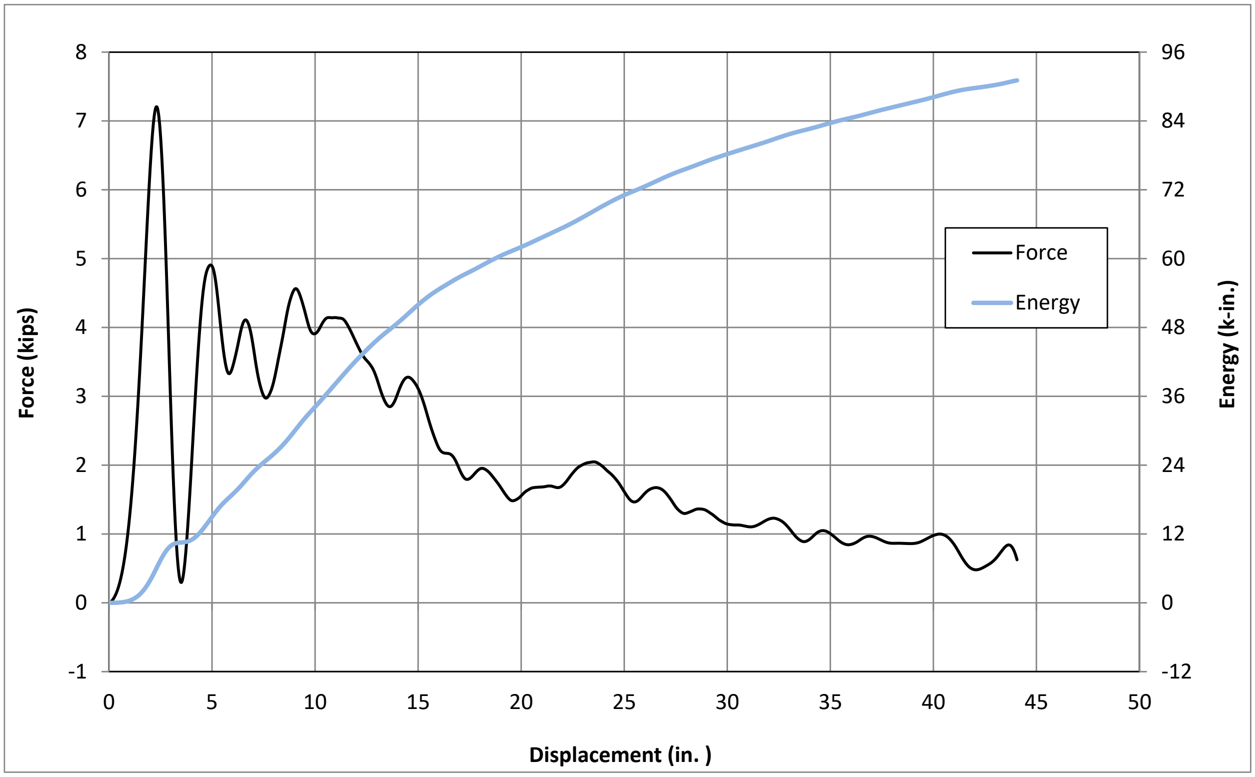

Figure 34. Force vs. Deflection and Energy vs. Deflection, Test No. CTPS-2

IMPACT

0.020 sec

0.040 sec

0.080 sec

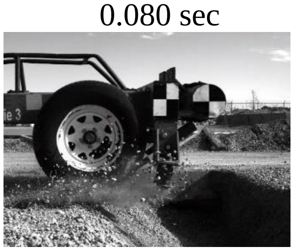

0.120 sec

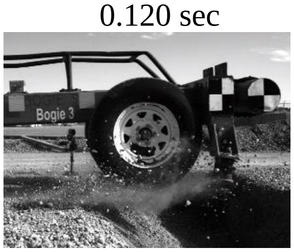

0.160 sec

Figure 35. Time-Sequential, Pretest and Post-Test Photographs, Test No. CTPS-2

7.3 Discussion

For tests nos. CTPS-1 and CTPS-2, dynamic component tests were conducted on MTPs with offset distances of 12 in. (305 mm) and 6 in. (152 mm) from the slope break point of a 1.8H:1V slope, respectively. The goal of these comparisons was to determine a minimum offset from the slope break point where the full flexural capacity of the MTP post could be developed.

The results of the dynamic component testing comparison are summarized in Table 5 and a comparison of the force versus displacement and energy versus displacement data for the post tests are shown in Figures 36 and 37. Comparison of the forces and energies from the tests found that the two tests of the MTP post adjacent to a 1.8H:1V slope developed similar average forces and energy dissipated through 10 in. (254 mm) of displacement. After 10 in. (254 mm) of post displacement, test no. CTPS-2 with the 6 in. (152mm) offset from the slope developed higher average post forces and energies.

A comparison was also made with respect to the post deformation in the two dynamic component tests. The deformed post geometries from test nos. CTPS-1 and CTPS-2 are shown in Figure 38. In test no. CTPS-1 the post hinged at groundline at the weakened area of the post section. This behavior was similar to that observed during the development of the MTP when evaluated on level terrain. Test no. CTPS-2 formed a hinge in the post below grade through the entire post section. The difference in the location of the plastic hinge in the post tests indicated that the soil resistance changed significantly with the reduced offset from the slope.

These results indicated that the forces developed by the posts and the energy absorbed were strongly related to the amount of displacement of the post deflecting through the soil. In each of the tests, the posts plastically hinged and collapsed, allowing the bogie to pass over the deflected posts. After plastic hinge collapse occurred, the force sustained by the post dropped. However, when soil plowing or displacement occurred, the post resistance was sustained over a longer duration before plastic collapse. Therefore, the weaker soil configuration of test no. CTPS-2 resulted in the highest average forces and energy absorbed through 10, 15, and 20 in. (254, 381, and 508 mm) of deflection.

While the force and energy levels were higher for the smaller post offset in these two tests, there was concern that the 6 in. (152 mm) post offset from the slope break point was transitioning the post behavior away from the behavior of the MTP post on level terrain. The post in test no. CTPS-2 caused the soil at the slope break point to heave and break out behind the post, whereas the post in test no. CTPS-1 rotated and plastically deformed in the soil with little to no damage to the slope break point. Additionally, reduced slope offset in test no. CTPS-2 resulted in plastic hinging of the post well below grade, which was a departure from the behavior of the MTP post when evaluated on level terrain. These factors led to concern that the use of a 6 in. (152 mm) offset to the slope break point may lead to inconsistent post loading and energy dissipation. Therefore, researchers recommend a minimum offset of the posts from the SBP of 12 in. (305 mm) to ensure that the behavior of the MTP post adjacent to slope was consistent with its behavior when installed on level terrain.

Table 5. Dynamic Testing Results, Test Nos. CTPS-1 and CTPS-2

Test No.	Post Description	Embedment Depth in. (mm)	Peak Force kips (kN)	Average Force kips (kN)				Energy kip-in. (kJ)					Maximum Deflection in. (mm)
				@ 5"	@ 10"	@ 15"	@ 20"	@ 5"	@ 10"	@ 15"	@ 20"	Total	
CTPS-1	HSS3x2x⅛	40 (1,106)	6.73 (30.0)	3.15 (14.0)	3.26 (14.5)	2.82 (12.5)	2.51 (11.2)	15.8 (1.78)	32.6 (3.68)	42.3 (4.78)	50.2 (5.67)	70.9 (8.01)	40.0 (1,016)
CTPS-2	HSS3x2x⅛	40 (1,106)	7.20 (32.0)	3.02 (13.4)	3.42 (15.2)	3.47 (15.4)	3.10 (13.8)	15.1 (1.71)	34.2 (3.87)	52.0 (5.87)	62.1 (7.01)	91.1 (10.29)	44.0 (1,118)

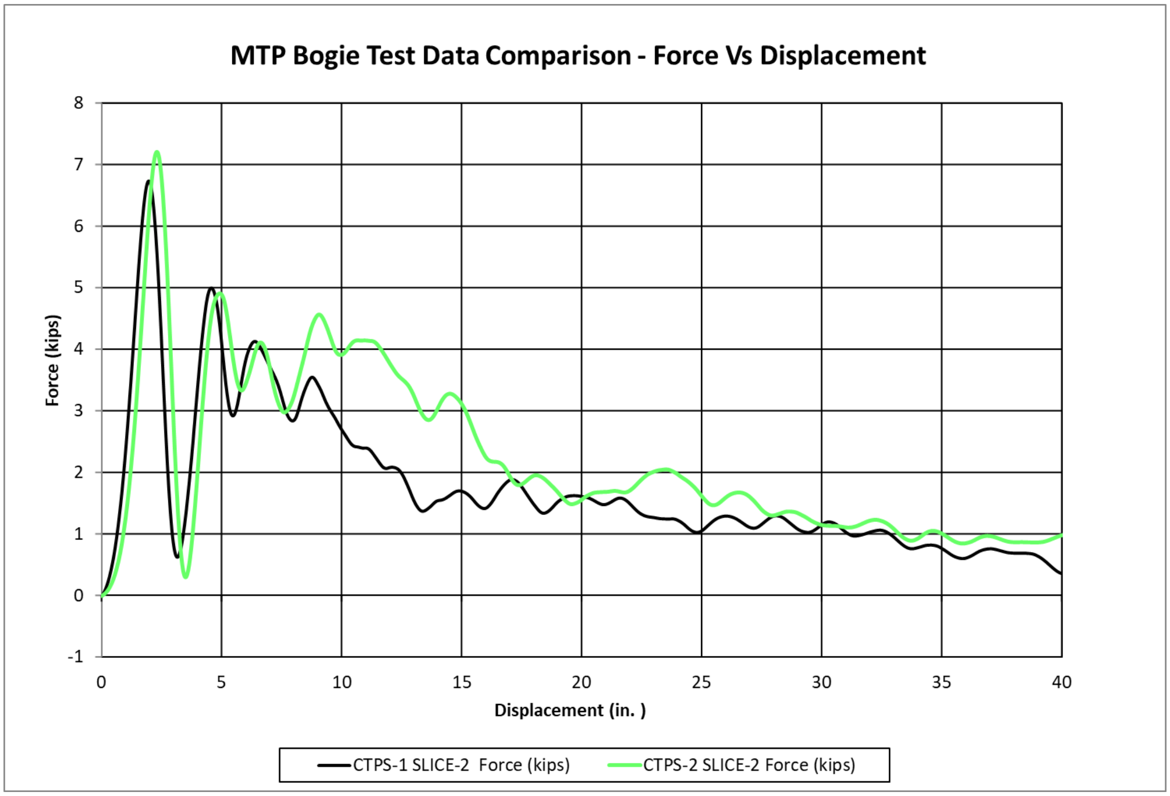

Figure 36. Force-Displacement Comparison, Test Nos. CTPS-1 and CTPS-2

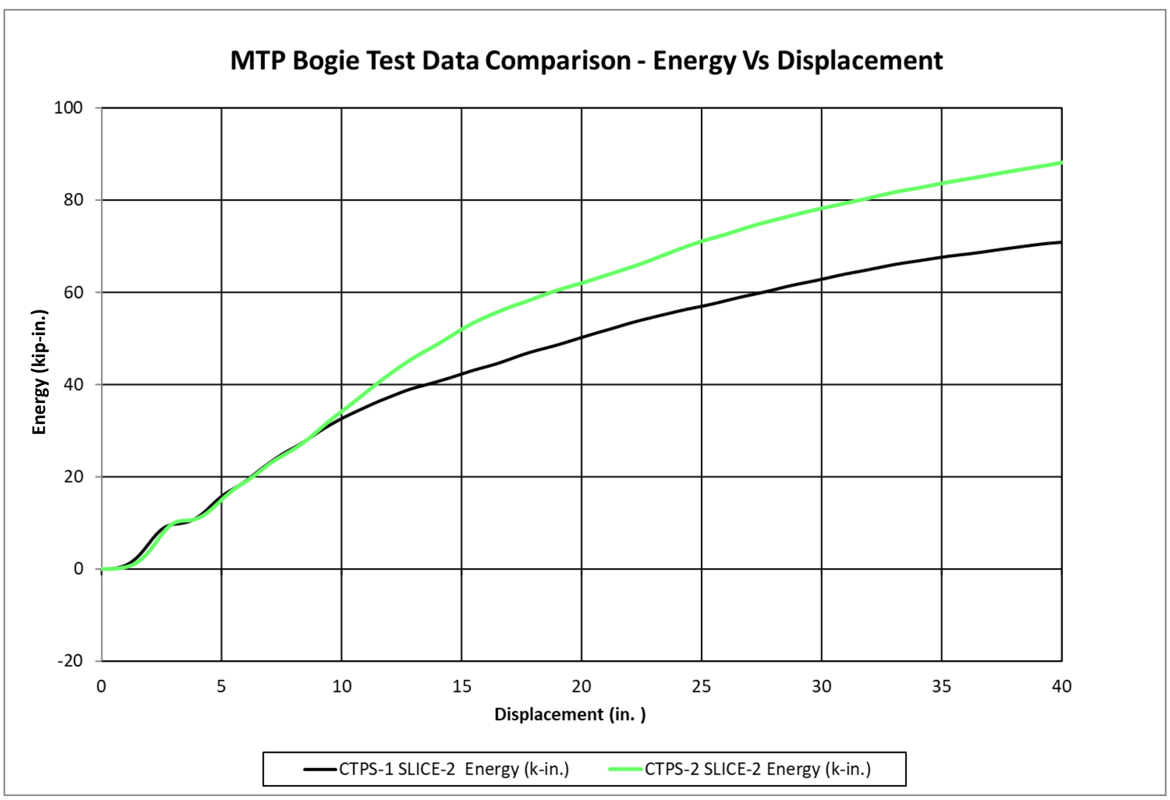

Figure 37. Energy vs. Deflection Comparison, Test Nos. CTPS-1 and CTPS-2

Figure 38. Comparison of Deformed Posts Shapes, Test Nos. CTPS-1 (Top) and CTPS-2 (Bottom)

8 LOW-TENSION CABLE BARRIER SIMULATION MODELING

The finite element analysis (FEA) software LS-DYNA [14] was used to develop and evaluate potential design configurations for the revised, low-tension cable system adjacent to slopes as steep as 1.8H:1V. In order to evaluate potential design configurations with LS-DYNA, several computer simulation modeling efforts has to be undertaken. First, vehicle models for both the NCHRP Report 350 and MASH pickup truck vehicles were collected for use in calibration of a cable barrier models and simulation of new design configurations. Models of the various components of the previous low-tension cable barrier and the proposed low-tension cable barrier were then acquired from previous research efforts or developed and validated as part of this research effort. Next simulation models of test nos. CS-1 and CS-2 on the original low-tension cable barrier adjacent to slope were developed and validated in order to provide confidence in modeling of new design alternatives. Finally, LS-DYNA models of alternative low-tension cable barrier adjacent to steep slopes were simulated with variation of post spacing, cable heights, and slope offset to determine if a revised barrier design could be developed that was capable of meeting MASH TL-3. The simulation results were summarized, and configurations which were believed to have the highest likelihood of passing MASH TL-3 were identified. Details on the various components of the LS-DYNA simulation efforts are provided in subsequent sections.

8.1 Vehicle Models

In order to model the original cable barrier system adjacent to steep slopes and the proposed modified designs, two vehicle models were required. The original cable barrier adjacent to slopes was evaluated under NCHRP Report 350 TL-3. As such, the development and validation of the barrier model for that system required a model of the 2000P vehicle used in NCHPR Report 350 and crash test nos. CS-1 and CS-2. As the objective of this research effort was development of a MASH TL-3 low-tension cable barrier adjacent to steep slopes, simulation of potential design modifications required the use of a MASH 2270P vehicle model.

For the 2000P vehicle, the researchers used a modified model of a Chevrolet C2500 pickup truck originally developed at the National Crash Analysis Center (NCAC). The Chevrolet C2500 pickup is compliant with the 2000P pickup truck vehicle described in NCHRP Report 350. MwRSF has revised and refined the model of the Chevrolet C2500 pickup truck over the years to include improvements in the model mesh, steering and suspension, tires, contacts, and other model features. This model had been calibrated and validated in many simulation efforts at MwRSF prior to the adoption of the MASH safety. The UNL Chevrolet C2500 pickup truck model used in simulations of test nos. CS-1 and CS-2 is shown in Figure 39.

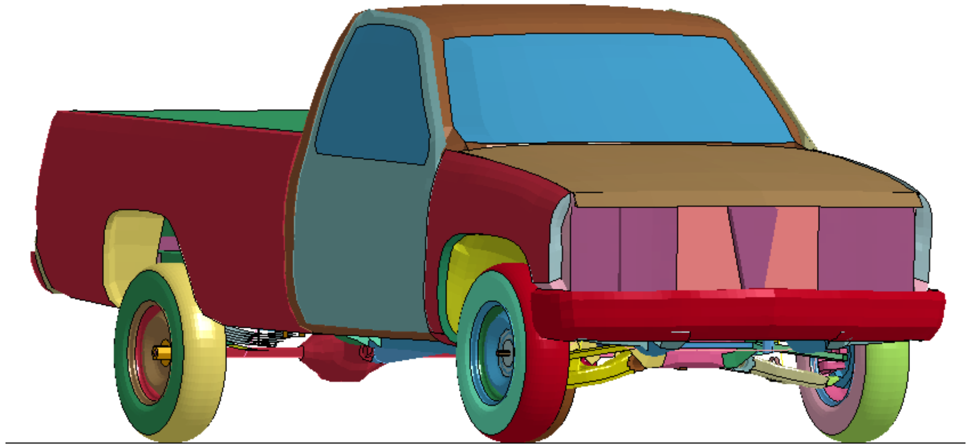

Figure 39. 2000P Chevrolet C2500 Pickup Truck Model used to Simulate Test Nos. CS-1 and CS-2

For the MASH TL-3 simulations of the revised low-tension cable barrier adjacent to steep slopes, a 2007 Chevrolet Silverado half-ton, quad cab pickup truck model, first produced by NCAC and modified at MwRSF, was used. This pickup model is approximately consistent with the MASH 2270P pickup truck and has been used to investigate the performance of a variety of roadside hardware systems under MASH impact conditions. MwRSF has developed three primary versions of the Chevrolet Silverado vehicle model. Version 2 (V2), Version 3 (V3), and Version 3 – Reduced (V3r). All three versions of the vehicle model represented the same Chevrolet Silverado quad cab vehicle, but there were differences in the tires, steering, vehicle-to-ground friction, and mesh size, among other factors. The UNL V3r model was used for the simulation analysis in this study.

Early simulation results suggested that the MwRSF Silverado pickup truck model did not have a stable interaction with the beam element cable model. The model was subsequently revised by adding null-material beam elements with a 0.08-in. (2-mm) diameter to every free shell edge of the truck on the impact side. These beams were included in the contact definition with the wire rope beam elements, which significantly improvement the vehicle contact and model stability for the simulations. An image of the revised MwRSF truck model with contact beam elements is shown in Figure 40. Similar beam elements were added to the C2500 model as well.

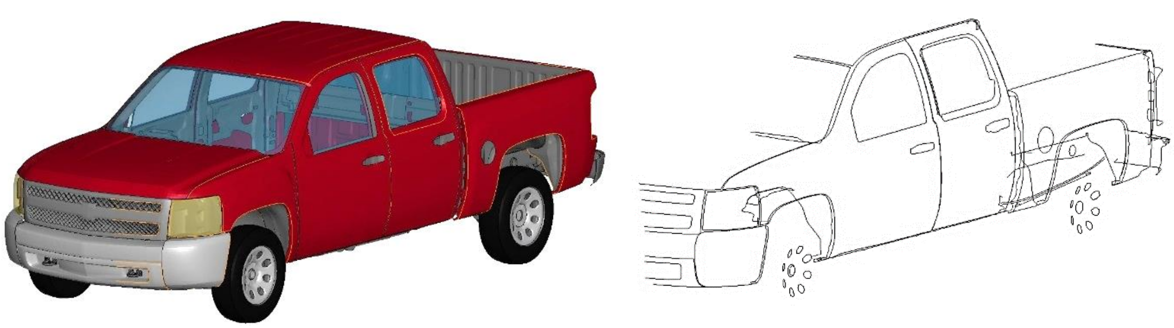

Figure 40. MwRSF Revised 2270P Model (2007 Chevrolet Silverado Quad Cab)

8.2 Cable Barrier Component Models

Models of the major components of the low-tension cable barrier system adjacent to steep slope were either collected from previous research or developed and validated as part of this study. The low-tension cable barrier components required for the simulation modeling effort included (1) a S3x5.7 steel post; (2) an HSS3x2x⅛ tubular post; (3) ⁵⁄₁₆-in. (8-mm) diameter J-bolt cable-to-post attachments; and (4) 3x7 wire rope or cable. Details on the various low-tension cable barrier model components are outlined below.

8.2.1 S3x5.7 Post Models

The first component model developed for the low-tension cable barrier simulation was a model of the S3x5.7 post used in the original low-tension cable barrier adjacent to slope. In order to develop a model of the S3x5.7 post, the researchers validated models of the S3x5.7 post in a rigid sleeve to confirm the model's ability to simulate the response of solely the steel post in flexure along the strong and weak axis. Impacts to the post in soil were also simulated and validated to provide an adequate component model for simulation of test nos. CS-1 and CS-2.

The first component model of the S3x5.7 post consisted of simulation of a typical dynamic bogie test on the weak and strong axis of the post in a rigid sleeve. The impact simulation was setup to mimic previous strong- and weak-axis testing of S3x5.7 posts in rigid sleeves. Several previous dynamic component tests would serve as baselines for comparison with the simulation models. Test nos. CMPB-4 [15] and CP-4B [16] served as baseline models for the strong-axis impacts, and test no. CCP-5 [17] served as a baseline for the weak-axis impact. The model inserted the S3x5.7 post in a fixed sleeve made of shell elements with a rigid material definition and impacted the post with a simple impactor with a geometry similar to the impact head used for bogie testing at MwRSF. The simple impactor was defined with the mass and impact velocity of typical bogie tests. The basic rigid sleeve simulation setups are shown in Figure 41.

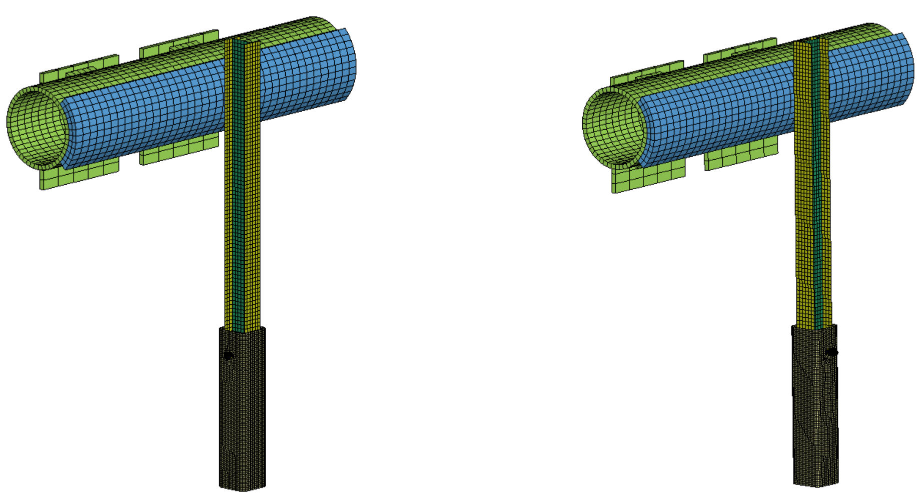

Figure 41. S3x5.7 Post in Rigid Sleeve Impact Simulation Setup

A model of the S3x5.7 post geometry was developed using 2-D shell elements. The post material was modeled with properties for ASTM A992 steel using MAT_24 ins LS-DYNA. Thin section metal components are typically modeled with shell elements with constant thickness in LS-DYNA. However, the S3x5.7 posts used in the original low-tension cable barrier do not have a consistent flange thickness. As such, two potential modeling techniques were considered for better representing the S3x5.7 post flange with shell elements: (1) the post flange was modeled with a constant-thickness shell element with a thickness representing the average thickness of the post flange; and (2) a variable thickness flange that used variable shell thickness across the flange to better represent the flange thickness variation. These two options are shown in Figure 42. Simulation of the two flange modeling options found only minimal difference in the behavior of the post. Thus, modeling of the post flange with a constant-thickness shell element with a thickness representing the average thickness of the post flange was selected for further modeling as it was simple in terms of model setup and the contact algorithm.

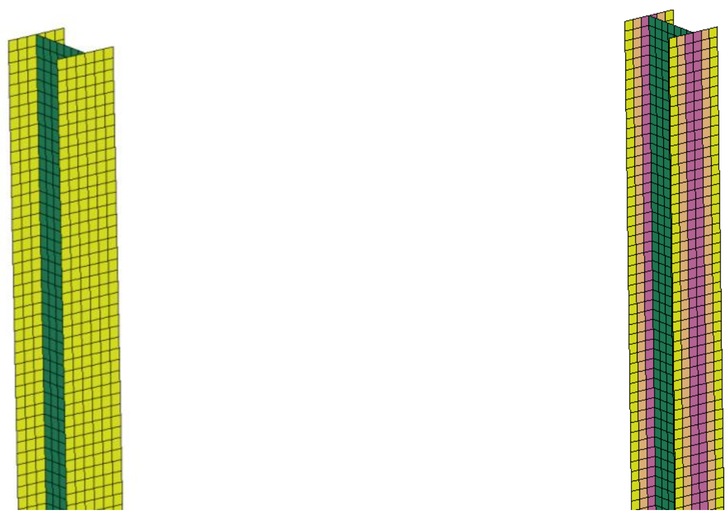

(a) Average Flange Thickness (b) Variable Flange Thickness

Figure 42. S3x5.7 Post Flange Modeling Options

The simulation results from the strong- and weak-axis S3x5.7 posts models in a rigid sleeve are shown graphically in Figures 43 and 44. Comparisons of the force versus deflection and energy versus deflections for the strong-axis simulation and baseline comparison tests, test nos. CP-4B and CMPB-4, are shown in Figures 45 and 46, respectively. Comparisons of the force versus displacement and energy versus displacement for the weak-axis simulation and baseline comparison test, test no. CCP-5, are shown in Figures 47 and 48, respectively. Simulation of the strong-axis impact on the S3x5.7 post found reasonably good correlation with the available dynamic component test data. The force versus displacement and energy versus displacement curves from the simulation fell directly between the values of the test nos. CP-4B and CMPB-4. Similarly, the simulation of the S3x5.7 post in the weak axis correlated very well with the force and energy levels observed in test no. CCP-5. The positive correlation of strong- and weak-axis simulations to the physical test data led the researchers to believe that the LS-DYNA model of the 3x5.7 post was capable of accurately reproducing the behavior of the steel section when loaded dynamically.

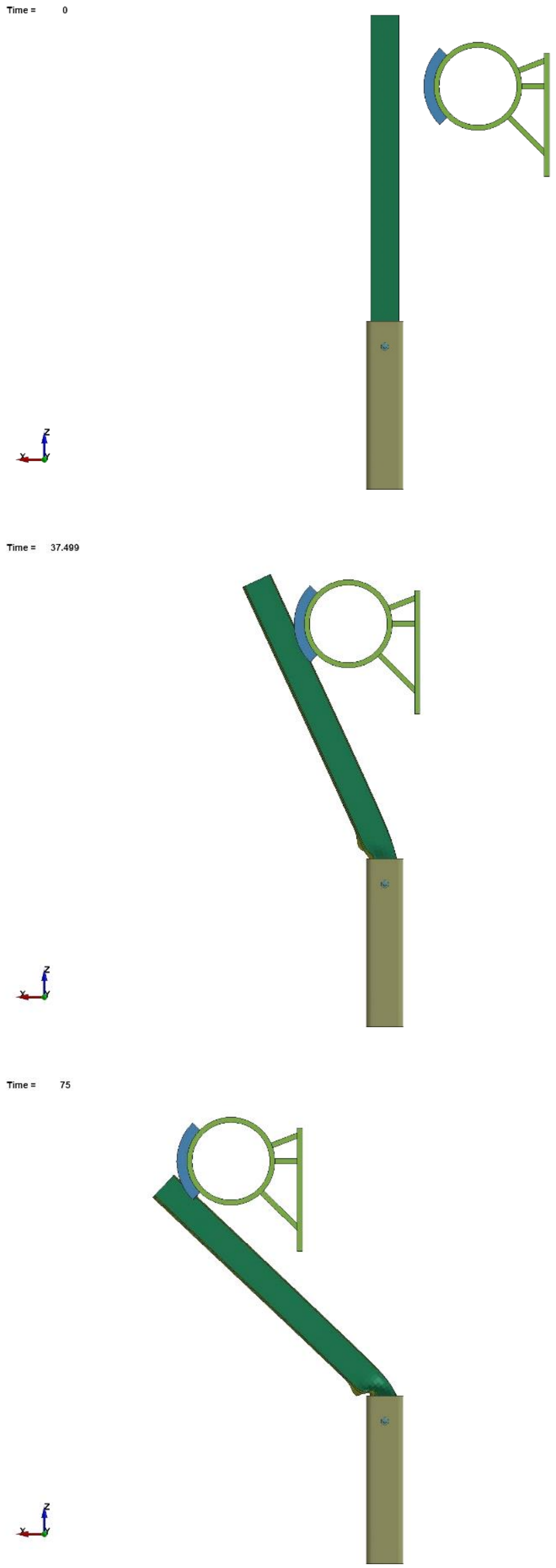

Figure 43. Simulation of Strong-Axis Impact of S3x5.7 Post in Rigid Sleeve

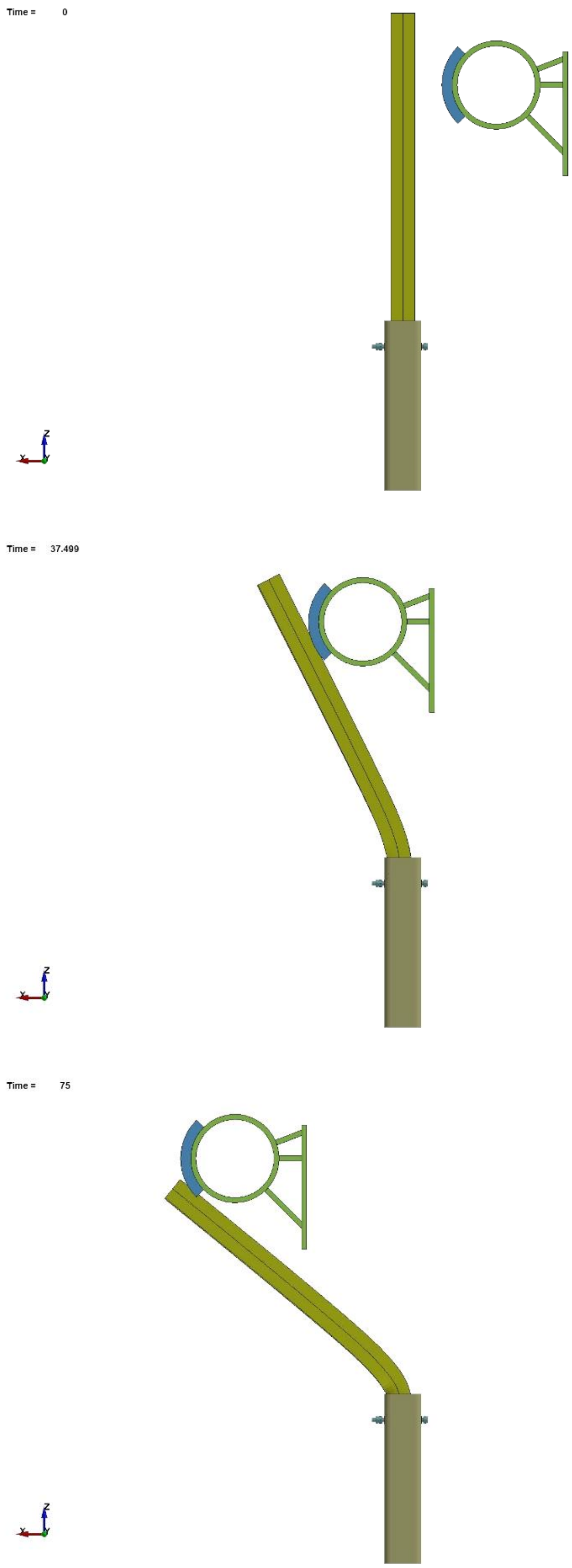

Figure 44. Simulation of Weak-Axis Impact of S3x5.7 Post in Rigid Sleeve

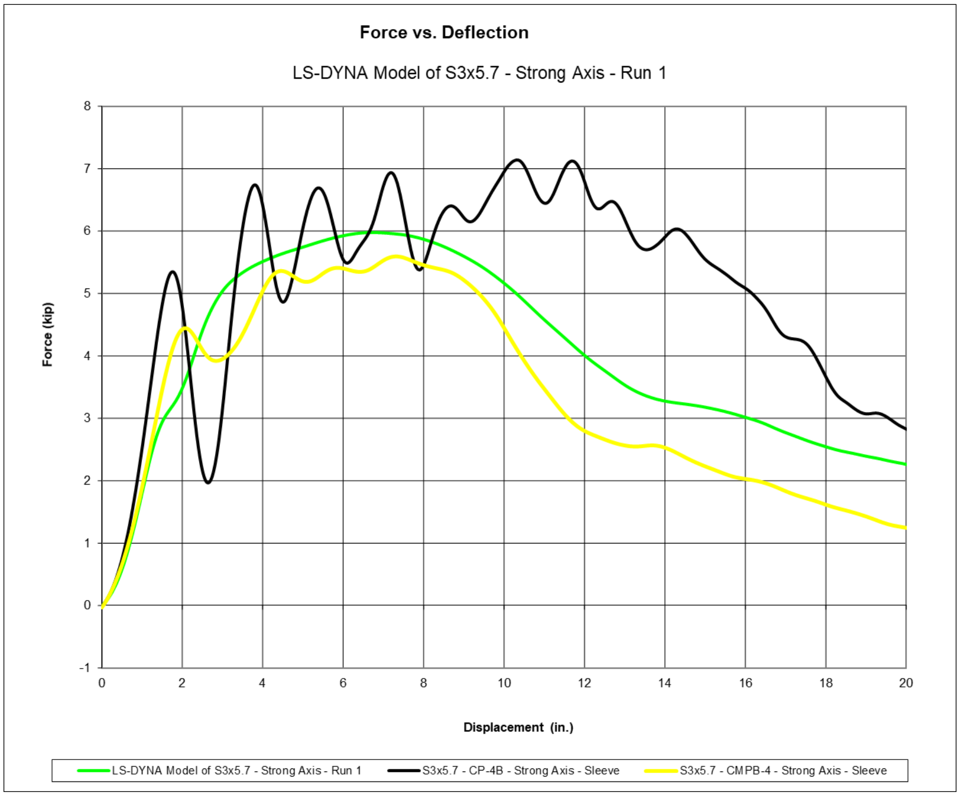

Figure 45. Force vs. Displacement Comparison, Strong-Axis of S3x5.7 Post in Rigid Sleeve

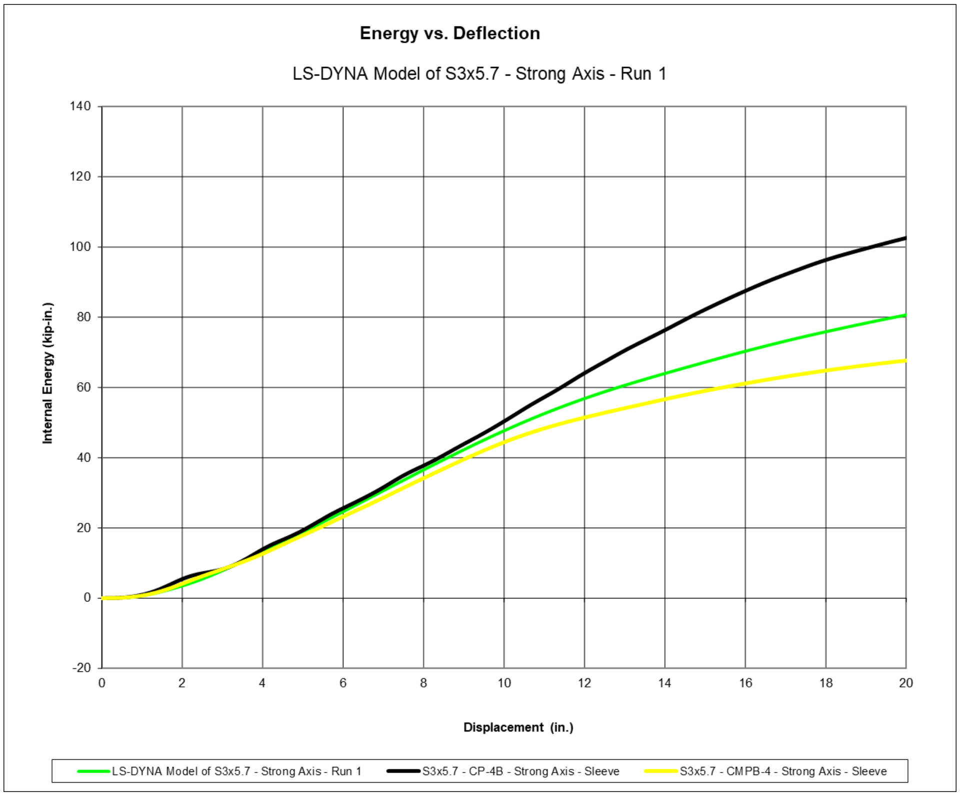

Figure 46. Energy vs. Displacement Comparison, Strong-Axis of S3x5.7 Post in Rigid Sleeve

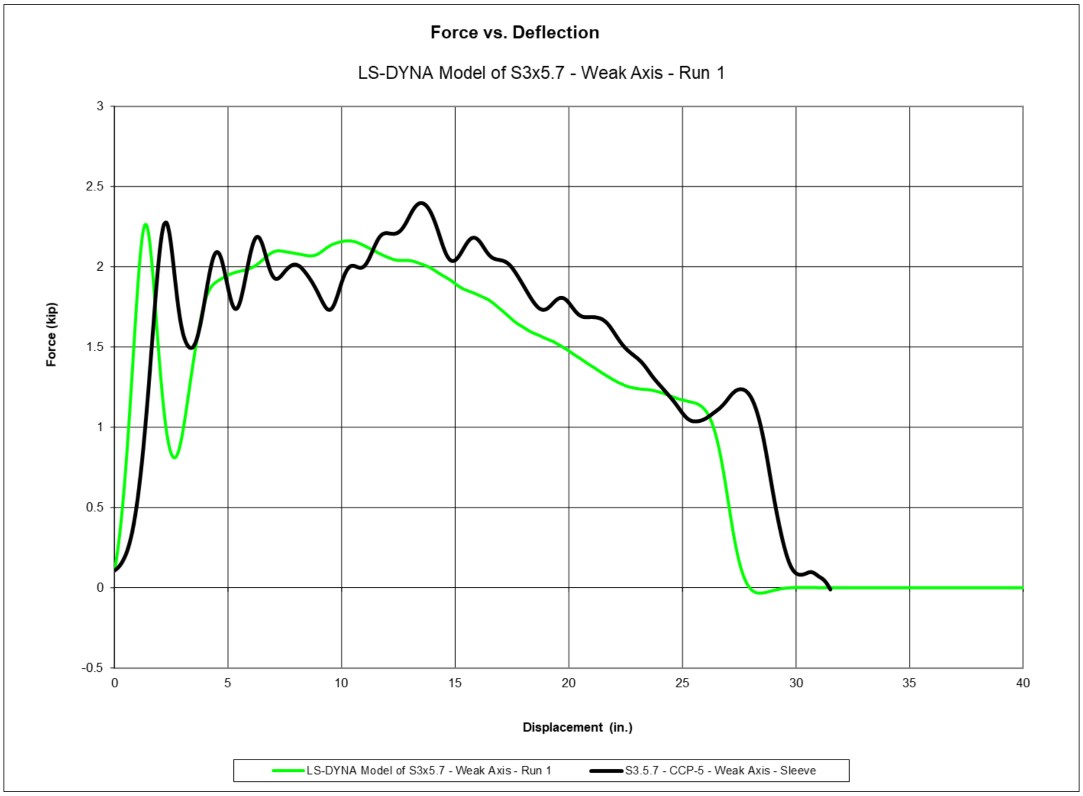

Figure 47. Force vs. Displacement Comparison, Weak-Axis of S3x5.7 Post in Rigid Sleeve

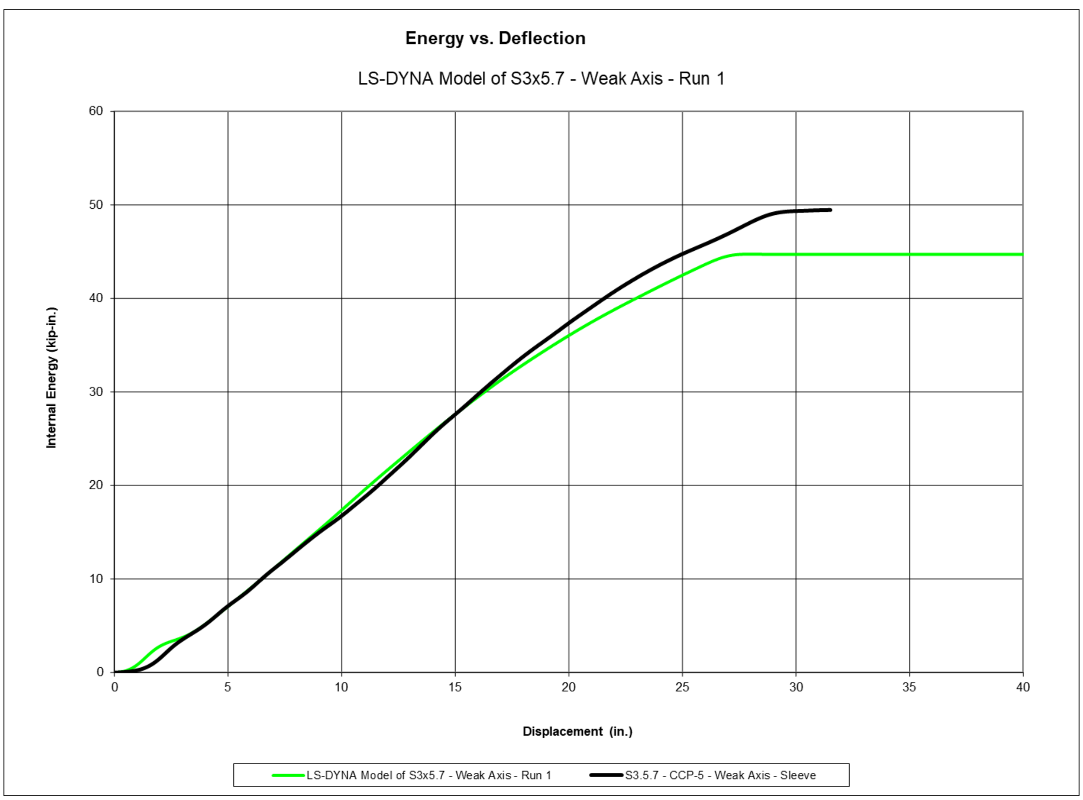

Figure 48. Energy vs. Displacement Comparison, Weak-Axis of S3x5.7 Post in Rigid Sleeve

A second series of strong-axis simulations were conducted on the S3x5.7 post with a simulated soil resistive force to ensure that the post could be used to replicate lateral barrier stiffness and deflection of test nos. CS-2. Weak-axis simulation was not conducted as weak-axis post testing in soil was not available. Additionally, S3x5.7 posts impacted along their weak axis tend to displace very little in soil during full -scale crash testing prior to yielding, which would indicate that the simulation of the weak-axis impact in soil was less critical. Simulation of the soil response was done using a tube of rigid elements around the base of the tube that was supported by discrete spring elements providing the soil resistive force. The top of the rigid tube was flared slightly to allow for more gradual bending and flexure of the post without an abrupt stress concentration at ground line. The force versus displacement curves for the soil springs were taken from baseline soil testing performed on soil as part of the MASH soil criteria for full-scale crash testing using W6x16 posts with a 40 in. (1,016 mm) embedment depth. The baseline soil response curve was then adjusted for the post section along both the strong- and weak-axis to provide a soil response for the S3x5.7 post. Note that the post simulation did not include a soil plate. The effect of the soil plate was compensated for by not scaling the soil forces on the S3x5.7 post section for the 25 percent reduction in embedment of the S3x5.7 post used in the test no. CS-2. Simulation of the post impact used a similar impactor as the previous simulations in a rigid foundation. The basic simulation setup is shown in Figure 49. Test nos. LTCB-1 and LTCB-2, strong-axis impacts of S3x5.7 posts in soil on level terrain conducted earlier in this research, served as baselines for the strong-axis impact simulations and were used to determine the accuracy of the model.

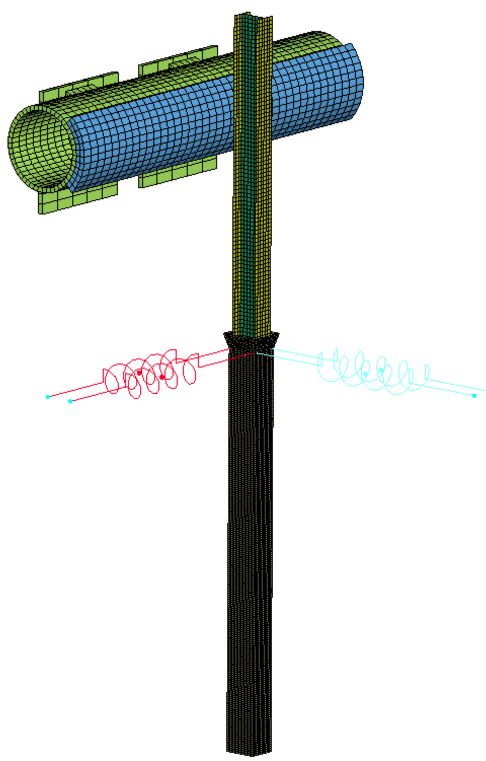

Figure 49. S3x5.7 Post in Soil Strong-Axis Simulation Setup

The simulation results from the strong-axis S3x5.7 post model in a soil are shown graphically in Figure 50. Comparisons of the force versus displacement and energy versus displacement for the strong-axis simulation and baseline comparison tests, test nos. LTCB-1 and LTCB-2, are shown in Figures 51 and 52, respectively. Simulation of the strong-axis impact on the S3x5.7 post in soil found good correlation with the available dynamic component test data. Post deformations were also similar between the test and the simulation. The simulated force versus displacement compared very well to the tests through the entire post displacement. Corresponding energy dissipation of the post also correlated very well with the physical tests. The positive correlation of strong-axis simulation to the physical test data suggested that the soil-spring model used could accurately simulate the response of the S3x5.7 post with soil plate used in test no. CS-2.

It should be noted that test no. CS-1 used the same post configuration as test no. CS-2, but it had a reduced lateral offset of the post relative to the slope break point of 12 in. (305 mm). This reduction in the post offset reduced the soil resistive forces on the post which allowed the posts in that test to deflect and rotate out of the soil on the slope. In order to simulate this behavior, the soil-spring model forces were scaled down 29 percent and the spring displacements were scaled down 50 percent. This reduced soil response was determined based on calibration of the full-scale test simulations of test no. CS-1 which will be discussed further in a subsequent section.

Figure 50. Simulation of Strong-Axis Impact of S3x5.7 Post in Soil

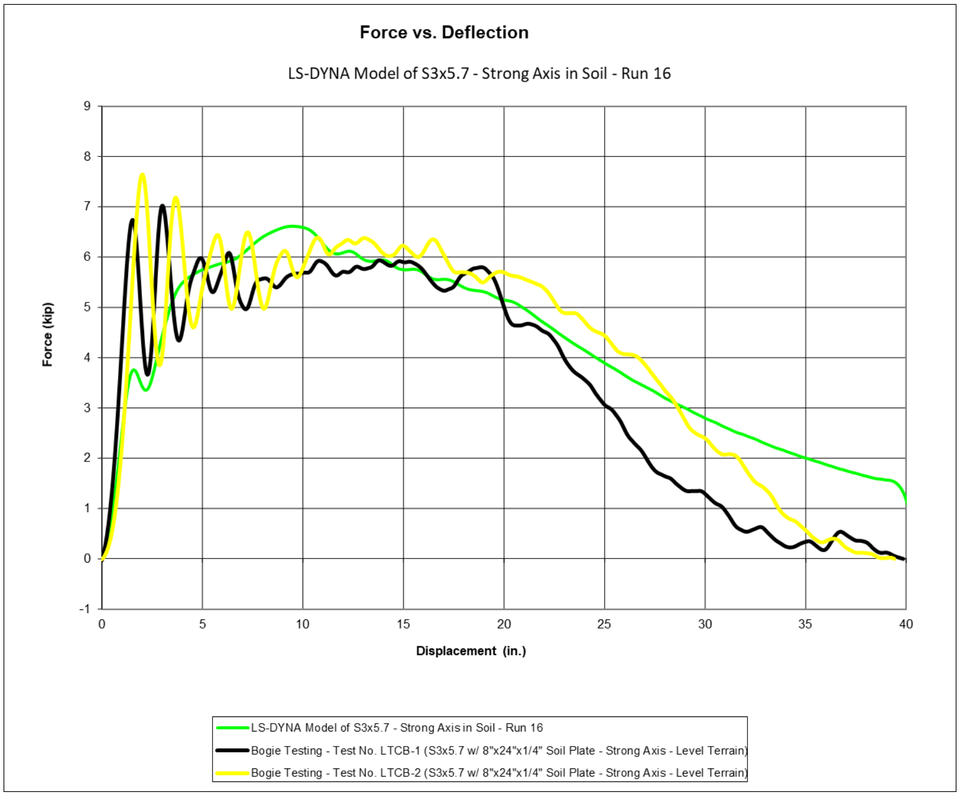

Figure 51. Force vs. Displacement Comparison, Strong-Axis of S3x5.7 Post in Soil

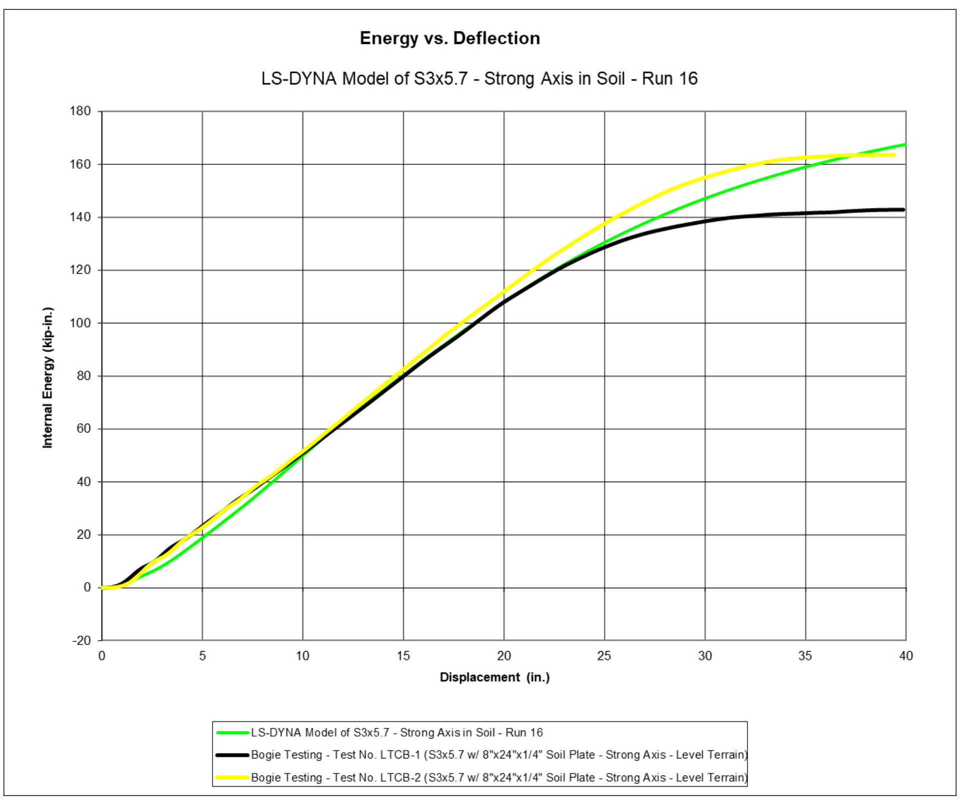

Figure 52. Energy vs. Displacement Comparison, Strong-Axis of S3x5.7 Post in Soil

8.2.2 HSS3x2x⅛ Post

As noted previously, the revised low-tension cable barrier adjacent to steep slope design intended to use the MTP post section to mitigate concerns for floorboard tearing and penetration. As such, simulation of design configurations using this post required that an accurate component model of the MTP post be developed. The MTP model development was similar to the methodology used for the development of the S3x5.7 post model. Models of the MTP post in a rigid foundation and in soil were developed and calibrated against available physical testing of the MTP post.

The first component model of the MTP post consisted of simulation of a dynamic bogie test on the weak and strong axis of the post in a rigid sleeve. The impact simulation was setup to mimic previous strong- and weak-axis testing of MTP posts in rigid sleeves. Test no. CTPB-19 served as a baseline model for the strong-axis impact, and test no. CTPB-16 served as a baseline for the weak-axis impact [12]. The model inserted the MTP post in a fixed sleeve made of shell elements with a rigid material definition and impacted the post with a simple impactor with a geometry similar to the impact head used for bogie testing at MwRSF. The simple impactor was defined with the mass and impact velocity of typical bogie tests. Note that the impact height for the strong- and weak-axis simulations were adjusted to match the setup for test nos. CTPB-19 and CTBP-16. A model of the MTP post geometry was developed using 2-D shell elements. The post material was modeled with properties for ASTM A500 Grade B steel using MAT_24 in LS-DYNA. The basic rigid sleeve simulation setups are shown in Figure 53.

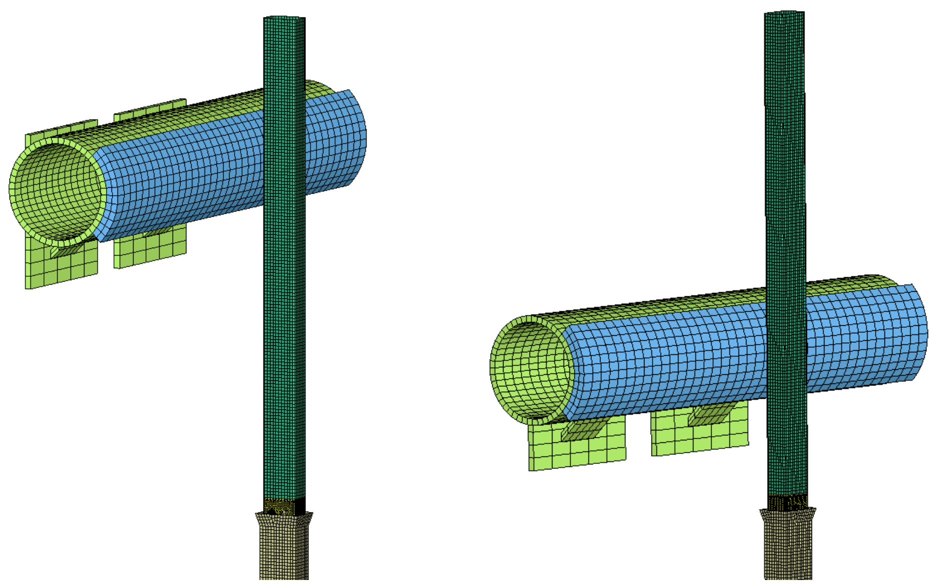

Figure 53. MTP Post in Rigid Sleeve Impact Simulation Setup

The simulation results from the strong- and weak-axis MTP posts models in a rigid sleeve are shown graphically in Figures 54 and 55, respectively. Comparisons of the force versus displacement and energy versus displacement for the strong-axis simulation and baseline test, test no. CTPB-19, are shown in Figures 56 and 57, respectively. Comparisons of the force versus displacement and energy versus displacement for the weak-axis simulation and baseline test, test no. CTPB-16, are shown in Figures 58 and 59, respectively. Simulation of the strong-axis impact on the MTP post found good correlation with the available dynamic component test data. The force versus displacement and energy versus displacement curves from the simulation were very similar to test no. CTPB-19 throughout the displacement of the post. The simulation of the MTP post in the weak axis correlated well with the force and energy levels observed in test no. CTPB-16 during the initial 5 in. (127 mm) of post

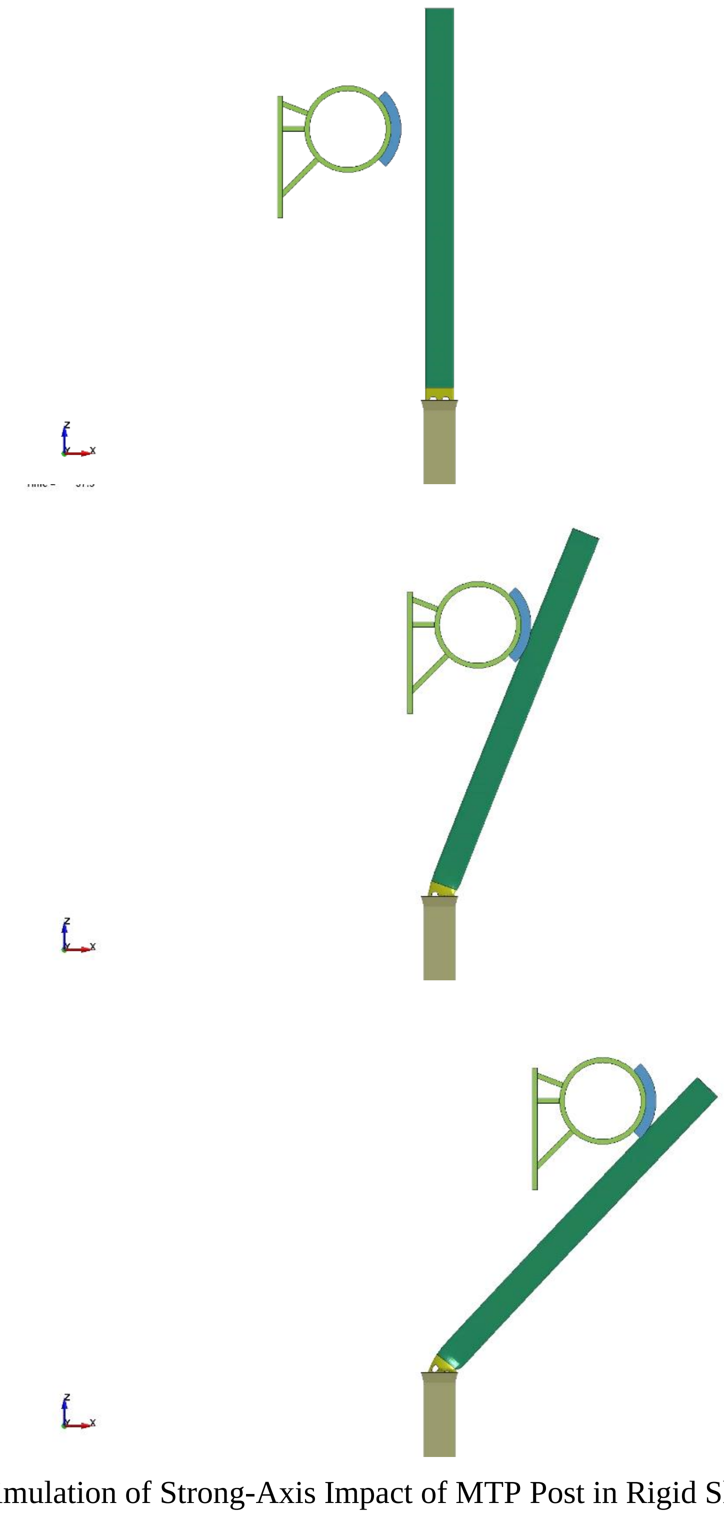

Figure 54. Simulation of Strong-Axis Impact of MTP Post in Rigid Sleeve

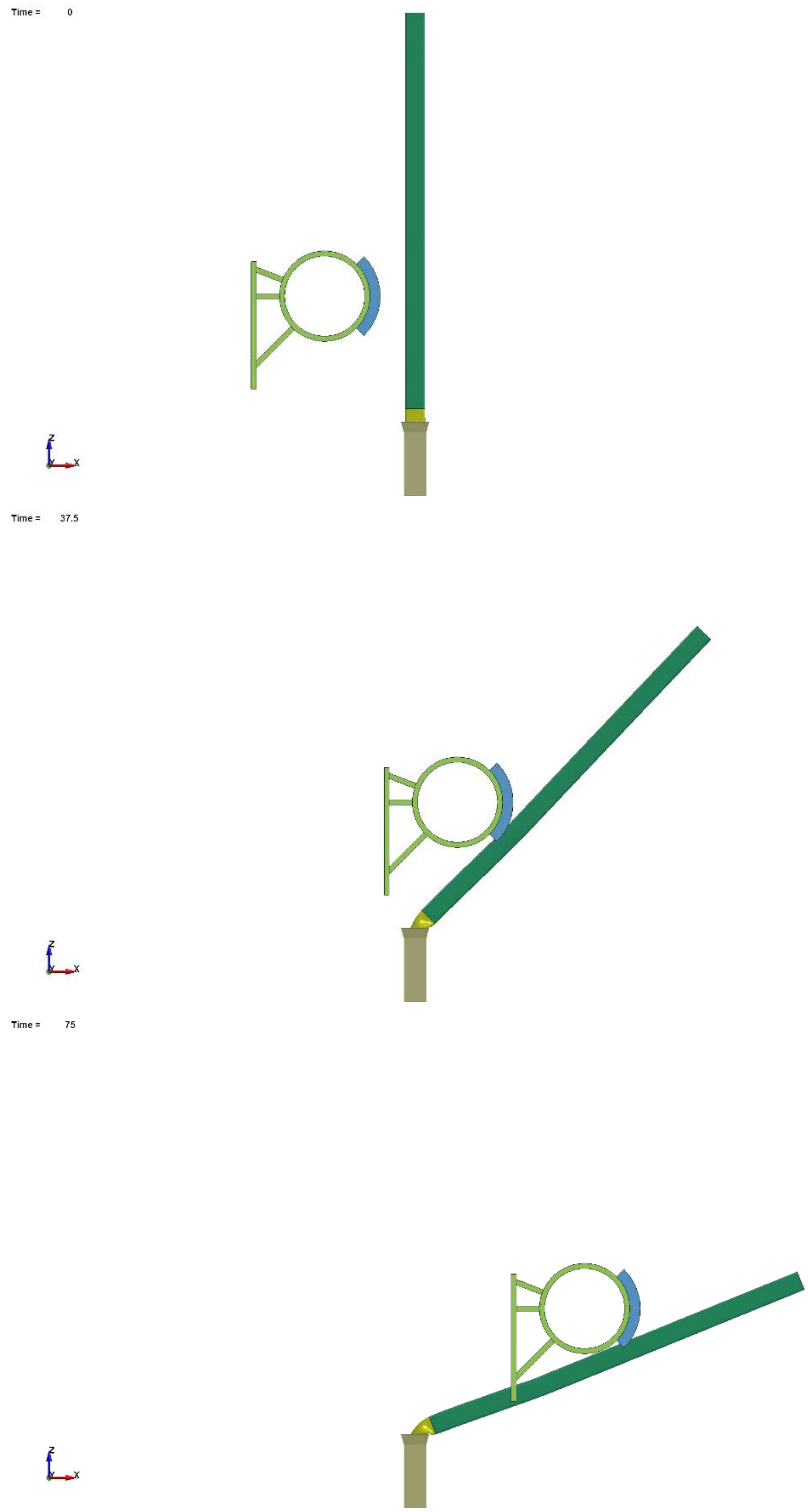

Figure 55. Simulation of Weak-Axis Impact of MTP Post in Rigid Sleeve

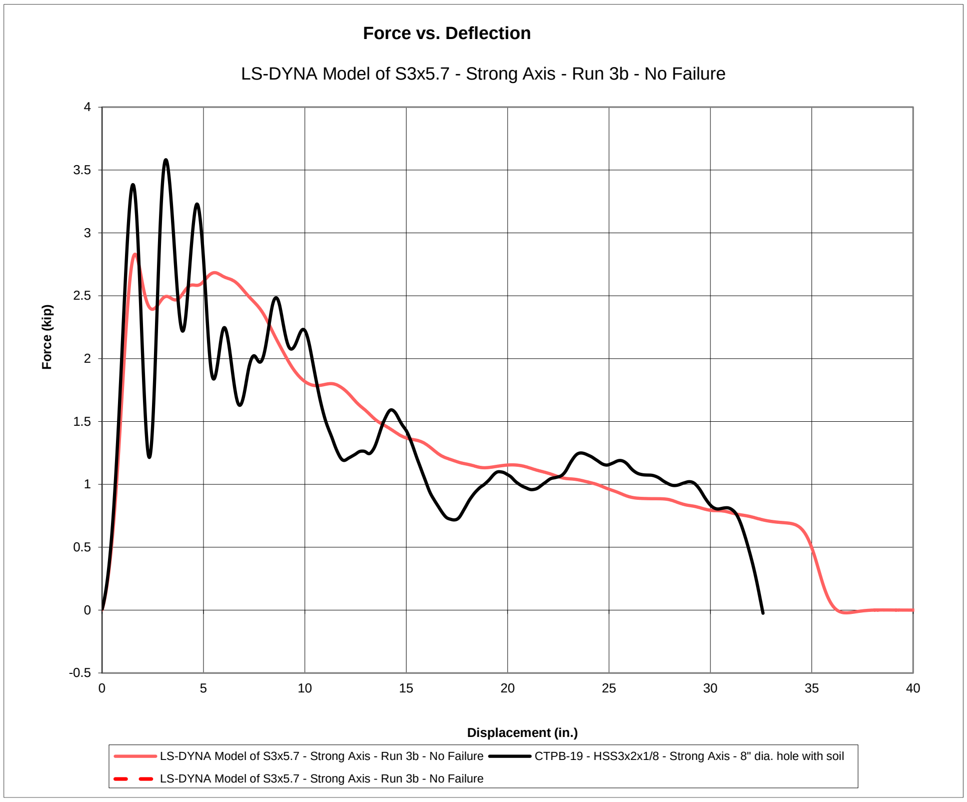

Figure 56. Force vs. Displacement Comparison, Strong-Axis of MTP Post in Rigid Sleeve

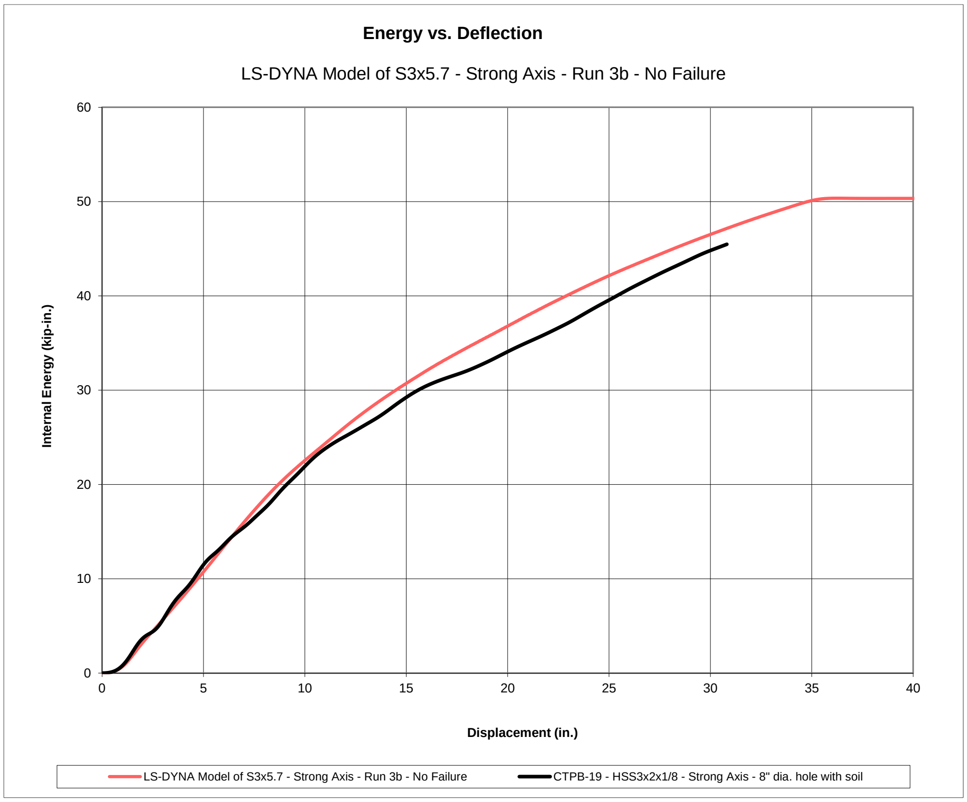

Figure 57. Energy vs. Displacement Comparison, Strong-Axis of MTP Post in Rigid Sleeve

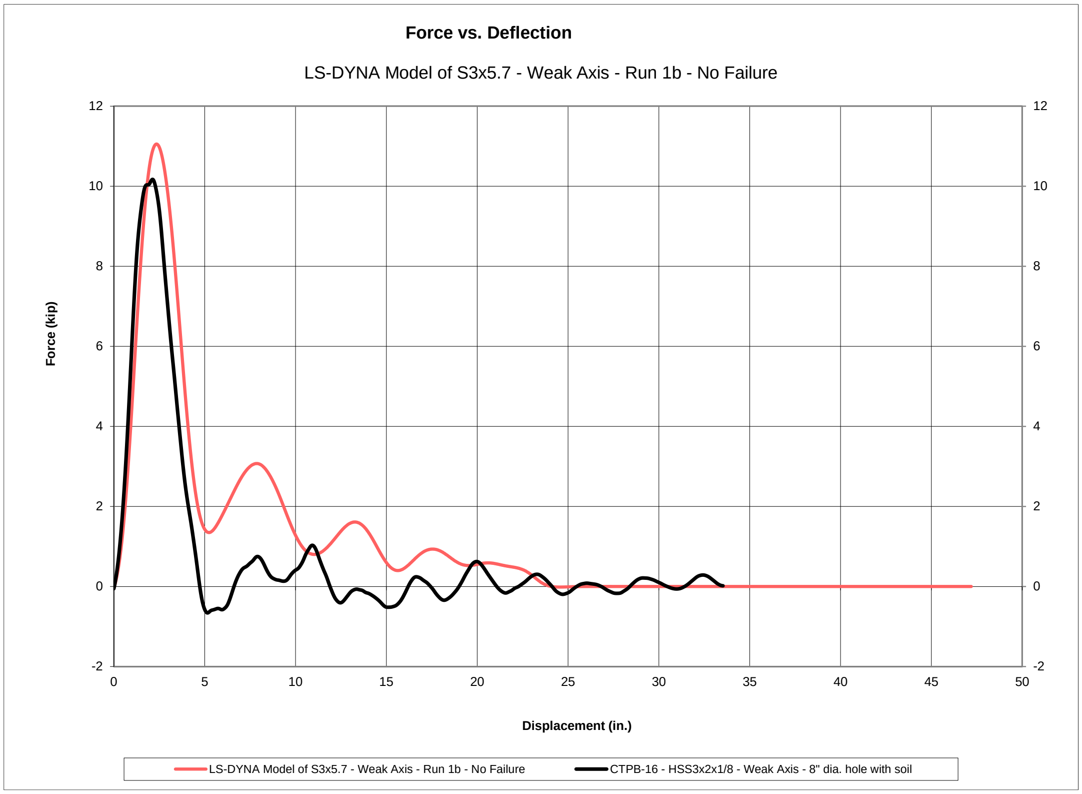

Figure 58. Force vs. Displacement Comparison, Weak-Axis of S3x5.7 Post in Rigid Sleeve

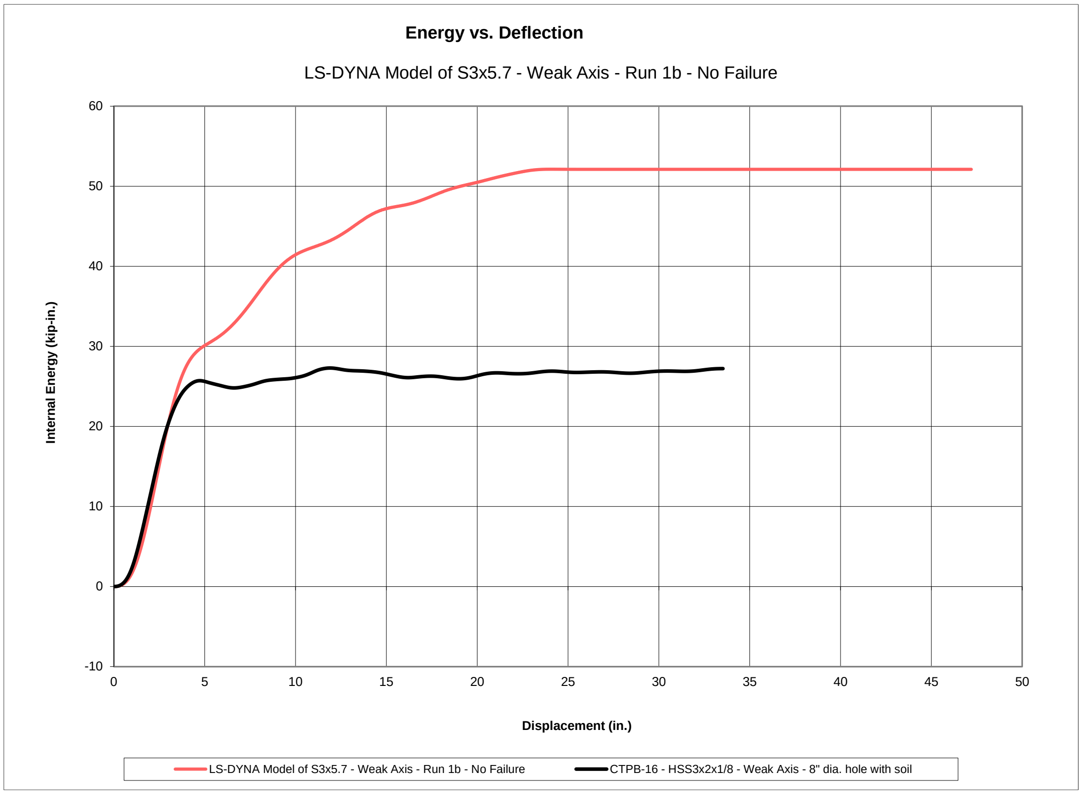

Figure 59. Energy vs. Displacement Comparison, Weak-Axis of S3x5.7 Post in Rigid Sleeve

displacement. After the initial 5 in. (127 mm) of post displacement, the force levels in test no. CTPB-16 dropped to zero, while the simulation post still developed load as the post displaced. The difference between the test and simulation behavior was linked to the fracture of the post at the weakening holes. In the physical test, the post section fractured at ground line due to the weakening holes added the to the post section, as shown in Figure 60. The simulation model of the MTP did not have failure strain criteria defined, and failure of the post did not occur in the simulation model. Simulation models with failure strain included were attempted in both strong- and weak-axis impact orientations. However, the iterations of these model suffered from an inability to accurately capture the fracture during weak-axis impacts, or the model would induce incorrect post fracture during the strong axis simulations. Because the initial force and displacement of the post in the weak-axis simulation correlated well with the test data and the implementation of failure strain criteria in the model did not improve the simulation performance, it was decided to move forward with the existing post model in for the MTP post in soil simulations.

Figure 60. MTP Post Fracture in Weak-Axis Impact, Test No. CTPB-16

A second series of strong-axis simulations were conducted on the MTP post with a simulated soil resistive force to ensure that the post could be used to predict lateral barrier stiffness and deflection of test no. CS-2. Weak-axis simulation was not conducted MTP posts impacted along their weak axis tend to displace very little in soil, which would indicate that the simulation of the weak-axis impact in soil was less critical. Simulation of the soil response was done using a tube of rigid elements around the base of the tube that was supported by discrete spring elements providing the soil resistive force. The top of the rigid tube was flared slightly to allow for more gradual bending and flexure of the post without an abrupt stress concentration at ground line. The force versus displacement curves for the soil springs were taken from baseline soil testing performed on soil as part of the MASH soil criteria for full-scale crash testing using W6x16 posts with a 40 in. (1,016 mm) embedment depth. The baseline soil response curve was then adjusted for the post section along both the strong- and weak-axis to provide a soil response for the MTP. Note that soil forces were scaled by 0.6 to account for the placement of the post at a 12-in. (305-mm) offset from the slope break point. Simulation of the post impact used a similar impactor as the previous simulations in a rigid foundation. The basic simulation setup is shown in Figure 61. Test nos. test nos. CTPS-1, a strong-axis impact of the MTP in soil at a 12-in. (305-mm) offset from the slope break point, conducted earlier in this research, served as the baseline comparison for the strong-axis impact simulation of the MTP in soil.

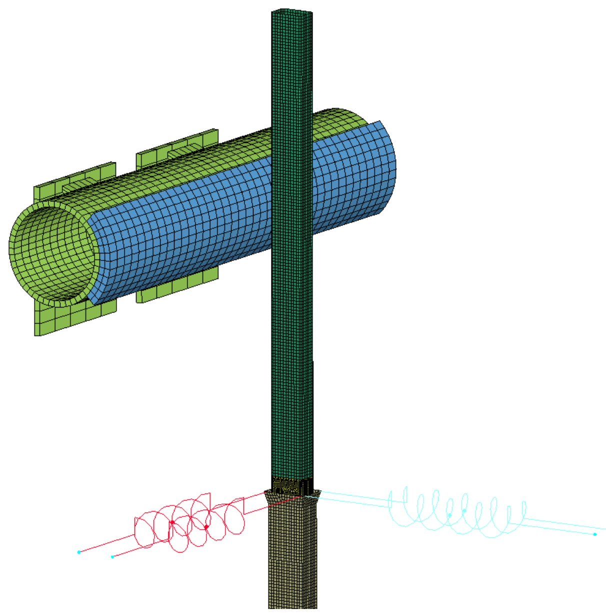

Figure 61. MTP Post in Soil Strong-Axis Simulation Setup

The simulation results from the strong-axis MTP post model in a soil are shown graphically in Figure 62. Comparisons of the force versus displacement and energy versus displacement for the strong-axis simulation and baseline test, test no. CTPS-1, are shown in Figures 63 and 64, respectively. Simulation of the strong-axis impact on the MTP post in soil found good correlation with the available dynamic component test data. Post deformation and displacement in the soil compared closely between the test and the simulation, as shown in Figure 65. The simulated force versus displacement and energy versus displacement compared well to test no. CTPS-1. Initial forces developed by the post were lower in the simulation model due to differences in the initial inertia peaks in the curve, but the overall force versus displacement curves compared well. Energy dissipation for the simulated post was also generally lower, but this also appeared to be due to inertial peaks in the physical test that were not captured in the simulation. Overall, the positive correlation of strong-axis simulation to the physical test data suggested that the model of the MTP in soil could be applied to simulate potential barrier configurations for the low-tension cable barrier adjacent to steep slopes.

Figure 62. Simulation of Strong-Axis Impact of MTP Post in Soil

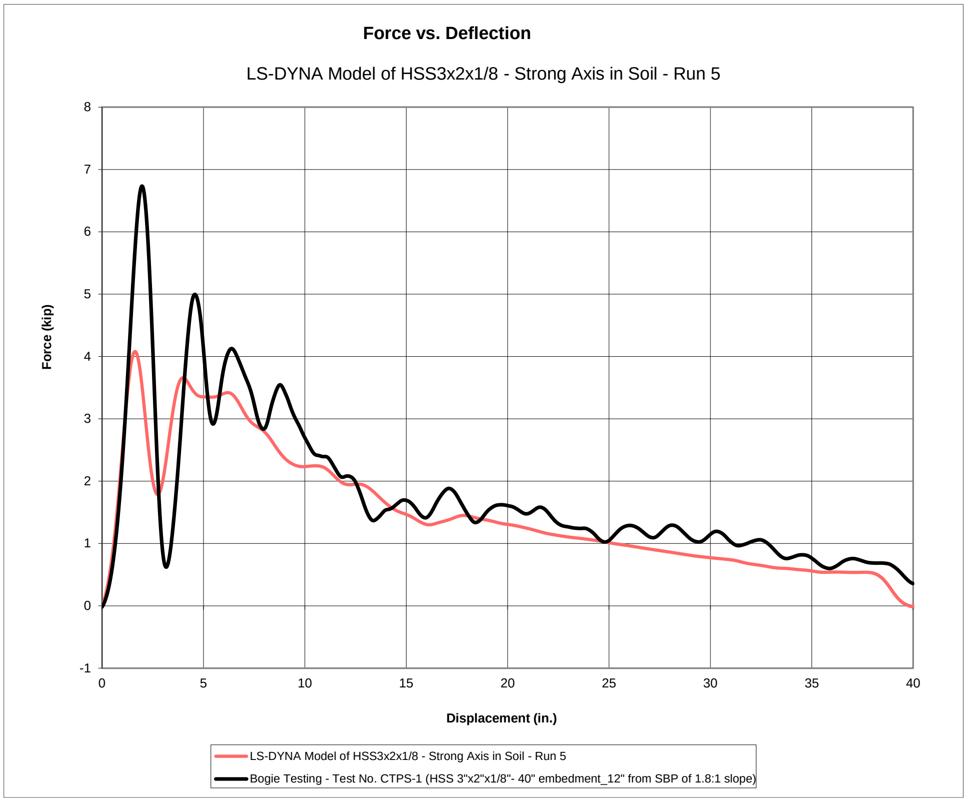

Figure 63. Force vs. Displacement Comparison, Strong-Axis of MTP Post in Soil

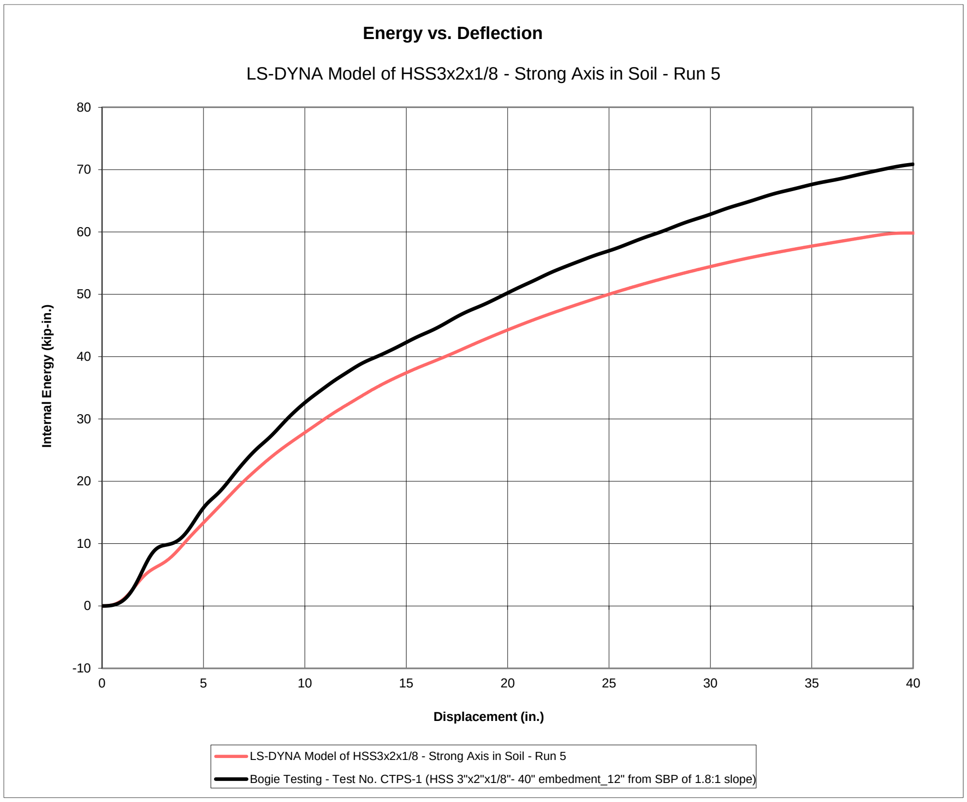

Figure 64. Energy vs. Displacement Comparison, Strong-Axis of MTP Post in Soil

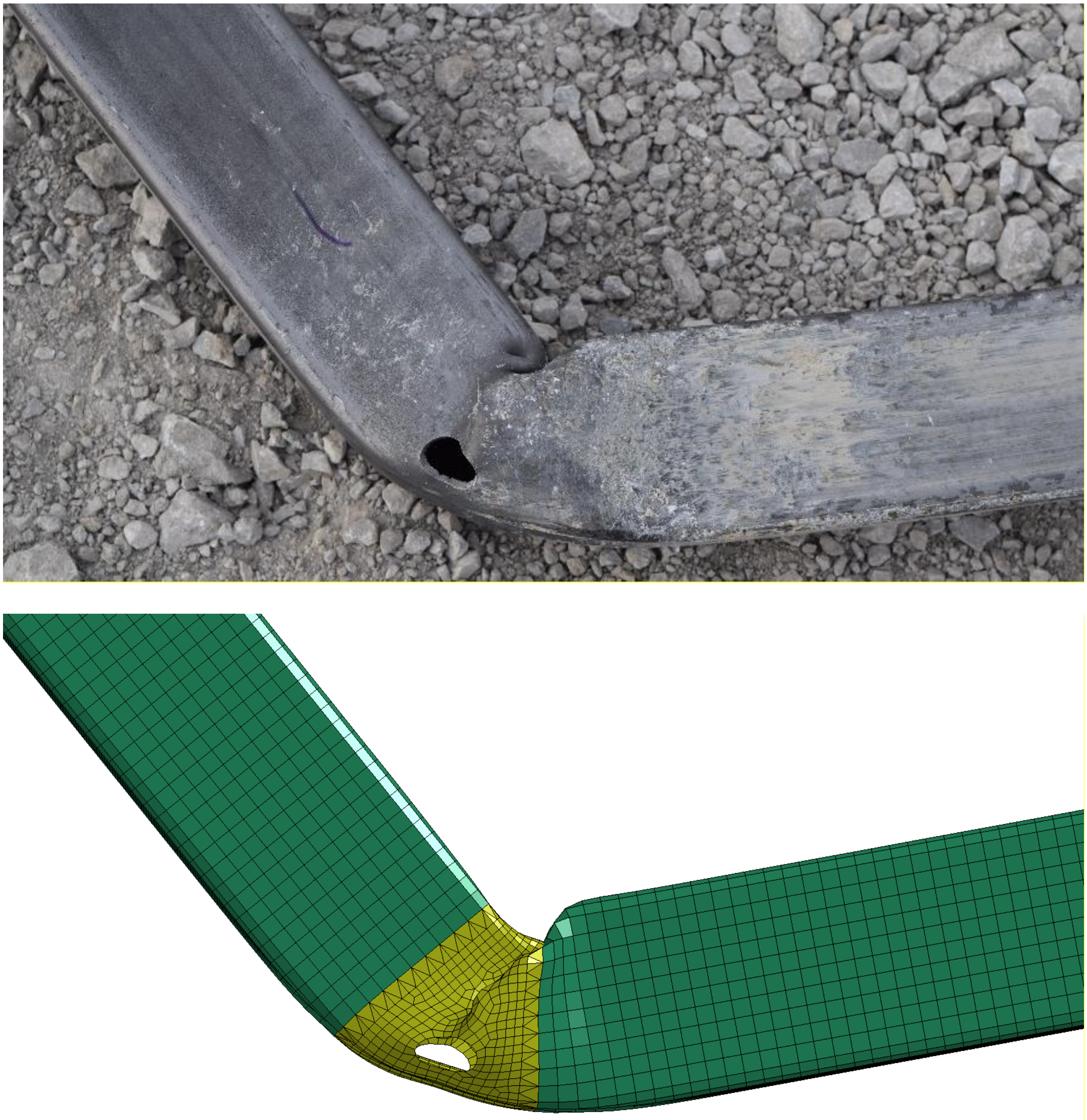

Figure 65. Post Deformation Comparison, Strong-Axis of MTP Post in Soil

8.2.3 Cable-to-Post Attachments

The cable-to-post attachments in the original low-tension cable barrier system and the revised system were ⁵⁄₁₆-in. (8-mm) diameter hook bolts typically used in low-tension cable barrier systems, as shown in Figure 66. Models of these hook bolts had previously been developed and validated by Coon, et al. [18] and later refined by Stolle, et al. [19]. Solid element models of a rod of equivalent diameter to the cable clips were created and simulated in tension, bending, and torsion using material properties consistent with available ASTM A307 steel material properties. The resulting tension-strain, bending moment-curvature, and torque-rate of twist curves were inserted into beam element models of the clips using the *MAT_MOMENT_CURVATURE_BEAM material model with a type 2 Belytschko-Schwer beam element section. This model was applied to both the simulations of test nos. CS-1 and CS-2 and the simulations of revised design alternatives for the low-tension cable barrier adjacent to steep slope.

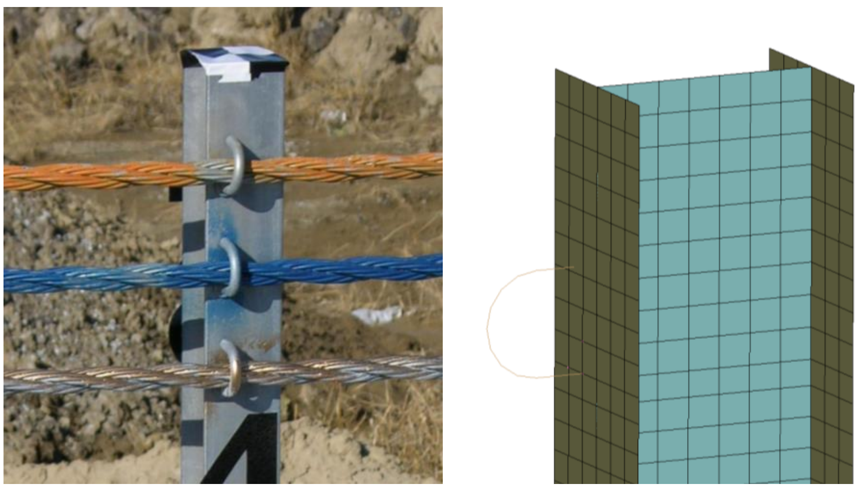

Figure 66. Cable J-bolt Attachment and Beam Element Model

8.2.4 Wire Rope (Cable) Model

The wire ropes used in test nos. CS-1 and CS-2 were consistent with ¾-in. (19-mm) diameter 3x7 XIPS construction. Models of this wire rope were generated using Belytschko-Schwer beam elements and a *MAT_MOMENT_CURVATURE_BEAM material model previously developed and validated for wire rope used in cable barriers [20-21] This model has previously been evaluated in cable barrier system models for roadside or median applications [22].

8.3 Calibration of Low-Tension Cable Guardrail Adjacent to Steep Slope: NCHRP Report 350 Test Nos. CS-1 and CS-2

Next, researchers evaluated models of existing low-tension roadside cable barrier systems installed adjacent to steep slopes to validate computer simulation models. Good correlation between these models and the two MwRSF full-scale crash tests should provide confidence in further computer simulation modeling when investigating MASH impact conditions and alternative designs of low-tension cable barrier systems using the tubular post options.

8.3.1 Description of Models

The full-scale system evaluated during test no. CS-1 consisted longitudinal roadside cable barrier system installed 12 in. (305 mm) from the slope break point of a 1.5H:1V slope. Three ¾-in. diameter, 3x7 wire ropes were supported using ⁵⁄₁₆-in. (8-mm) diameter J-bolts at heights of 24, 27, and 30 in. (610, 686, and 762 mm) using S3x5.7 steel posts spaced 16 ft (4.9 m) on center and installed with the back flange of the post located 12 in. (305 mm) from the slope break point.

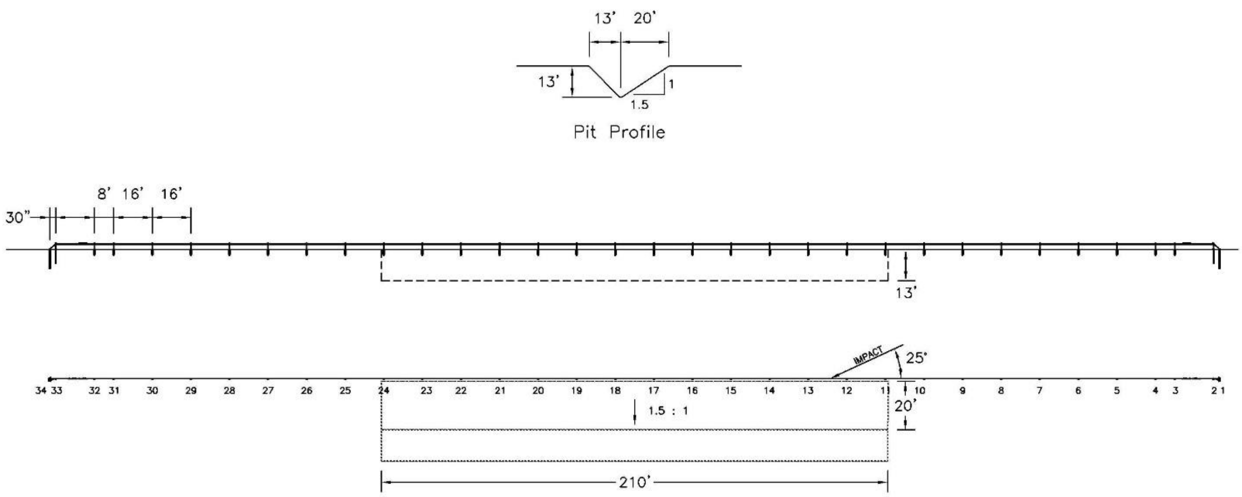

Figure 67. Test Article Layout, Test No. CS-1

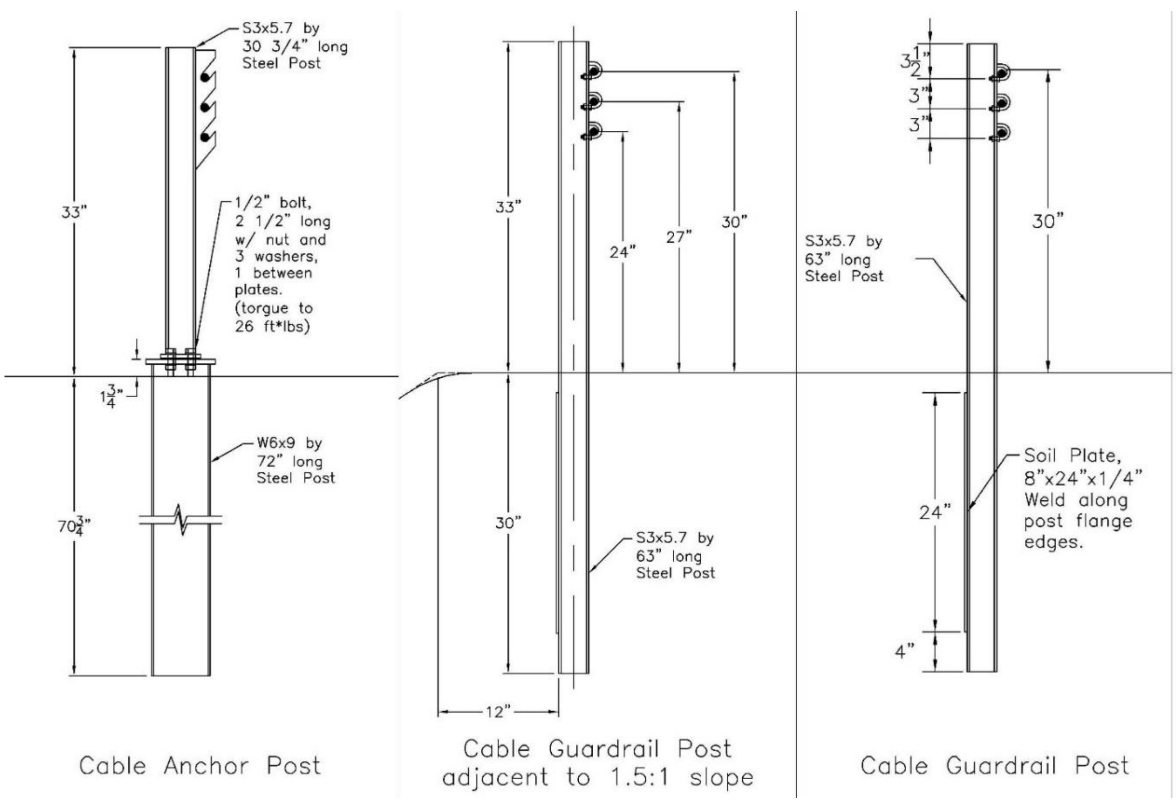

Figure 68. Post and Cable Attachment Details, Test No. CS-1

The simulation model of test no. CS-1 used a barrier model comprised of the previously detailed S3x5.7 steel post model in soil, the validated ⁵⁄₁₆-in. (8-mm) diameter J-bolt cable-to-post connection models, and three low-tension, beam-element cable models. Discrete element springs were placed on the ends of each wire rope in the simulation to provide the simulated stiffness and deflection of the cable anchors at the end of the system. A separate beam element was added to each wire rope to allow for tensioning of the cables. A rigid plane ground was used to represent the level terrain and adjacent 1.5H:1V slope. As mentioned previously, the soil model for the simulation of test no. CS-1 scaled down the soil spring forces 29 percent and the spring displacements 50 percent to compensate for the reduced soil resistive forces observed in the test due to the small offset from the slope break point. A comparison of the line post from test no. CS-1 and the FEA model of a line post and cable connections is shown in Figure 69. The low-tension cable barrier model of test no. CS-1was impacted with the C2500 pickup truck model described previously at a speed of 61.0 mph (98.1 km/h) and at an angle of 26.2 degrees, which matched the impact conditions for full-scale crash test no. CS-1.

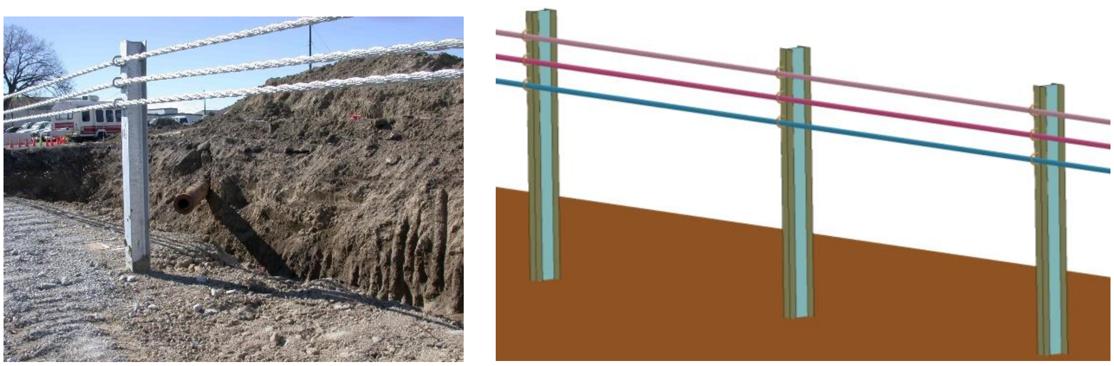

Figure 69. Test No. CS-1 (a) Post-and-Cable Configuration (b) Simulation Model

For simulation of test no. CS-2 the same basic model configuration was used, but the model was modified to use S3x5.7 steel posts spaced 4 ft (1.2 m) on center and installed with the back flange of the post located 48 in. (305 mm) from the slope break point. Soil spring forces were also returned to their nominal levels from the component simulations. The low-tension cable barrier model of test no. CS-2 was impacted with the C2500 pickup truck model described previously at a speed of 61.6 mph (99.1 km/h) and at an angle of 23.6 degrees, which matched the impact conditions for full-scale crash test no. CS-2.

8.3.2 Simulation of Test No. CS-1

Following the simulation of test no. CS-1, comparisons of the simulation model performance and the full-scale test were made. Comparison of sequential images from the simulation model and the full-scale crash test are shown in Figures 70 and 71. The behavior of the simulation model closely matched that of the full-scale crash test. In both cases, the pickup truck was initially captured by the low-tension cable barrier with all three cables. As the impact continued, the vehicle extended past the slope break point and began to roll counterclockwise due to the lack of vertical support to the left-side wheels. As the pickup continued to redirect, the cables did not capture the rear bumper of the vehicle, which allowed the rear of the pickup truck to continue to roll. This motion eventually caused the barrier to lose vehicle capture and the vehicle to rollover in both the simulation and the full-scale crash test. Timing of the rollover event compared very well between the model and the simulation. The timing and magnitude of the post deflections during the simulation and the crash test also showed good correlation. Comparison of dynamic system deflection was not conducted as the cables in the full-scale crash test were not visible on the overhead film.

Based on these comparisons, the simulation model proved capable of replicating the failure mode of the initial configuration of the low-tension cable barrier adjacent to steep slope. This provided the researchers with confidence that the simulation model could potentially indicate a similar failure mode when modeling the revised barrier design options.

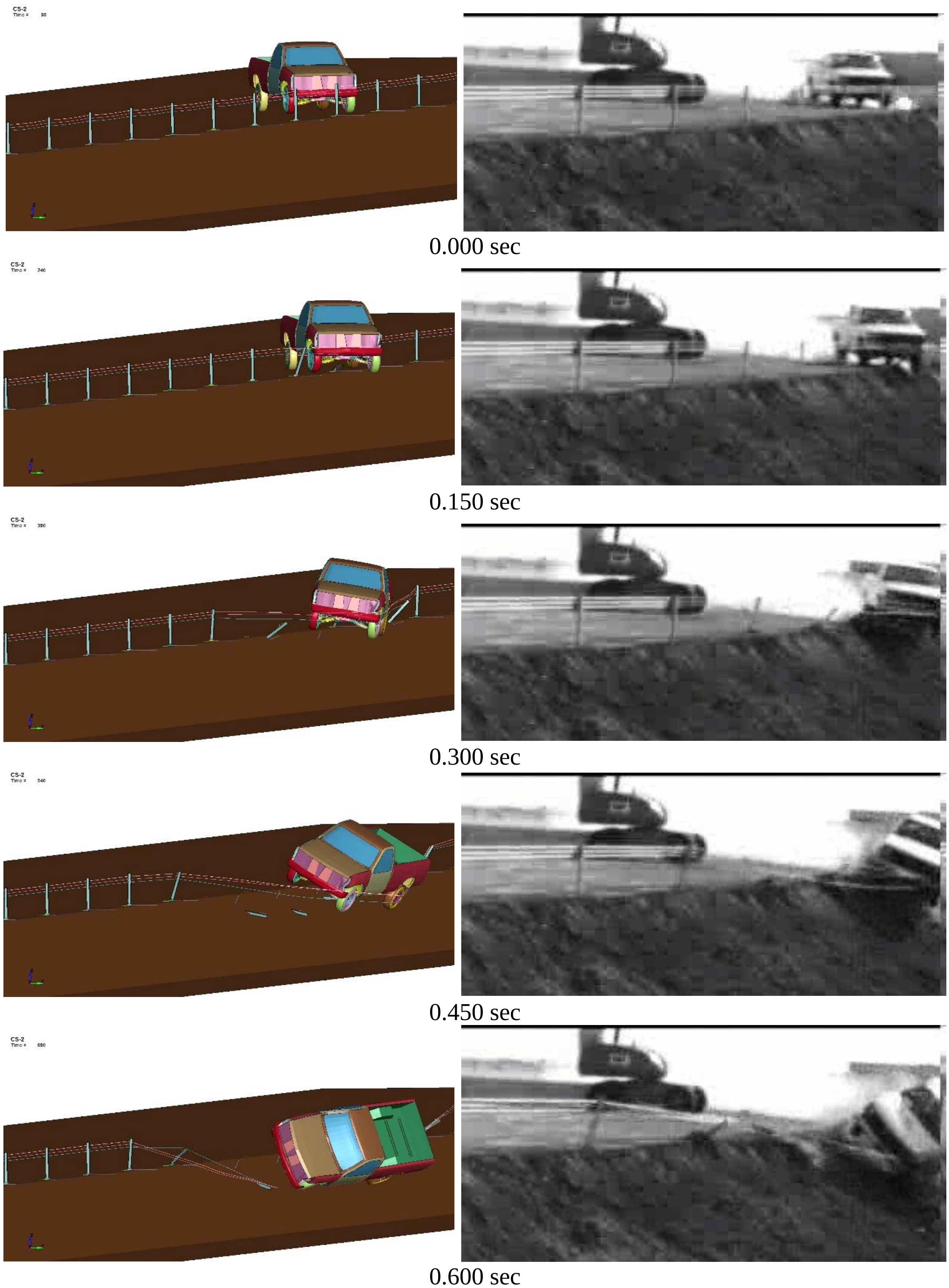

Figure 70. Sequential Images of the Simulation Model and Full-Scale Test No. CS-1

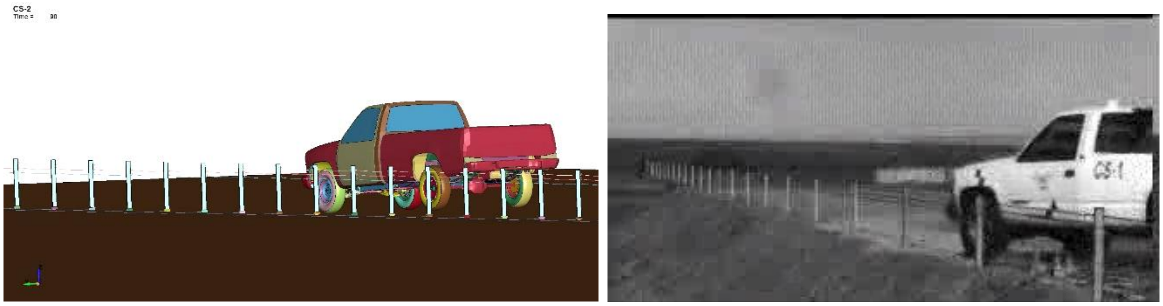

0.000 sec

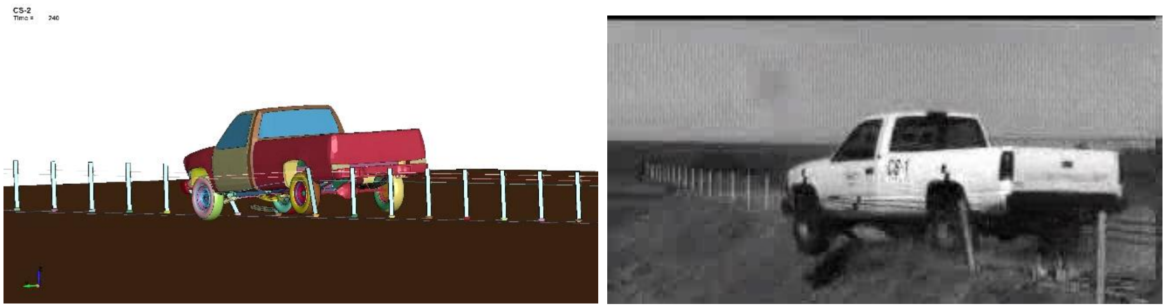

0.150 sec

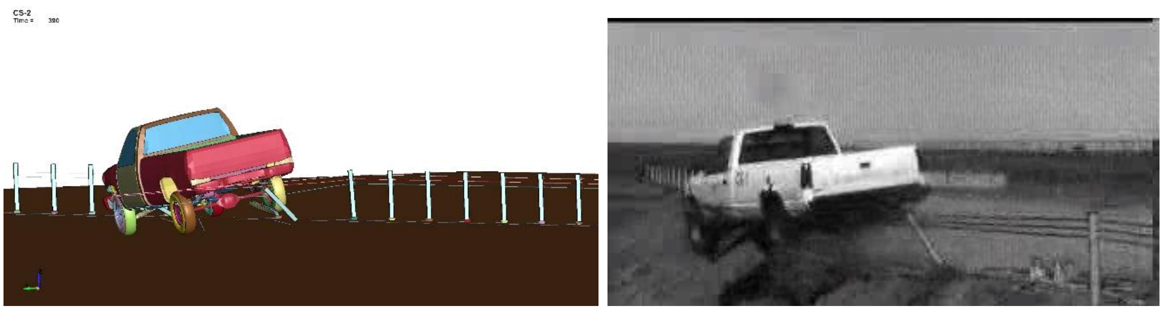

0.300 sec

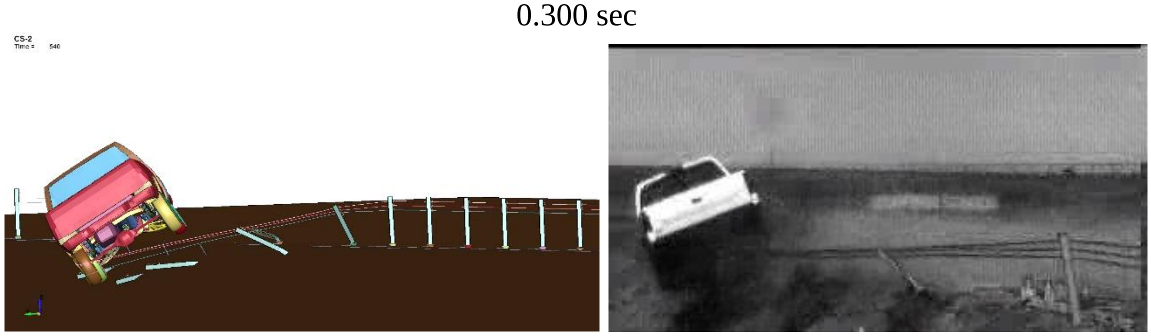

0.450 sec

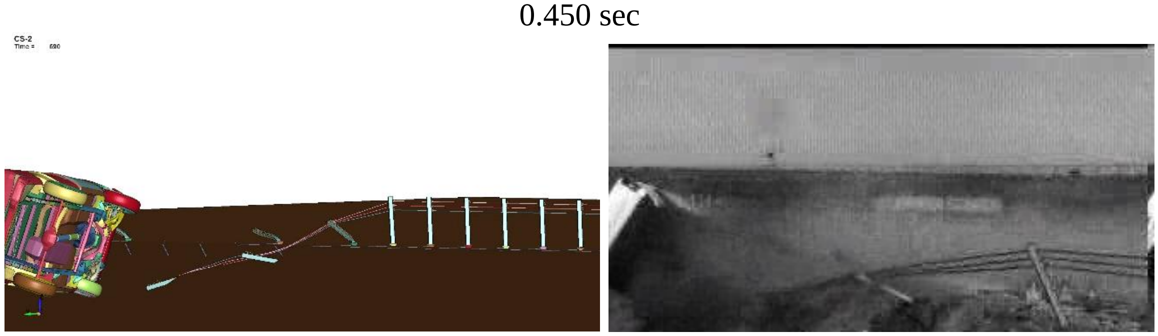

0.600 sec

Figure 71. Sequential Images of the Simulation Model and Full-Scale Test No. CS-1

8.3.3 Simulation of Test No. CS-2

Following the simulation of test no. CS-2, comparisons of the simulation model performance and the full-scale test were made. Sequential images from the simulation model and the full-scale crash test are shown in Figures 72 and 73. The behavior of the simulation model closely matched that of the full-scale crash test. In both cases, the pickup truck was captured by the low-tension cable barrier with all three cables above the bumper. As the impact continued, the vehicle extended past the slope break point and began to roll counterclockwise. During vehicle redirection, both left-side wheels of the truck contacted the slope, which helped limit the roll of the pickup. As the pickup continued to redirect, the rear of the vehicle in both the test and the simulation was captured as the cables engaged over the left-rear wheel but under the rear bumper. The vehicle was then redirected back up the slope in both the simulation and the full-scale crash test. The timing and magnitude of the post deflections during the simulation and the crash test correlated well. The maximum dynamic lateral barrier deflection was measured to be 80¼ in. (2,038 mm) in the simulation model and 77⅞ in. (1,978 mm) in the full-scale crash test. The lateral barrier deflection noted herein is lower than the published value to in the original research report. This value was revised during this research as the original, published value overestimated the cable deflection based on the position of the pickup truck and did not account for the engagement of the cable in the rear wheel well underneath the truck body or the vehicle roll appropriately.

Based on these comparisons, the simulation model proved capable of replicating vehicle capture, redirection, and overall barrier deflections of the low-tension cable barrier adjacent to steep slope. This provided the researchers with confidence that the simulation model could potentially predict an acceptable safety performance when modeling the revised barrier design configurations.

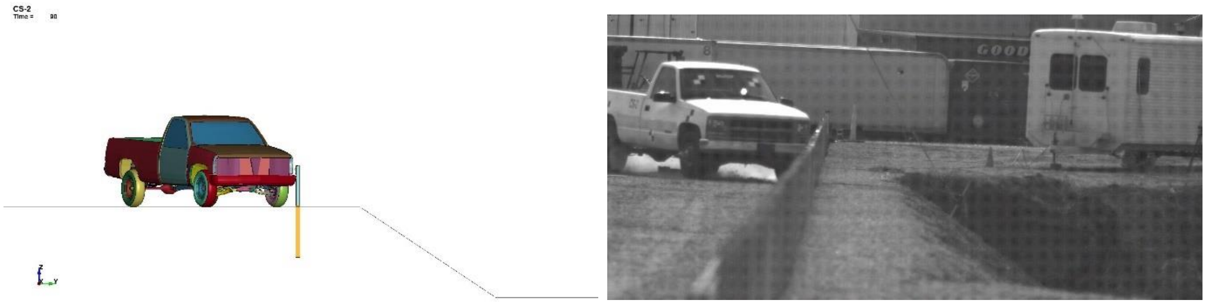

0.000 sec

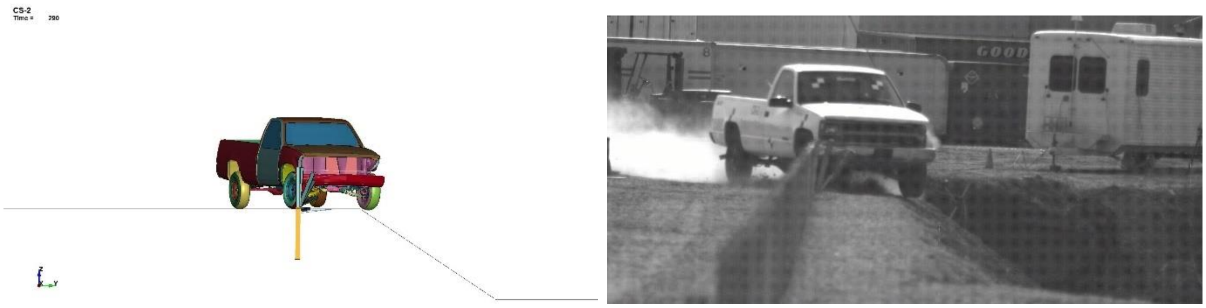

0.200 sec

0.400 sec

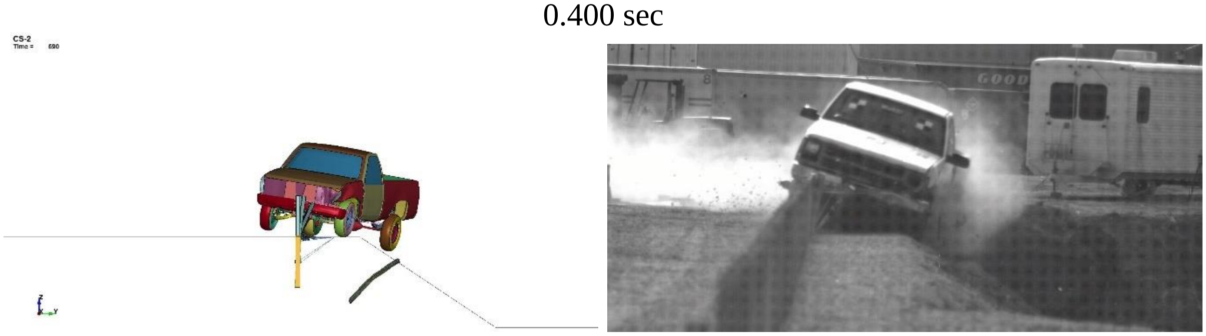

0.600 sec

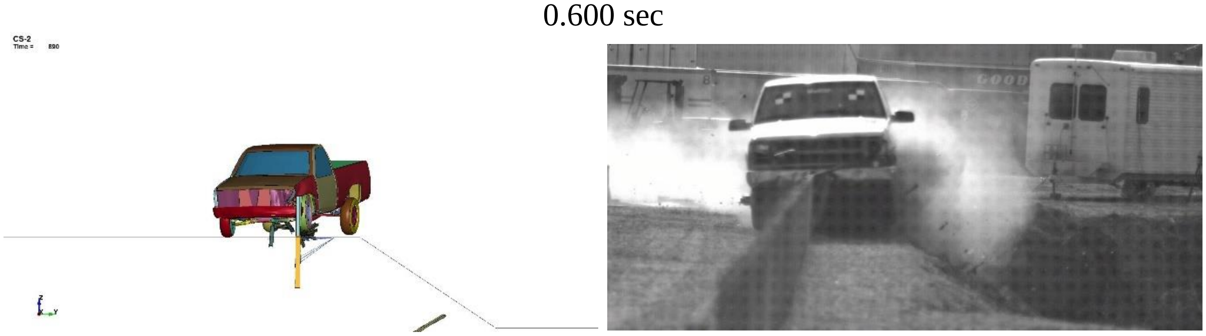

0.800 sec

Figure 72. Sequential Images of the Simulation Model and Full-Scale Test No. CS-2

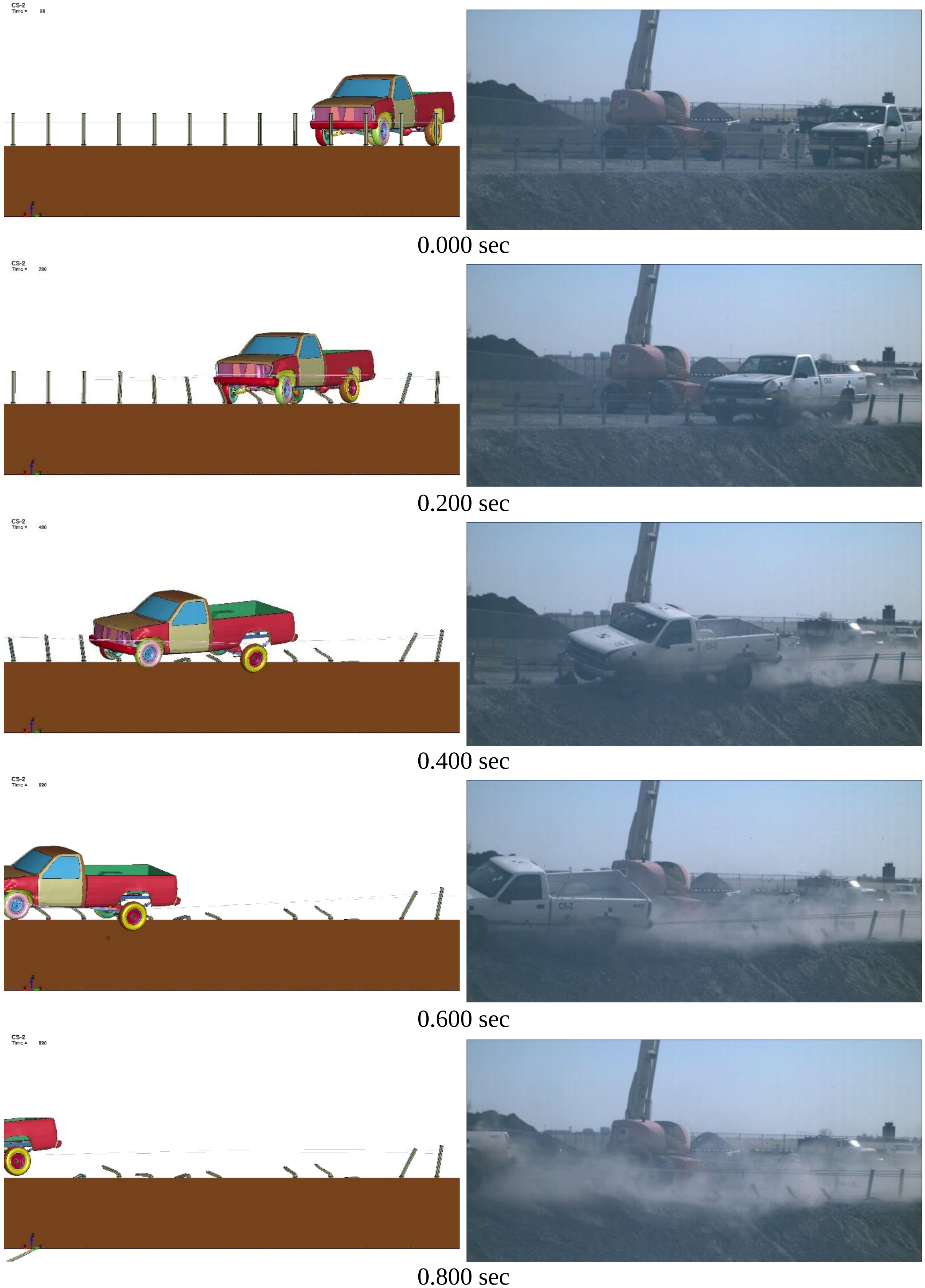

Figure 73. Sequential Images of the Simulation Model and Full-Scale Test No. CS-2

8.3.4 Discussion & Conclusions

Results of the simulations of test nos. CS-1 and CS-2 suggested that the baseline models adequately captured the vehicle response, dynamic deflections, working widths, system damage, and truck-to-steep slope interactions. Upstream and downstream damage to the cable system posts and cable-to-post attachments, as well as cable interlock on the simulated vehicle compared to the test vehicles, suggested that the baseline models were accurately depicting the event sequences in test nos. CS-1 and CS-2. Based on these findings, and correlation of the component models of the MTP posts with component test results, researchers had the confidence to investigate alternative configurations for the low-tension cable barrier systems installed adjacent to steep slopes using the MTP post.

8.4 Alternative Designs for Low-Tension Cable Barrier Adjacent to Steep Slope

The low-tension cable barrier system model developed for simulated test nos. CS-1 and CS-2 was modified by replacing the S3x5.7 posts with the MTP post. A 6-in. (152-mm) vertical cable spacing was utilized. The slope was also modified to 1.8H:1V to be consistent with the design criteria. The same ⁵⁄₁₆-in. (8-mm) diameter J-bolt cable-to-post attachment models from the baseline models were used for the revised system configuration. The modeled cable lengths for each system were equal to 500 ft (152.6 m) and simulated end anchor stiffness was applied to each cable using discrete spring elements. The UNL V3r Chevy Silverado model was used to represent the 2270P vehicle in the simulations, and an impact speed and angle were 62.1 mph (100 km/h) and 25 degrees were applied consistent with MASH TL-3 impact conditions.

Researchers investigated multiple parameters/modifications for the low-tension cable barrier system adjacent to steep slope. As noted previously, the design modifications focused primarily on post spacing, barrier offset, and cable mounting heights. The design configurations simulated are summarized in Table 6. The offset from the slope break point was varied from 1 ft to 4 ft (305 mm to 1,219 mm). Post spacing was evaluated at 4 ft, 6 ft, and 8 ft (1,219 mm, 1,829 mm, and 2,438 mm). Finally, two cable height configurations with 6-in. (152-mm) vertical cable spacing were investigated. The first configuration had cables mounted at heights of 22 in., 28 in., and 34 in. (559 mm, 711 mm, and 864 mm). The second configuration had cables mounted at heights of 24 in., 30 in., and 36 in. (610 mm, 762 mm, and 914 mm). For each simulation, the locations of the weakening holes of the tubular posts were maintained at ground level, and the top of the post was located 3 in. (76 mm) above the top cable. To maintain similar post lengths, the embedment depths for posts with 24-in. (611 mm) bottom cable height was 2 in. (51 mm) less than posts with a 22-in. (559 mm) bottom cable height. An example of one of the system configurations is shown in Figure 74. An example of the initial impact configuration is shown in Figure 75.

Some simulations became numerically unstable before the point of maximum dynamic deflection (typically around 700 msec) and before researchers could determine if the vehicle would remain stable during impact. Some minor modifications were explored to improve stability which were not believed to otherwise affect simulation outcomes. When these efforts were not successful, these simulations were noted and were not included in the final analysis of vehicle stability, maximum dynamic deflection, or recommendations. A summary of the simulation data is shown in Table 7. Further analysis on the effects of cable heights, post spacing, and offset from SBP is provided below.

Table 6. Summary of Simulated Cable Barrier System Configurations

Post Spacing, ft (m)	Cable Heights, in. (mm)	System Offset from SBP, ft (m)
4 (1.22)	22, 28, 34 (559, 711, 864)	2 (0.61)
		3 (0.91)
		4 (1.22)
	24, 30, 36 (610, 762, 914)	2 (0.61)
		3(0.91)
		4 (1.22)
6 (1.83)	22, 28, 34 (559, 711, 864)	2 (0.61)
		3 (0.91)
		4 (1.22)
	24, 30, 36 (610, 762, 914)	2 (0.61)
		3 (0.91)
		4 (1.22)
8 (2.44)	22, 28, 34 (559, 711, 864)	1 (0.31)
		2 (0.61)
		3 (0.91)
		4 (1.22)
	24, 30, 36 (610, 762, 914)	2 (0.61)
		3 (0.91)
		4 (1.22)

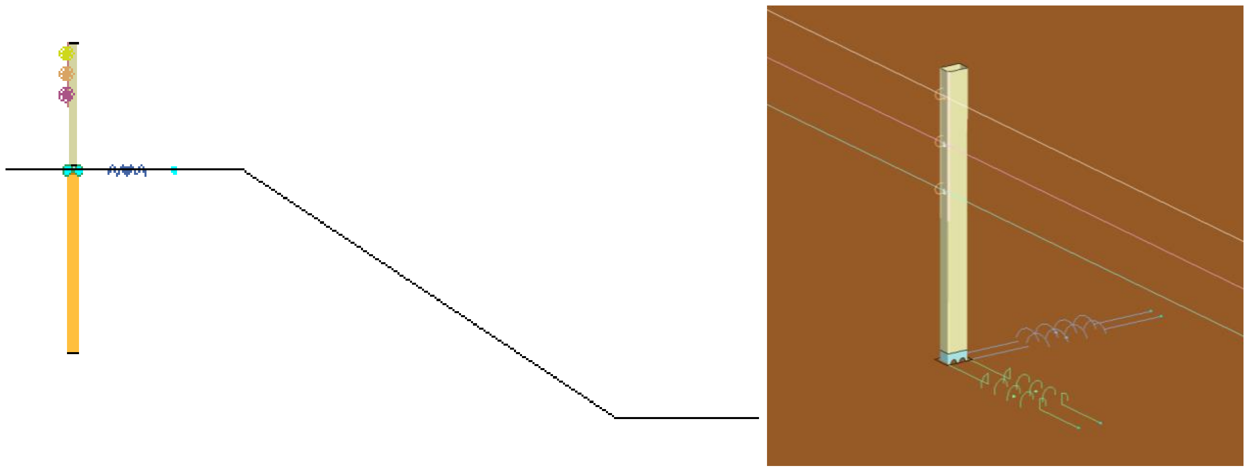

Figure 74. Example Low-Tension Roadside Cable Barrier Model Configuration

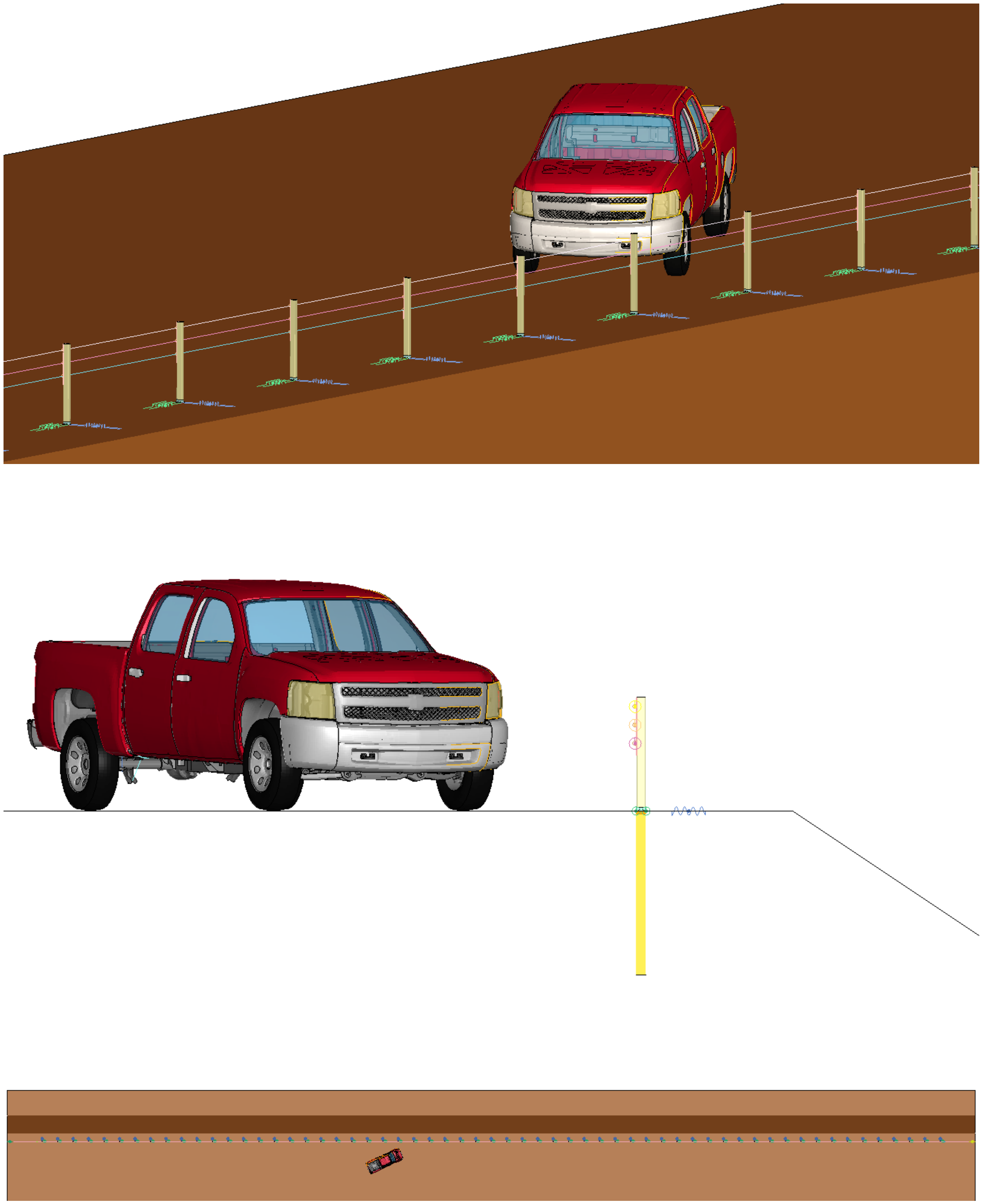

Figure 75. Example Simulation Configuration: Chevrolet Silverado and Low-Tension Cable Barrier Model Adjacent to Steep Slope

Table 7. Summary of LS-DYNA Simulation Data

Post Spacing ft (m)	Barrier Offset ft (mm)	Bottom Cable Height ft (mm)	Simulation Time sec	Max Roll Angle deg.	Max Pitch Angle deg	Max Change in Yaw deg	Max Lateral Barrier Displacement in. (mm)	Pickup CG Displacement past Slope Break Point in. (mm)
4 (1.22)	2 (0.61)	22 (559)	0.915	58.6	23.4	31.5	73.3 (1,862)	49.3 (1,252)
4 (1.22)	3 (0.91)	22 (559)	0.832	39.7	17.9	34.2	69.8 (1,773)	33.8 (859)
4 (1.22)	4 (1.22)	22 (559)	0.329	3.0	1.4	7.0	20.4 (518)	-27.6 (-701)
4 (1.22)	2 (0.61)	24 (610)	0.976	32.5	17.9	28.1	63.6 (1,615)	39.6 (1,006)
4 (1.22)	3 (0.91)	24 (610)	1.000	27.6	13.8	28.2	63.1 (1,603)	27.1 (688)
4 (1.22)	4 (1.22)	24 (610)	0.339	2.0	1.0	9.3	20.6 (523)	-27.4 (-696)
6 (1.83)	2 (0.61)	22 (559)	0.466	8.5	3.1	13.2	60.1 (1,527)	36.1 (917)
6 (1.83)	3 (0.91)	22 (559)	1.000	44.8	20.4	30.5	86.4 (2,195)	53.4 (1,356)
6 (1.83)	4 (1.22)	22 (559)	1.000	44.8	22.9	28.6	91.3 (2,319)	43.3 (1,100)
6 (1.83)	2 (0.61)	24 (610)	1.000	42.5	20.7	28.9	79.5 (2,019)	55.5 (1,410)
6 (1.83)	3 (0.91)	24 (610)	0.324	2.6	0.6	5.7	19.4 (493)	-16.6 (-422)
6 (1.83)	4 (1.22)	24 (610)	0.626	18.7	10.3	29.4	78.1 (1,984)	30.1 (765)
8 (2.44)	1 (0.31)	22 (559)	1.000	89.1	53.5	29.0	121.2 (3,078)	109.2 (2,774)
8 (2.44)	2 (0.61)	22 (559)	0.493	13.7	3.2	13.5	71.8 (1,824)	47.8 (1,214)
8 (2.44)	3 (0.91)	22 (559)	1.000	53.4	24.4	29.4	109.4 (2,779)	73.4 (1,864)
8 (2.44)	4 (1.22)	22 (559)	0.712	32.7	19.6	33.1	101.5 (2,578)	53.5 (1,359)
8 (2.44)	2 (0.61)	24 (610)	1.000	93.4	28.4	31.9	90.7 (2,304)	66.7 (1,694)
8 (2.44)	3 (0.91)	24 (610)	1.000	49.0	22.7	31.9	92.5 (2,350)	56.5 (1,435)
88 (2.44)	4 (1.22)	24 (610)	0.737	38.3	28.6	31.8	91.7 (2,329)	43.7 (1,110)

Note: Shaded cells indicated simulations which became numerically unstable prior to the vehicle reaching maximum lateral extension/deflection.

8.4.1 Bottom Cable Height

The researchers reviewed the results of the simulated configurations based on cable height variation. Maximum lateral vehicle c.g. displacement vs. bottom cable height is shown graphically in Figure 76. Note that insufficient data existed to compare results with 6-ft (1.8-m) post spacing for 22- and 24-in. (559- and 610-mm) bottom cable heights due to model instabilities. Simulation modeling of the cable height options found that the increased cable height configuration reduced overall deflections across the range of offsets and post spacings simulated. In general, a lower cable height of 22 in. (559 mm) did not engage the truck and was instead overridden by the wheel, whereas a cable located at 24 in. (610 mm) remained in contact with the bumper. The additional capture cable increased the lateral redirection force on the pickup truck by applying shear load lower on the post, meaning the post contributed more lateral redirection load with the same plastic bending capacity. The average decrease in maximum c.g. displacement was approximately 13 percent, and the average decrease in lateral barrier deflections were approximately 15 percent.

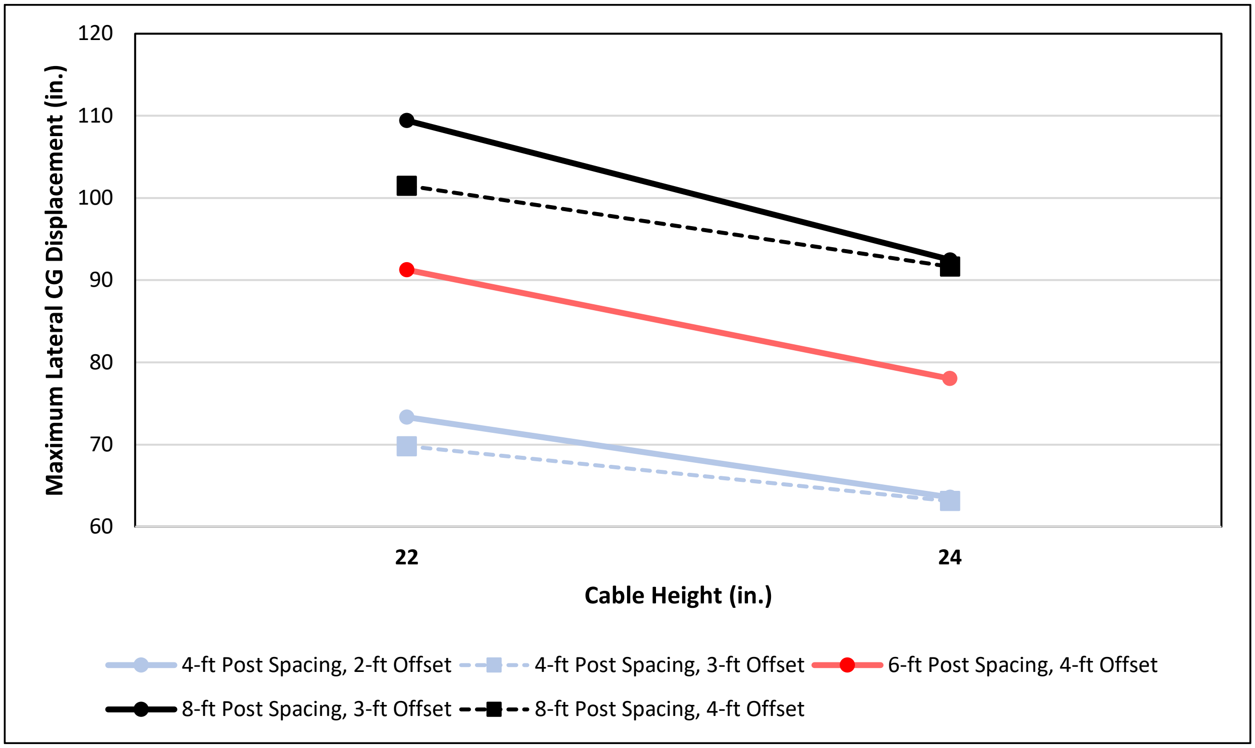

Figure 76. Maximum Lateral c.g. Displacement vs. Bottom Cable Height

Review of previous full-scale crash testing of the Midwest Cable Median Barrier system (test nos. MTP-1 and MWP-2) [23-24] and New York cable barriers (NYC test series) [25] had cables mounted at heights of 23 in. (584 mm) and demonstrated similar pickup truck capture with those cables, which would indicate that the reductions in deflection and improved pickup truck capture observed in the simulations was valid. Small car capture with a bottom cable height of 24 in. (610 mm) was not investigated in this study. Review of previous testing of sedans and small car geometries with cable heights similar to the proposed cable heights indicated that both 22 in. and 24 in. bottom cables could capture the smaller passenger vehicles and that the middle cable would also likely contribute to vehicle capture [26]. It was noted that having the top cable at 36 in.

(914 mm) versus 34 in. (914 mm) provided minimal benefit. Thus, it was proposed that the second cable height option would be equally effective if heights of 24 -in., 29 in., and 34 in. (610 mm, 737 mm, and 864 mm) were applied.

8.4.2 Post Spacing

Post spacings of 4 ft, 6 ft, and 8 ft were evaluated to determine a cost-effective configuration of the system which was believed to be capable of passing MASH test no. 3-11. Vehicle stability, lateral barrier deflection, and vehicle displacement improved significantly as post spacing decreased. Compared to models with 4-ft (1.2-m) spacings, models with 6-ft spacings showed a 25 percent increase in c.g. displacement, a 22 percent increase in deflection past the slope, and were more prone to rollover. Models with 8-ft (2.4-m) spacings showed a 44 percent increase in c.g. displacement, a 36 percent increase in deflection past the slope, and were much more prone to rollover compared to 4-ft (1.2-m) post spacing.

As noted previously, increasing the height of the bottom cable reduced dynamic deflections of the pickup truck, as shown in Figure 77. Systems with 4-ft (1.2-m) spacings and a 22-in. (559-mm) bottom cable height were comparable to systems with 6-ft spacings and a 24-in. bottom cable height with regard to dynamic deflections, vehicle roll angles, and lateral deflections. The same was true when comparing 6-ft (1.8-m), 22-in. (559-mm) and 8-ft (2.4-m), 24-in. (610-mm) systems. Results indicated that the maximum c.g. displacement was reduced by approximately 0.7 in. (18 mm) for every 1-in. (25-mm) reduction of post spacing for systems with a 22-in. (559-mm) bottom cable height, and deflections were reduced by approximately 0.6 in. (15 mm) for every 1-in. (25-mm) reduction in post spacing for systems with a 24-in. (610-mm) bottom cable height.

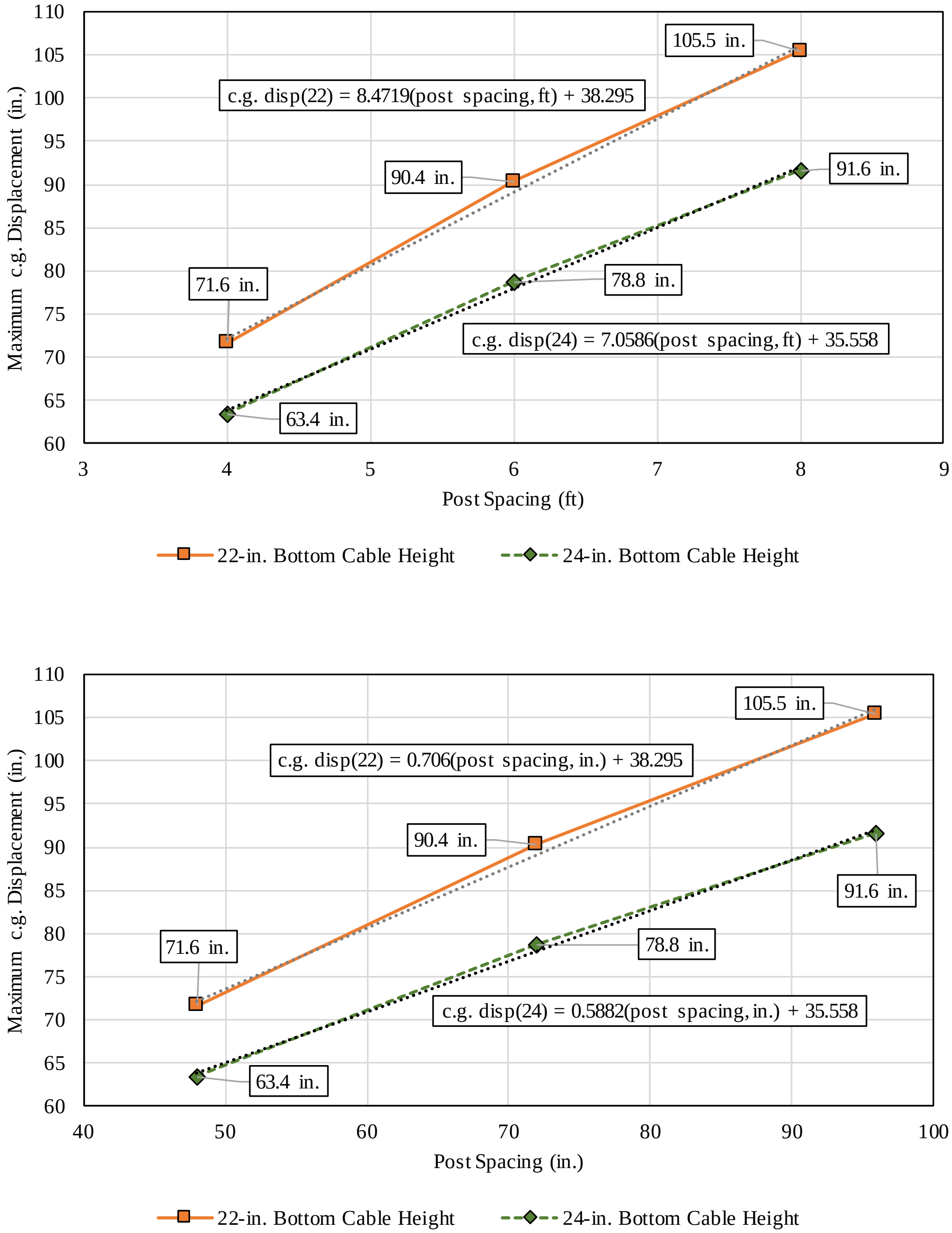

Figure 77. Maximum c.g. Displacement Based on Post Spacing and Bottom Cable Height

8.4.3 System Offset from SBP

Simulation of variable slope offsets found that the barrier offset from the slope had a minimal effect on the lateral deflections of the barrier and the impacting vehicle. This can be seen in a comparison of the vehicle c.g. lateral displacement past the original longitudinal line of the barrier, as shown in Figure 78. However, the simulation models found a significant effect on the vehicle extension down the slope, which affected vehicle capture and stability. No barrier offsets to the slope less than 2 ft demonstrated the ability to capture and redirect the impacting vehicle.

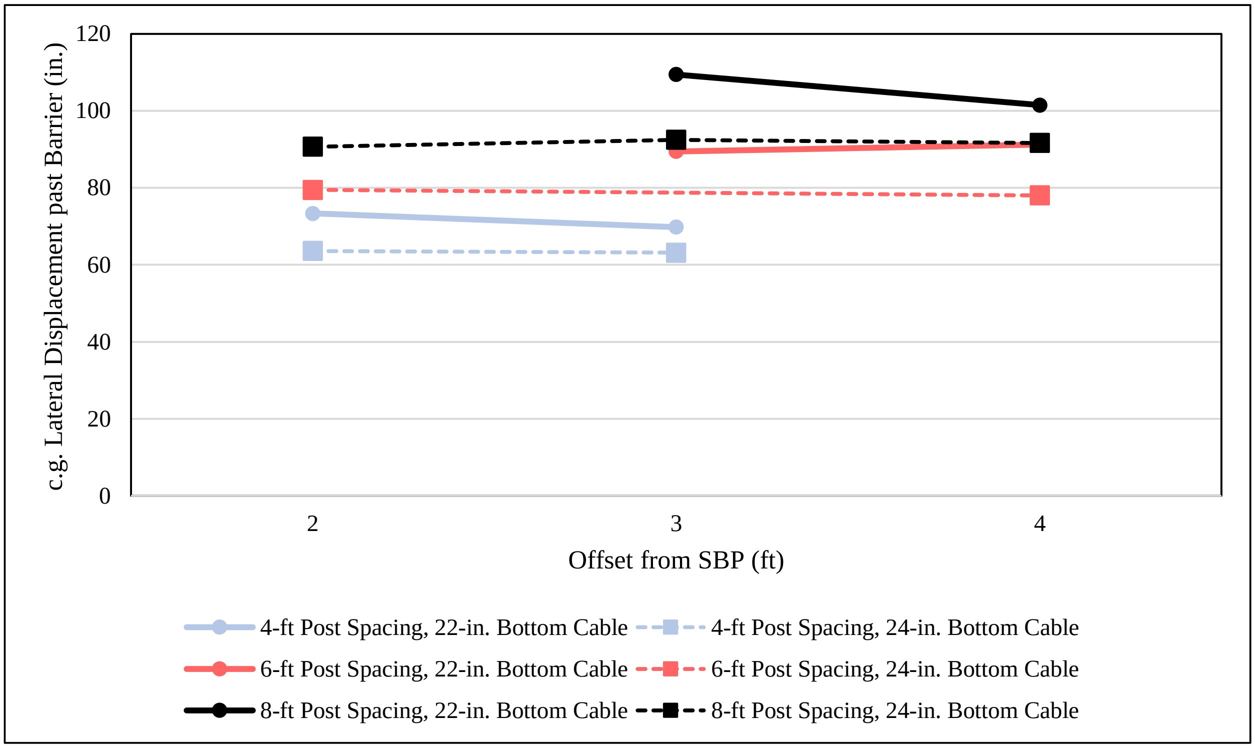

Figure 78. Vehicle c.g. Lateral. Displacement Past Barrier vs. Offset from SBP

8.5 Discussion

Following a review of the simulations of the various barrier configurations, the researchers attempted to determine which low-tension cable barrier configurations adjacent to steep slopes provided the potential to meet MASH TL-3. The researchers found that barrier configurations that allowed all four of the pickup truck wheels to extend past the slope break point had reduced vehicle capture and much higher instability as compared to simulations where the non-impact side wheels remained on the shoulder or level terrain during redirection. An example of the vehicle extension down the slope on vehicle stability is shown graphically for two different cable configurations in Figure 79.This observation correlated well with the previous full-scale testing and rollover observed in test no. CS-1 and the subsequent success of the modified cable barrier system in test no. CS-2. A comparison of the simulated barrier configurations and their associated wheel extension over the slope is shown in Figure 80. As such, it was believed that vehicle stability and probability of successfully passing MASH test designation no. 3-11 would be greatly improved by retaining wheels on the flat shoulder region.

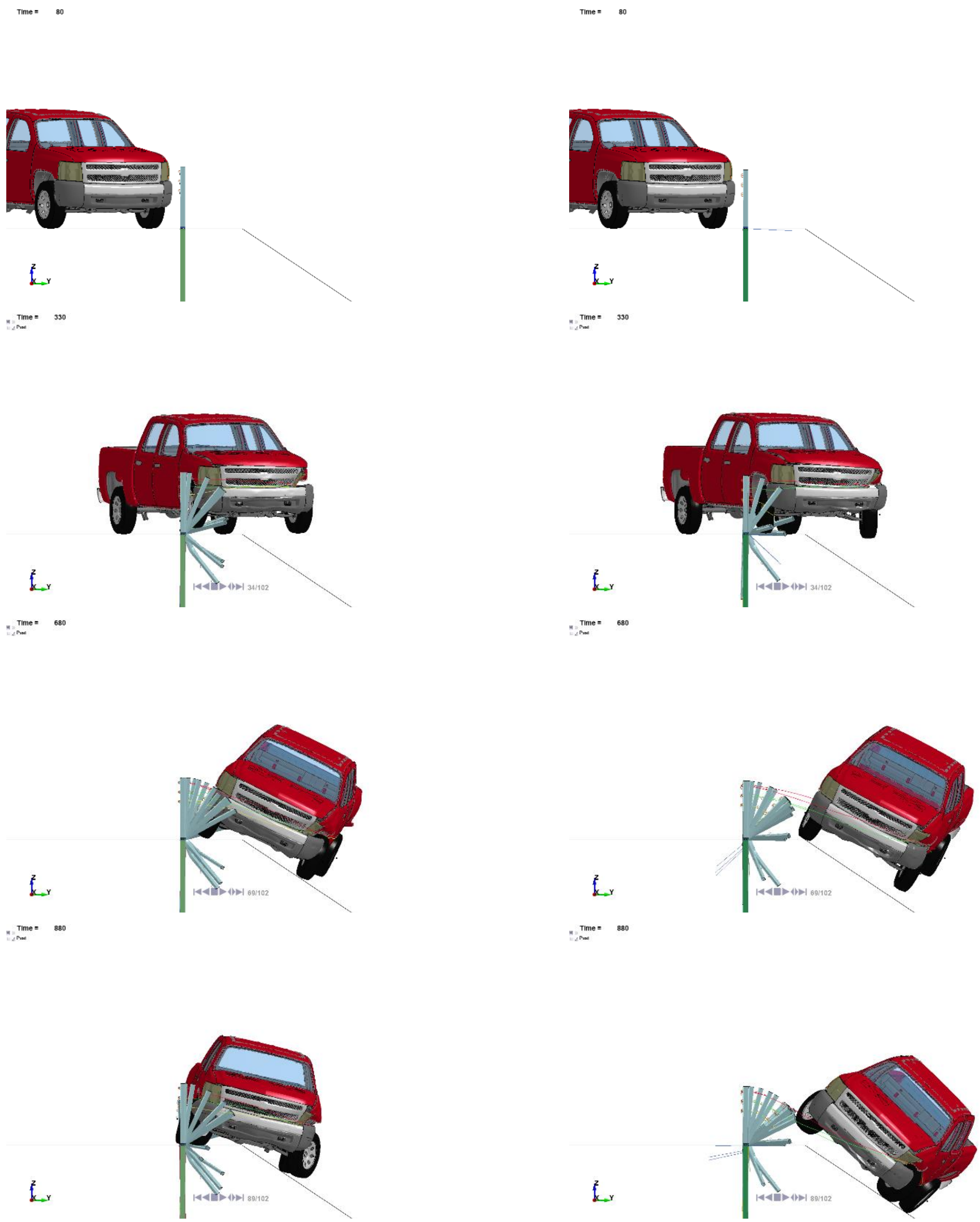

4-ft Post Spacing
3-ft Offset to Slope Break Point
24-in., 30-in., and 36-in. Cable Heights

6-ft Post Spacing
3-ft Offset to Slope Break Point
22-in., 28-in., and 34-in. Cable Heights

Figure 79. Effect of Barrier Offset on Cable Barrier Vehicle Extension Down Slope

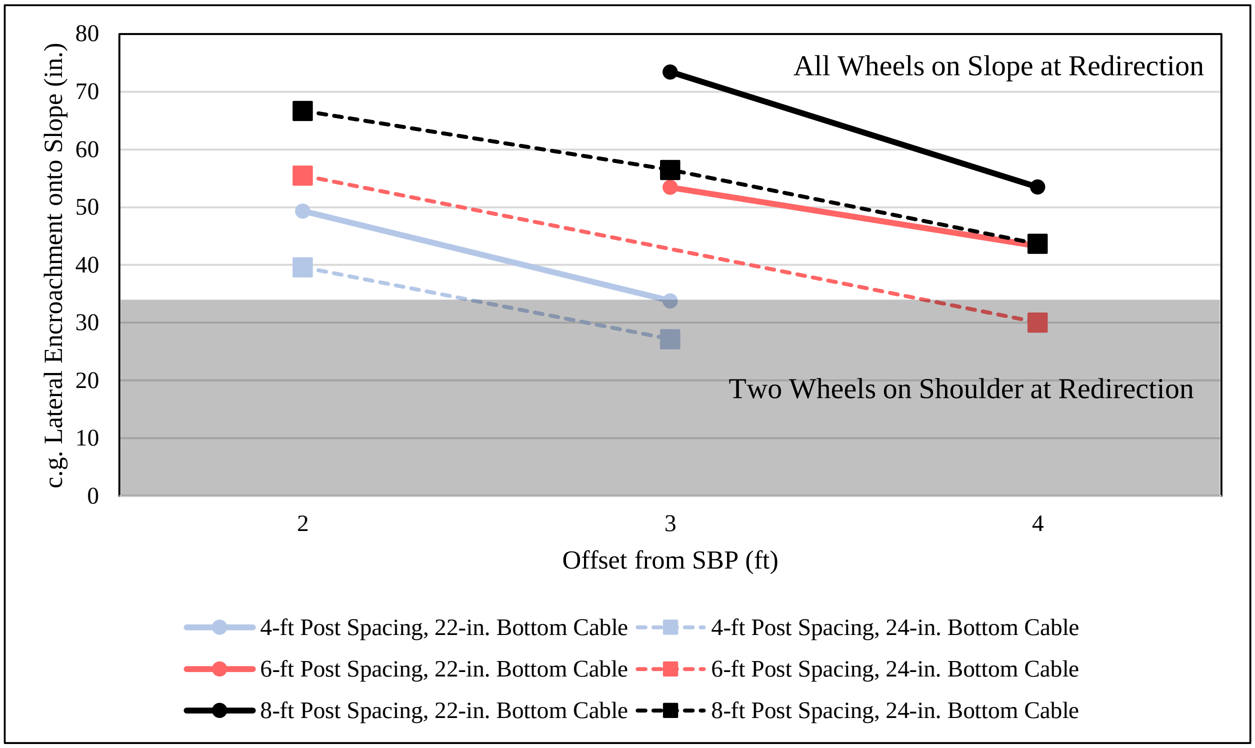

Figure 80. Vehicle c.g. Lateral. Encroachment onto Slope vs. Offset from SBP

Based on this criteria, low-tension cable barrier configurations were identified and recommended which indicated that at least two wheels (one side of the vehicle) would remain on the flat terrain behind the system. These systems were believed to provide the highest potential for the low-tension cable barrier to satisfy MASH criteria for test designation no. 3-11 when installed adjacent to slopes as steep as 1.8H:1V. Recommended system configurations which satisfy this condition are denoted in Table 8. The three recommended configurations are shown schematically in Figure 81.

As noted previously, a top cable height of 36 in. (914 mm) did not provide additional benefit, while a bottom cable height of 24 in. (610 mm) did provide for reduced system deflection due to increased lower cable engagement with the vehicle. Thus, the recommended low-tension cable barrier configurations had two sets of cable heights. The first used cable heights of 22 in., 28 in., and 34 in. (559 mm, 711 mm, and 864 mm). The second used cable heights of 24 in., 29 in., and 34 in. (559 mm, 711 mm, and 864 mm). The recommended configurations used either 4-ft or 6-ft (1,219-mm or 1,828-mm) post spacing depending on the offset from the slope break point. The offset from the slope break point for the recommended configurations was either 3 ft or 4ft (914 mm or 1,219 mm). Full-scale testing of these recommended configurations would be required prior to implementing these designs in order to verify their safety performance.

Table 8. Evaluation of Configurations of Low-Tension Cable Barrier Adjacent to Steep Slope

Potential MASH TL-3 Performance	Cable Barrier Configurations with 22-in., 28-in., and 34-in. Cable Heights	Cable Barrier Configurations with 24-in., 29-in., and 34-in. Cable Heights
Good	4-ft post spacing offset 3 ft from slope break point	4-ft post spacing offset 3 ft from slope break point
		6-ft post spacing offset 4 ft from slope break point
Poor	6-ft post spacing offset ≤ 4 ft from slope break point	4-ft post spacing offset ≤ 2 ft from slope break point
		6-ft post spacing offset ≤ 3 ft from slope break point
	8-ft post spacing offset ≤ 4 ft from slope break point	8-ft post spacing offset ≤ 4 ft from slope break point

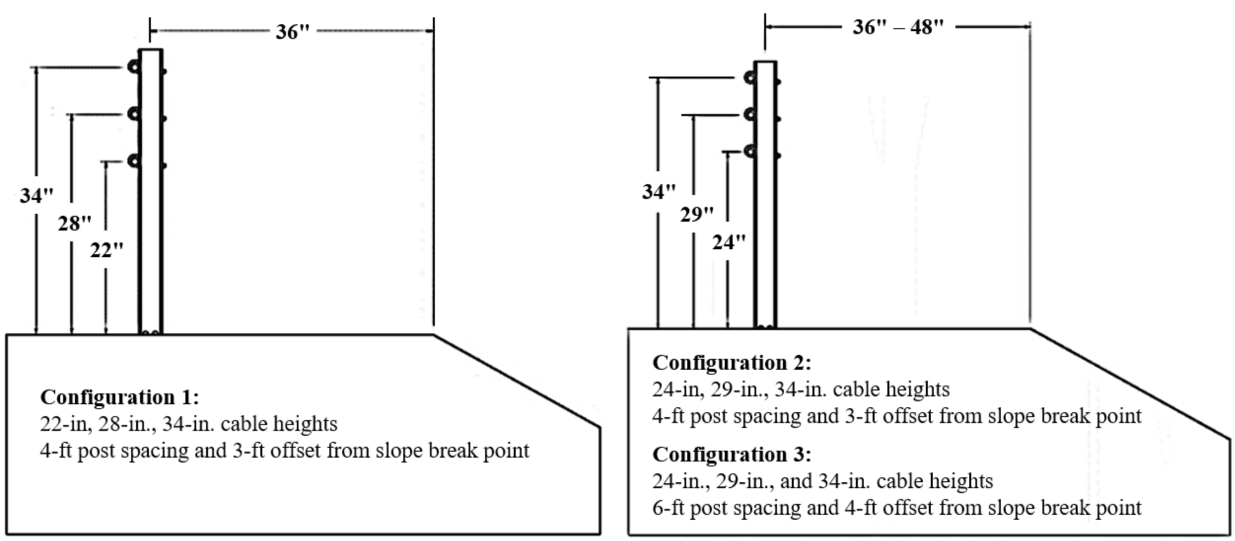

Figure 81. Recommended Configurations, Low-Tension Cable Barrier Adjacent to Steep Slope

9 COST COMPARISON

A critical aspect regarding the feasibility of the low-tension system is a comparison of the cost of different options for treating steep roadside slopes. Recall that one of the objectives of the research effort was to develop a revised, low-tension cable barrier that was lower in cost than the original low-tension cable barrier adjacent to slope design and NDOT's current MGS adjacent to slope design which was evaluated to MASH TL-3 previously [27]. This previous MGS system adjacent to steep slopes consisted of an MGS with 8-ft (2.43-m) long W6x8.5 posts at 75-in. (1,905-mm) spacing installed at the slope break point of a 2H:1V slope. NDOT also utilizes 4H:1V fill slopes adjacent to their roadways as this slope is considered traversable according to the AASHTO *Roadside Design Guide* [28]. Researchers investigated the costs of installing different configurations of the newly recommended low-tension cable barrier system adjacent to steep slope as compared to the original low-tension cable barrier adjacent to slope, the MGS adjacent to steep slope with and without blockouts, and a traversable 4H:1V fill slope.

In order to compare the cost of these alternatives, costs were estimated for each alternative based on material costs and the cost of the associated grading for each alternative. Installation labor and other factors were not considered. For each alternative, steel costs were estimated by summing up the total weight of steel per linear foot for the system and multiplying the weight per foot by a steel cost $2.00 per pound. Note that the newly recommended low-tension cable barrier configuration costs were separated into two categories based on slope offset and post spacing. In the previous section, three alternatives were listed due to differences in cable height, slope offset, and post spacing. However, the variation in cable height did not affect the material costs of the system, so the newly recommended low-tension cable barrier costs were compared based solely on post spacing and slope offset. Finally, timber blockout costs for the MGS were estimated to be $0.50 per pound.

Grading costs were estimated based on a cost of $12 per cubic yard based on information provided by NDOT. Grading cost varied based on the assumed height of the fill slope. As such, a basic grading geometry, as shown in Figure 82, was established for all barriers with an assumed length of 12 ft (3.66 m) and a 2H:1V slope. An assumed length for the grading was selected to allow calculation of soil volume so a subsequent cost per linear foot could be derived. A 2H:1V slope was used for all of the barrier alternatives to provide a more consistent cost comparison. Then, fill slopes of 5 ft, 10 ft, and 20 ft (1.52 m, 3.05 m, and 6.10 m) were developed and the costs per foot of the grading were calculated based $12 per cubic yard estimate provided. Each barrier alternative and the traversable slope were compared at each assumed slope height. It should be noted that the assumptions for the grading costs were based on an assumed soil volume and may not reflect the actual methodology that grading costs would be determined. However, it provided a reasonable starting point for comparison and insight on whether or not the proposed cable on slope systems were feasible. Results of the benefit-to-cost evaluation are shown in Tables 9 through 11.

Review of the cost comparison found that the material costs for the proposed, low-tension cable barrier adjacent to steep slope configurations were less expensive than the original low-tension cable barrier evaluated in test no. CS-2 and the MGS with and without blockouts. This was true even when 4-ft (1.22-m) post spacing was considered. When grading costs were added to the analysis, the proposed, low-tension cable barrier adjacent to steep slope configurations were less expensive that the other barrier alternatives for 5-ft and 10-ft (1.52-m and 3.05-m) high slopes but became slightly more expensive when a 20-ft (6.10-m) tall slope was considered. Application of a traversable 4H:1V slope appeared to be cost effective for only the lowest slope heights. This would suggest that the proposed, low-tension cable barrier configuration would provide for reduced costs in most installation situations. However, final determination of whether or not to use the proposed, low-tension cable barrier adjacent to slope may depend on the size of the slope and the grading costs involved.

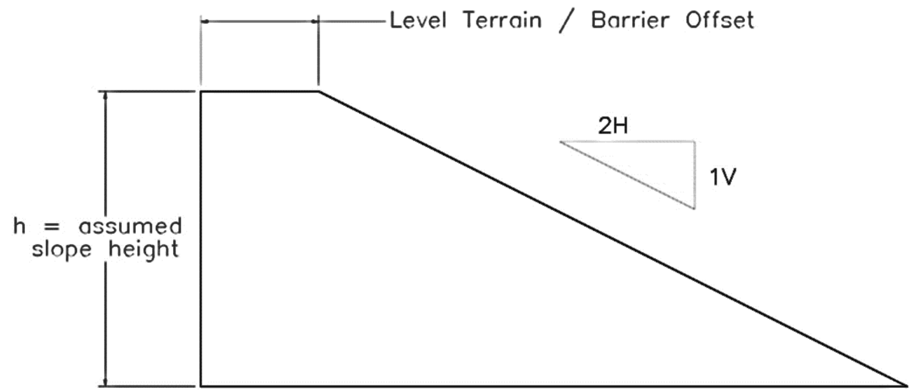

Figure 82. Assumed Geometry for Grading Cost Estimation

Table 9. Cost Comparison for Barrier and Slope Configurations: 2H:1V Slope with 5-ft (1.52-m) Slope Height

Summary of Comparative Costs for Barrier Systems (Slope Height = 5 ft)			
Barrier System	Barrier Material Cost/linear ft	Grading Cost/linear ft	Total Cost/linear ft
Original CS-2 Low-Tension Cable Barrier Adjacent to 2:1 Slope	$27.03	$31.11	$58.14
Proposed Low-Tension Cable Barrier Adjacent to 2:1 Slope, 4 ft post spacing and 3 ft offset	$18.17	$28.89	$47.06
Proposed Low-Tension Cable Barrier Adjacent to 2:1 Slope, 6 ft post spacing and 4 ft offset	$13.88	$31.11	$45.00
Standard MGS @ SBP with 8 ft posts Adjacent to 2:1 Slope	$37.17	$25.56	$62.72
Non-Blocked MGS @ SBP with 8 ft posts Adjacent to 2:1 Slope	$36.17	$22.22	$58.39
4:1 Traversable Slope with No Barrier	$0.00	$44.44	$44.44

Table 10. Cost Comparison for Barrier and Slope Configurations: 2H:1V Slope with 10-ft (3.05-m) Slope Height

Summary of Comparative Costs for Barrier Systems (Slope Height = 10 ft)			
Barrier System	Barrier Material Cost/linear ft	Grading Cost/linear ft	Total Cost/linear ft
Original CS-2 Low-Tension Cable Barrier Adjacent to 2:1 Slope	$27.03	$62.22	$89.25
Proposed Low-Tension Cable Barrier Adjacent to 2:1 Slope, 4 ft post spacing and 3 ft offset	$18.17	$57.78	$75.95
Proposed Low-Tension Cable Barrier Adjacent to 2:1 Slope, 6 ft post spacing and 4 ft offset	$13.88	$62.22	$76.11
Standard MGS @ SBP with 8 ft posts Adjacent to 2:1 Slope	$37.17	$51.11	$88.28
Non-Blocked MGS @ SBP with 8 ft posts Adjacent to 2:1 Slope	$36.17	$44.44	$80.61
4:1 Traversable Slope with No Barrier	$0.00	$88.89	$88.89

Table 11. Cost Comparison for Barrier and Slope Configurations: 2H:1V Slope with 20-ft (6.10-m) Slope Height

Summary of Comparative Costs for Barrier Systems (Slope Height = 20 ft)			
Barrier System	Barrier Material Cost/linear ft	Grading Cost/linear ft	Total Cost/linear ft
Original CS-2 Low-Tension Cable Barrier Adjacent to 2:1 Slope	$27.03	$124.44	$151.47
Proposed Low-Tension Cable Barrier Adjacent to 2:1 Slope, 4 ft post spacing and 3 ft offset	$18.17	$115.56	$133.73
Proposed Low-Tension Cable Barrier Adjacent to 2:1 Slope, 6 ft post spacing and 4 ft offset	$13.88	$124.44	$138.33
Standard MGS @ SBP with 8 ft posts Adjacent to 2:1 Slope	$37.17	$102.22	$139.39
Non-Blocked MGS @ SBP with 8 ft posts Adjacent to 2:1 Slope	$36.17	$88.89	$125.06
4:1 Traversable Slope with No Barrier	$0.00	$177.78	$177.78

10 SUMMARY, CONCLUSIONS, AND RECOMMENDATIONS

In this research effort, modified configurations for a low-tension cable barrier for use adjacent to steep slopes were developed for a barrier system originally developed under NCHRP Report 350 safety criteria. The new, low-tension cable barrier configurations were required to have the capability to meet MASH TL-3 criteria when installed adjacent to slopes as steep as 1.8H:1V. Additionally, it was desired that the new, low-tension cable barrier designs be more cost effective than the MGS installed adjacent to steep slopes and the previous NCHRP Report 350 low-tension cable barrier adjacent to steep slopes.

The research effort began with a literature review, a review of design criteria for the new, low-tension cable barrier system, and development of an initial design concept. The design for the new cable barrier system was based on the original NDOT low-tension cable barrier with basic modifications. The cable heights were raised and the spacing between cables was increased to maintain vehicle capture and stability as the vehicle was redirected and partially traversing a steep slope. A S3x5.7 post section with a soil plate was retained from the original NDOT low-tension cable barrier. Targeted post spacings were 6 ft to 8 ft (1,829 mm to 2,438 mm) and the lateral barrier offset from the slope breakpoint was targeted as 1 ft to 2 ft (305 mm to 610 mm) in order to reduce the cost of the system. The researchers believed that proper performance of the system relied on developing the flexural capacity of the post to limit barrier deflection over the steep slope and maintain vehicle capture during redirection. In order to evaluate the potential for reduced lateral offset from the slope, dynamic component testing of the posts adjacent to a steep slope was conducted to evaluate potential minimum offsets for the posts adjacent to a steep slope and to aid in development of LS-DYNA computer simulation models.

A series of dynamic component tests were conducted on S3x5.7 steel posts to determine the potential minimum offset from the slope that would result in full development of the plastic section of the post. Two tests were conducted on posts installed on level terrain in order to serve as a baseline. Three additional tests were conducted at reduced lateral offsets to a 1.8H:1V slope. Lateral offsets of 24 in. (610 mm), 12 in. (305 mm), and 6 in. (152 mm), were evaluated and compared with the level terrain tests. The results from these tests found that a 6-in. (152-mm) offset from the 1.8H:1V slope may be at or past the limit for acceptable performance for the S3x5.7 as the post began to rotate through the soil instead of only bending near ground line. However, testing of the larger offsets indicated that the flexural strength of the post could be fully developed at offsets of 12 in. (305 mm) or greater.

Following the component testing of the S3x5.7 posts adjacent to slopes, the researchers reviewed ongoing research regarding a nonproprietary, high-tension cable median barrier. The nonproprietary, high-tension cable median barrier was being tested and evaluated with the newly developed Midwest Weak Post (MWP) section. The full-scale crash testing of the system with the 1100C small car vehicle indicated that the flanges of the MWP post could lacerate and penetrate the floorboard of the vehicle as it overrode the weak axis of the posts, which raised concerns that the flanges of the S3x5.7 post intended for the low-tension cable barrier adjacent to slopes could pose similar floorboard laceration and penetration issues. In order to evaluate that concern, a dynamic component test, test no. LTCB-6, was undertaken that overrode the S3x5.7 posts with a specialized bogie vehicle with a simulated floorboard. The results of test no. LTCB-6 indicated that the S3x5.7 would likely penetrate a vehicle floorboard.

In order to alleviate concerns for the S3x5.7 post penetrating the floorboard, an alternative cable post design developed for use in the high-tension cable median barrier was adopted for the design. The Midwest Tube Post (MTP), an HSS3x2x⅛ post with two ¾-in. (19-mm) diameter holes at ground line, was chosen for the post section as it met the design criteria for strong and weak axis post strength and showed the potential to mitigate floorboard tearing.

Additional dynamic component tests were conducted on the MTP post at reduced offsets to a steep slope to determine a minimum offset from the slope break point where the post bending capacity could be fully developed similar to the previous component testing of the S3x5.7 post. For tests nos. CTPS-1 and CTPS-2, dynamic component tests were conducted on MTPs with offset distances of 12 in. (305 mm) and 6 in. (152 mm) from the slope break point of a 1.8H:1V slope, respectively. The post in test no. CTPS-2 caused the soil at the slope break point to heave and break out behind the post, whereas the post in test no. CTPS-1 rotated and plastically deformed in the soil with little to no soil deformation. Additionally, reduced slope offset in test no. CTPS-2 resulted in plastic hinging of the post well below grade, which was a departure from the behavior of the MTP post when evaluated on level terrain. These factors led to concern that the use of a 6 in. (152 mm) offset to the slope break point may lead to inconsistent post loading and energy dissipation. Therefore, researchers recommend a minimum offset of the posts from the SBP of 12 in. (305 mm) to ensure that the behavior of the MTP post adjacent to slope was consistent with its behavior when installed on level terrain.

LS-DYNA computer simulation was used to evaluate potential configurations for the revised low-tension cable barrier adjacent to steep slopes. The researchers developed calibrated models of the posts, cable-to-post attachments, and utilized validated models of cables and vehicles. Simulation models of the original low-tension cable barrier adjacent to slope were conducted to build confidence in the simulation approach. Simulations of test nos. CS-1 and CS-2 on the original low-tension cable barrier adjacent to slope design compared favorably to test results. Therefore, researchers performed simulations with the MASH 2270P vehicle on modified configurations of the original low-tension cable barrier in order to redesign the barrier to meet the project objectives. The simulated low-tension barrier configurations adjacent to a 1.8H:1V slope utilized MTP posts, 6-in. (152-mm) vertical cable spacing, 22-in. or 24-in. (559-mm or 610-mm) bottom cable heights, 4-ft, 6-ft, or 8-ft (1.2-m, 1.8-m, or 2.4-m) post spacings, and 1-ft, 2-ft, 3-ft, or 4-ft (0.3-m, 0.6-m, 0.9-m, or 1.2-m) offsets from the slope break point to the back flange of the posts. The simulation results were then reviewed to identify which configurations had the greatest potential to meet MASH TL-3.

The simulation of the modified low-tension cable barrier configurations found that a bottom cable height of 24 in. (610 mm) allowed for capture of the vehicle with all three cables as opposed to two cables for the configurations with a bottom cable height of 22 in. (559 mm). This improved cable engagement and led to reduced barrier deflections and vehicle extension over the slope. Reduced post spacing had the largest effect on reducing barrier deflection. Slope offset did not tend to reduce barrier deflections, but it did reduce vehicle extension over the slope and consequently improved vehicle stability. The researchers found that barrier configurations that allowed all four of the pickup truck wheels to extend past the slope break point had reduced vehicle capture and much higher instability as compared to simulations where one side of the vehicle wheels remained on the shoulder or level terrain during redirection. Based on this criteria, low-tension cable barrier configurations were identified and recommended which indicated that at least two wheels (non-impact side of the vehicle) would remain on the flat terrain behind the system. These systems were believed to provide the highest potential for the low-tension cable barrier to satisfy MASH criteria for test designation no. 3-11 when installed adjacent to slopes as steep as 1.8H:1V.

Three barrier configurations were identified for potential use which met the design criteria and had a good probability of satisfying MASH TL-3 safety criteria.

1. Cables at heights of 22 in., 28 in., and 34 in. (559 mm, 711 mm, and 864 mm) supported by MWP posts spaced at 4 ft (1.2 m) on-center and offset 3 ft (0.9 m) from the slope break point.

2. Cables at heights of 24 in., 29 in., and 34 in. (610 mm, 739 mm, and 864 mm) supported by MWP posts spaced at 4 ft (1.2 m) on-center and offset 3 ft (0.9 m) from the slope break point.

3. Cables at heights of 24 in., 29 in., and 34 in. (610 mm, 739 mm, and 864 mm) supported by MWP posts spaced at 6 ft (1.8 m) on-center and offset 4 ft (1.2 m) from the slope break point.

Finally, the researchers investigated the costs of installing the three configurations of the newly recommended low-tension cable barrier system adjacent to steep slope as compared to the original low-tension cable barrier adjacent to slope, the MGS adjacent to steep slope with and without blockouts, and a traversable 4H:1V fill slope. The cost comparison found that the proposed, low-tension cable barrier adjacent to steep slope configurations were less expensive that the other barrier alternatives for 5-ft and 10-ft (1.52-m and 3.05-m) high slopes but became slightly more expensive when a 20-ft (6.10-m) tall slope was considered. This would suggest that the proposed, low-tension cable barrier configuration would provide for reduced costs in most installation situations.

In summary three potential options were developed for a low-tension cable barrier installed adjacent to slopes as steep as 1.8H:1V through computer simulation modeling with LS-DYNA. The newly developed options were all more cost effective than the current design and available guardrail options based on a simple cost analysis. Full-scale testing of the recommended configurations according to the MASH TL-3 requirements for cable barriers would be required prior to implementing these designs in order to verify their safety performance. Finally, the low-tension cable barrier options developed herein would also have the potential to be used as a MASH TL-3 generic, roadside cable barrier if they were full-scale crash tested. Currently no MASH TL-3 generic option exists for roadside cable barrier. Note that implementation of a generic, roadside cable barrier would also require development and evaluation of an end terminal for the system.

11 REFERENCES

1. Nelson, R.M., Sicking, D.L., Faller, R.K., Reid, J.D., Rohde, J.R., Polivka, K.A., Hascall, J.A., *Evaluation of Alternate Cable Anchor Designs and Three-Cable Guardrail Adjacent to Steep Slope*, Report No. TRP-03-155-05, Midwest Roadside Safety Facility, University of Nebraska-Lincoln, Lincoln, NE, February 3, 2005.

2. Ross, H.E., Sicking, D.L., Zimmer, R.A., and Michie, J.D., *Recommended Procedures for the Safety Performance Evaluation of Highway Features*, National Cooperative Highway Research Program (NCHRP) Report 350, Transportation Research Board, Washington, D.C., 1993.

3. Terpsma, R.J., Polivka, K.A., Sicking, D.L., Rohde, J.R., Reid, J.D., Faller, R.K., *Evaluation of a Modified Three Cable Guardrail Adjacent to Steep Slope*, Report No. TRP-03-192-08, Midwest Roadside Safety Facility, University of Nebraska-Lincoln, Lincoln, NE, March 4, 2008.

4. *Manual for Assessing Safety Hardware (MASH), Second Edition*, American Association of State Highway and Transportation Officials (AASHTO), Washington, D.C., 2016.

5. *Manual for Assessing Safety Hardware (MASH)*, American Association of State Highway and Transportation Officials (AASHTO), Washington, D.C., 2009.

6. Schmidt T., Lechtenberg K.A., Meyer C., Faller R.K., Bielenberg R., Reid J.D., Sicking D.L., *Evaluation on the New York Low-Tension Three-Cable Barrier on Curved Alignment*, Report No. TRP-03-263-12, Midwest Roadside Safety Facility, University of Nebraska-Lincoln, Lincoln, Nebraska, February 19, 2013.

7. Stolle C., Faller R.K., Lechtenberg K.A., *Dynamic Impact Testing of S76x8.5(S3x5.7) Steel Posts for Use in Cable Guardrail Systems*, Report No. TRP-03-186-07, Midwest Roadside Safety Facility, University of Nebraska-Lincoln, Lincoln, Nebraska, December 19, 2007.

8. Bielenberg R., Schmidt T., Faller R.K., Rosenbaugh S.K., Lechtenberg K.A., Reid J.D., Sicking D.L., *Design of an Improved Post for Use in a Nonproprietary High-Tension Cable Median Barrier*, Report No. TRP-03-286-15, Midwest Roadside Safety Facility, University of Nebraska-Lincoln, Lincoln, Nebraska, May 07, 2015.

9. Meyer, D.T., Lechtenberg, K.A., Faller, R.K., Bielenberg, R.W., Rosenbaugh, S.K., and Reid, J.D., *MASH Test No. 3-10 of a Nonproprietary, High-Tension Cable Median Barrier for Use in 6H:1V V-Ditch (Test No. MWP-8)*, Report No. TRP 03-331-17, Midwest Roadside Safety Facility, University of Nebraska-Lincoln, Lincoln, Nebraska, May 10, 2017.

10. Asadollahi Pajouh, M., Lechtenberg, K.A., Faller, R.K., Holloway, J.C., Bielenberg, R.W., Rosenbaugh, S.K., and Reid, J.D., *MASH Test No. 3-10 of a Nonproprietary, High-Tension, Cable Median Barrier for Use in 6H:1V V-Ditch (Test No. MWP-9)*, Report No. TRP 03-360-18, Midwest Roadside Safety Facility, University of Nebraska-Lincoln, Lincoln, Nebraska, March 30, 2018.

11. Rosenbaugh S.K., Hartwell J.A., Bielenberg R., Faller R.K., Holloway J., Lechtenberg K.A., *Evaluation of Floorboard Tearing and Cable Splices for Cable Barrier System*, Report No. TRP-03-324-17, Project No.: TPF-5(193), Midwest Roadside Safety Facility, University of Nebraska-Lincoln, Lincoln, Nebraska, May 16, 2017.

12. Asadollahi Pajouh, M., Faller, R.K., Lechtenberg, K.A., Holloway, J.C., and Bielenberg, R.W., *Design of Closed-Section Post for Use in a Nonproprietary High-Tension Cable Median Barrier*, Report No. TRP-03-380-19, Midwest Roadside Safety Facility, University of Nebraska-Lincoln, Lincoln, Nebraska, April 22, 2019.

13. Society of Automotive Engineers (SAE), *Instrumentation for Impact Test – Part 1 – Electronic Instrumentation*, SAE J211/1 MAR95, New York City, NY, July 2007.

14. Hallquist, J.O., *LS-DYNA Keyword User's Manual*, Livermore Software Technology Corporation, Livermore, California, 2007.

15. Kuipers, B.D. and Reid, J.D., *Testing of M203.7x9.7 (M8x6.5) and S76x8.5 (S3x5.7) Steel Posts - Post Comparison Study for the Cable Median Barrier*, Report No. TRP 03-143-03, Midwest Roadside Safety Facility, University of Nebraska-Lincoln, Lincoln, NE, October 24, 2003.

16. Schneider, A.J., Rosenbaugh, S.K., Faller, R.K., Sicking, D.L., Lechtenberg, K.A., and Reid, J.D., *Safety Performance Evaluation of Weak-Post, W-Beam Guardrail Attached to Culvert*, Report No. TRP 03-277-14, Midwest Roadside Safety Facility, University of Nebraska-Lincoln, Lincoln, Nebraska, February 12, 2014.

17. Luttig, M., Lechtenberg, K.A., *Cut Cable Post Bogie Testing, Test Nos. CCP-1 through CCP-11*, Internal Report for Midwest Roadside Safety Facility, Midwest Roadside Safety Facility, University of Nebraska-Lincoln, Lincoln, Nebraska, February 19, 2012.

18. Reid, J.D., and Coon, B.A., "Finite Element Modeling of Hook Bolts," 7th International LS-DYNA Users Conference, Dearborn, MI, May 19-21, 2002.

19. Stolle, C.S. Reid, J.D., and Bielenberg, R.W., *Improved Models of Cable-To-Post Attachments for High-Tension Cable Barriers*, Report No. TRP 03-267-12, Midwest Roadside Safety Facility, University of Nebraska-Lincoln, Lincoln, Nebraska, May 25, 2012.

20. C.S. Stolle and J.D. Reid, "Modeling Wire Rope Used in Cable Barrier Applications," *11th International LS-DYNA User's Conference*, Dearborn, MI, June 6-8, 2010, pp. 331-341.

21. Reid, J.D. and C.S. Stolle, *Development of a Wire Rope Model for Cable Guardrail Simulation*, International Journal of Crashworthiness, Vol 16, Issue 3, pp. 331-341, June 2011.

22. Stolle, C.S., Sicking, D.L., Faller, R.K., and Reid, J.D., *Cable Median Barrier Failure Analysis and Remediation Phase II*, Report No. TRP 03-319-13, Midwest Roadside Safety Facility, University of Nebraska-Lincoln, Lincoln, Nebraska, June 30, 2013.

23. Lechtenberg, K.A., Ball T.B., Faller, R.K., Holloway, J.C., and Loken, A.E., *MASH Test Nos. 3-11 & 3-17 of a Nonproprietary, High-Tension Cable Median Barrier with Closed-Section Posts*, Draft Report to the Midwest State's Pooled Fund Program, Report No. TRP 03-431-21, Midwest Roadside Safety Facility, University of Nebraska-Lincoln, Lincoln, Nebraska, July 16, 2020.

24. Asadollahi Pajouh, M., Lechtenberg, K.A., Faller, R.K., Holloway, J.C., Bielenberg, R.W., Rosenbaugh, S.K., and Reid, J.D., *MASH Test No. 3-10 of a Nonproprietary, High-Tension, Cable Median Barrier for Use in 6H:1V V-Ditch (Test No. MWP-9)*, Report No. TRP 03-360-18, Midwest Roadside Safety Facility, University of Nebraska-Lincoln, Lincoln, Nebraska, March 30, 2018.

25. Schmidt, T.L., Lechtenberg, K.A., Meyer, C.L., Faller, R.K., Bielenberg, R.W., Reid, J.D., and Sicking, D.L., *Evaluation of the New York Low-Tension Three-Cable Barrier on Curved Alignment*, Report No. TRP 03-263-12, Midwest Roadside Safety Facility, University of Nebraska-Lincoln, Lincoln, Nebraska, February 19, 2013.

26. Mongiardini, M., Faller, R.K., Rosenbaugh, S.K., and Reid, J.D., *Test Matrices for Evaluating Cable Median Barriers Placed in V-Ditches*, Report No. TRP-03-265-12, Midwest Roadside Safety Facility, University of Nebraska-Lincoln, Lincoln, Nebraska, July 13, 2012.

27. Wiebelhaus, M.J., Lechtenberg, K.A., Faller, R.K., Sicking, D.L., Bielenberg, R.W., Reid, J.D., Rohde, J.R., and Dey, Gopi, *Development and Evaluation of the Midwest Guardrail System (MGS) Placed Adjacent to a 2:1 Fill Slope*, Report No. TRP-03-185-10, Midwest Roadside Safety Facility, University of Nebraska-Lincoln, Lincoln, Nebraska, February 24, 2010.

28. *Roadside Design Guide, 4th Edition, 2011*, American Association of State Highway and Transportation Official (AASHTO), Washington, D.C., 2011.

12 APPENDICES

Appendix A. Material Specifications

Table A-1. Bill of Materials, Test Nos. LTCB-1 through LTCB-6

Item No.	Description	Material Specification	Reference
a1	S3x5.7 by 63"[1,575] Long Steel Post with 8"x24"x¼" [203x610x6] Soil Plate	ASTM A992, ASTM A572-Grade 50, ASTM A709-Grade 50	H#59058160/03 H#A412401 H#B408682
N/A	HSS3x2x⅛ by 78" [1,981] Long Steel Post	ASTM A500 Grade B	H#843Y67990

N/A – Not Applicable

GERDAU

US-ML-MIDLOTHIAN
300 WARD ROAD
MIDLOTHIAN, TX 76065
USA

CERTIFIED MATERIAL TEST REPORT

Page 1/1

CUSTOMER SHIP TO	CUSTOMER BILL TO	GRADE	SHAPE / SIZE	
STEEL & PIPE SUPPLY CO INC 1003 FORT GIBSON RD CATOOSA,OK 74015-3033 USA	STEEL & PIPE SUPPLY CO INC MANHATTAN,KS 66505-1688 USA	A36/A57250	Standard I-Beam / 3 X 5.7# / 75 X 8.5	
		LENGTH 40'00"	WEIGHT 8,208 LB	HEAT / BATCH 59058160/03
SALES ORDER 812105/000020	CUSTOMER MATERIAL Nº 000000000035357040	SPECIFICATION / DATE or REVISION A36/A36M-08 A572/A572M-07 ASTM A6/A6M-11		

CUSTOMER PURCHASE ORDER NUMBER	BILL OF LADING	DATE
4500221191	1327-0000099969	04/02/2014

CHEMICAL COMPOSITION

C %	Mn %	P %	S %	Si %	Cu %	Ni %	Cr %	Mo %	Sn %	V %	Nb %	Al %
0.09	0.79	0.014	0.026	0.20	0.36	0.11	0.06	0.027	0.009	0.001	0.011	0.003

CHEMICAL COMPOSITION

CEqyA6 %
0.3

MECHANICAL PROPERTIES

YS KSI	UTS KSI	YS MPa	UTS MPa	G/L Inch	G/L mm
53.4	69.5	382	468	8.000	200.0
55.3	67.9	368	479	8.000	200.0

MECHANICAL PROPERTIES

Elong. %	Y/T rati %
23.20	0.786
23.60	0.796

COMMENTS / NOTES

Low Tension Cable Barrier R# 15-0470
Soil-plated S3x5.7 posts
QTY 5
SMT March 2015

The above figures are certified chemical and physical test records as contained in the permanent records of company. This material, including the billets, was melted and manufactured in the USA. CMTR complies with EN 10204 3.1.

Bhaskar — BHASKAR YALAMANCHILI, QUALITY DIRECTOR

Tom L Harrington — TOM HARRINGTON, QUALITY ASSURANCE MGR.

Figure A-1. Material Specifications, S3x5.7 Steel Posts, Test Nos. LTCB-1 through LTCB-6

STEEL AND PIPE SUPPLY
SPS Coil Processing Tulsa
5275 Bird Creek Ave.
Port of Catoosa, OK 74015

METALLURGICAL TEST REPORT

PAGE 1 of 1
DATE 02/24/2015
TIME 11:35:46
USER GIANGRER

SOLD TO
12946
Wheeler Metals, Inc.
3100 W. 40th Street North
Muskogee OK 74401

SHIP TO
20484
Wheeler Metals, Inc. - CPU
5275 Bird Creek Avenue
Catoosa OK 74015

Order	Material No.	Description	Quantity	Weight	Customer Part	Customer PO	Ship Date
1805391-0140	70872120	1/4 72 X 120 A36 STP MIL PLT				MSK-0217-JP	02/24/2015

Chemical Analysis

Heat No. A412401 Vendor STEEL DYNAMICS COLUMBUS DOMESTIC Mill SEVERSTAL COLUMBUS **Melted and Manufactured in the USA**
Batch 0003708996 6 EA 3,675.600 LB **Produced from Coil**

Carbon	Manganese	Phosphorus	Sulphur	Silicon	Nickel	Chromium	Molybdenum	Boron	Copper	Aluminum	Titanium	Vanadium	Columbium	Nitrogen	Tin
0.1900	0.8100	0.0150	0.0030	0.0200	0.0300	0.0700	0.0100	0.0001	0.0700	0.0320	0.0010	0.0040	0.0010	0.0062	0.0040

Mechanical/ Physical Properties

Mill Coil No. A412401-05

Tensile	Yield	Elong	Rckwl	Grain	Charpy	Charpy Dr	Charpy Sz	Temperature	Olsen
79800.000	57400.000	26.90			0	NA			
75400.000	53100.000	27.60			0	NA			
74700.000	53100.000	28.10			0	NA			

THE CHEMICAL, PHYSICAL, OR MECHANICAL TESTS REPORTED ABOVE ACCURATELY REFLECT INFORMATION AS CONTAINED IN THE RECORDS OF THE CORPORATION.

Figure A-2. Material Specifications, S3x5.7 Steel Posts, Test Nos. LTCB-1 through LTCB-6

SPS Coil Processing Tulsa
5275 Bird Creek Ave.
Port of Catoosa, OK 74015

SPS STEEL & PIPE SUPPLY COMPANY INC.

METALLURGICAL TEST REPORT

PAGE 1 of 1
DATE 07/23/2014
TIME 16:01:58
USER MEHEULAL

SOLD TO

SHIP TO
13716
Warehouse 0040
401 New Century Parkway
New Century KS 66031

Order	Material No.	Description	Quantity	Weight	Customer Part	Customer PO	Ship Date
40225824-0020	701072120TM	5/16 72 X 120 A36 TEMPERPASSED STPMPL	13	9,952.800			07/23/2014

Chemical Analysis

Heat No. B408682 Vendor SEVERSTAL COLUMBUS DOMESTIC Mill SEVERSTAL COLUMBUS Melted and Manufactured in the USA

Batch 0003091201 13 EA 9,952.800 LB Produced from Coil

Carbon	Manganese	Phosphorus	Sulphur	Silicon	Nickel	Chromium	Molybdenum	Boron	Copper	Aluminum	Titanium	Vanadium	Columbium	Nitrogen	Tin
0.2000	0.8600	0.0140	0.0040	0.0200	0.0400	0.0700	0.0100	0.0001	0.0700	0.0250	0.0010	0.0060	0.0020	0.0058	0.0050

Mechanical/ Physical Properties

Mill Coil No. B408682-06

Tensile	Yield	Elong	Rckwl	Grain	Charpy	Charpy Dr	Charpy Sz	Temperature	Olsen
75300.000	51400.000	32.00	0	0.000	0	NA			
73700.000	50400.000	29.00	0	0.000	0	NA			

THE CHEMICAL, PHYSICAL, OR MECHANICAL TESTS REPORTED ABOVE ACCURATELY REFLECT INFORMATION AS CONTAINED IN THE RECORDS OF THE CORPORATION.

Figure A-3. Material Specifications, S3x5.7 Steel Posts, Test Nos. LTCB-1 through LTCB-6

MARUICHI LEAVITT PIPE AND TUBE

MATERIAL TEST REPORT

ORIGINAL

M/C No. MC0000048473
Date 11/28/2017

BL No. SH0000056242
Destination NORFOLK IRON&METAL - NORFOLK NE
Supplier NORFOLK IRON&METAL - BILLTO

MARUICHI LEAVITT PIPE & TUBE, LLC
1717 W. 115th St.
Chicago, IL 60643
TEL: (773) 239-7700 FAX: (773) 239-1023

	SPEC / SIZE / Customer PO No. / Customer Item No.	No of PCS / Calculated Wt(LBS)	Heat No	Chemical Composition(Ladle Analysis) C (%) x 100	Si (%) x 100	Mn (%) x 100	P (%) x 1000	S (%) x 1000	Cu (%) x 1000	Ni (%) x 1000	Cr (%) x 1000	Mo (%) x 1000	V (%) x 1000	Tensile Test Yield Strength (PSI)	Tensile Strength (PSI)	Elongation (%)	Hydrostatic Test Pressure (PSI) Result	Bending Test / Flattening Test	Remarks
1	ASTM A500/A500M-13 GRADE B ERW TUBING 3IN x 2IN x 0.125IN x 20FT HRB 01024356 / 00949	72 5,616	831Y07990	9	1	116	12	4	26	10	20	3	1	57,498	59,439	29			SA0000135198
2	ASTM A500/A500M-13 GRADE B ERW TUBING 3IN x 2IN x 0.125IN x 20FT HRB 01024356 / 00949	180 14,040	843Y67990	9	1	112	11	3	22	10	30	3	1	61,909	68,136	25			SA0000135198 A500 Grade B/C
3	ASTM A500/A500M-13 GRADE B ERW TUBING 3IN x 2IN x 0.125IN x 24FT HRB 01024356 / 00954	108 10,110	748227	8	2	124	13	5	20	10	40	10	2	56,829	61,113	29			SA0000135198
4	ASTM A500/A500M-13 GRADE B ERW TUBING 3IN x 2IN x 0.125IN x 24FT HRB 01024356 / 00954	144 13,480	748229	8	1	123	9	5	30	10	30	10	2	51,429	58,557	29			SA0000135198
5	ASTM A500/A500M-13 GRADE B ERW TUBING 4IN x 2IN x 0.188IN x 24FT HRB 01024356 / 00857	32 5,276	746684	17	1	76	10	5	20	10	30	10	2	59,320	67,794	32			SA0000135198 A500 Grade B/C

Made and Melted in The U.S.A.
This material has not come in direct contact with mercury during the manufacturing or testing processes. No Weld Repair.
Remarks:

We hereby certify that the material described herein conforms fully to the said specification.

Maruichi Leavitt Pipe & Tube, LLC

F-824-101 - Rev. 0

Figure A-4. Material Specifications, HSS3x2x⅛ Steel Posts, Test Nos. CPTS-1 through CTPS-2

Appendix B. Bogie Test Results, Test Nos. LTCB-1 through LTCB-6

The results of the recorded data from each accelerometer for every dynamic bogie test are provided in the summary sheets found in this appendix. Summary sheets include acceleration, velocity, and deflection vs. time plots as well as force vs. deflection and energy vs. deflection plots.

MIDWEST ROADSIDE SAFETY FACILITY

Bogie Test Summary

Test Information

Test Description:	S3x5.7 Low-Tension Cable Post on Level Terrain
Test Number:	LTCB-1
Test Date:	5/27/2015
Failure Type:	Post yielding and rotation in soil

Post Properties

Post Type:	S3x5.7 with 8"x24"x1/4" Soil Plate
Post Size:	S3x5.7
Post Length:	63
Embedment Depth:	30
Orientation:	Strong Axis

Soil Properties

Gradation:	072014
Moisture Content:	NA
Compaction Method:	HE8

Bogie Properties

Impact Velocity:	19.92 mph	(29.21 ft/s)
Impact Height:	22	
Bogie Mass:	1868 lb	

Data Acquired

Accelerometer:	SLICE-2
Camera Data:	AOS-8

Test Results Summary

Event Duration:	0.1397	sec
Max. Deflection:	39.8	in.
Peak Force:	7.0	k
Initial Linear Stiffness:	2.3	k/in.
Total Energy:	142.9	k-in.

	@ 5"	@ 10"	@ 15"	@20"
Average Force (k)	4.66	5.08	5.33	5.39
Energy (k-in.)	23.3	50.8	79.9	107.9

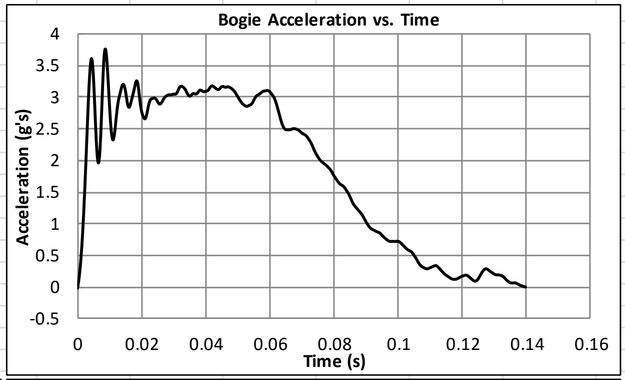

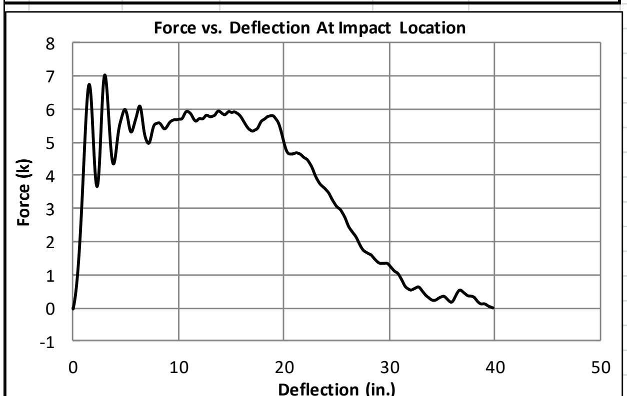

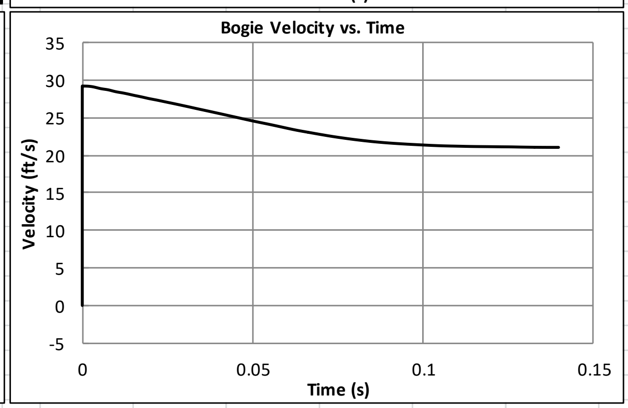

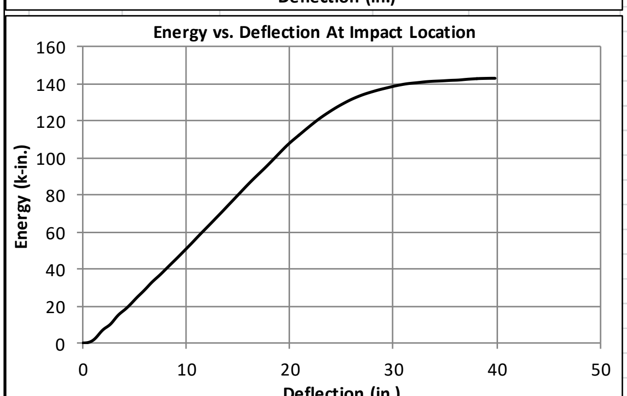

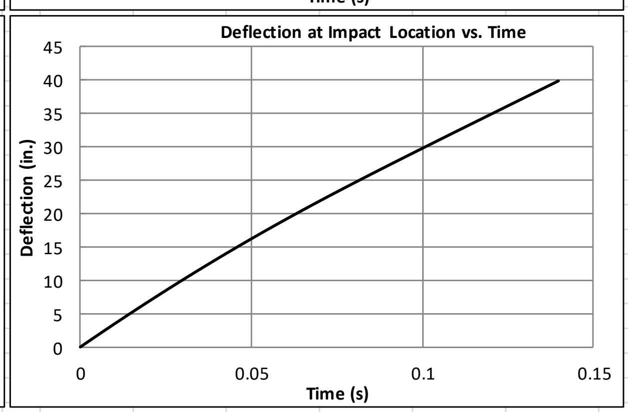

Figure B-1. Test No. LTCB-1 Results (SLICE-2)

MIDWEST ROADSIDE SAFETY FACILITY

Bogie Test Summary

Test Information	
Test Description:	S3x5.7 Low-Tension Cable Post on Level Terrain
Test Number:	LTCB-2
Test Date:	5/27/2015
Failure Type:	Post yielding and rotation in soil
Post Properties	
Post Type:	S3x5.7 with 8"x24"x1/4" Soil Plate
Post Size:	S3x5.7
Post Length:	63
Embedment Depth:	30
Orientation:	Strong Axis
Soil Properties	
Gradation:	072014
Moisture Content:	NA
Compaction Method:	HE8
Bogie Properties	
Impact Velocity:	21.88 mph (32.09 ft/s)
Impact Height:	22
Bogie Mass:	1868 lb
Data Acquired	
Accelerometer:	SLICE-2
Camera Data:	AOS-8

Test Results Summary		
Event Duration:	0.1225	sec
Max. Deflection:	39.4	in.
Peak Force:	7.6	k
Initial Linear Stiffness:	3.8	k/in.
Total Energy:	163.6	k-in.

	@ 5"	@ 10"	@ 15"	@20"
Average Force (k)	4.53	5.14	5.50	5.60
Energy (k-in.)	22.7	51.4	82.4	112.0

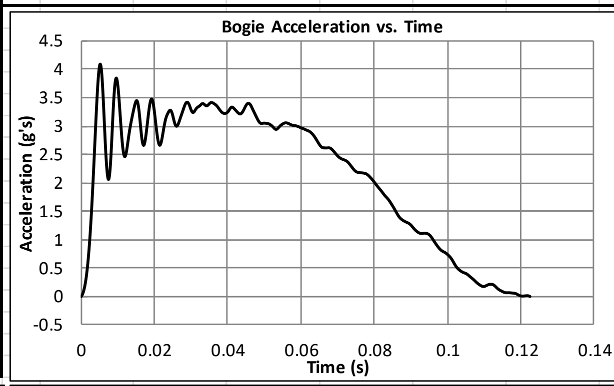

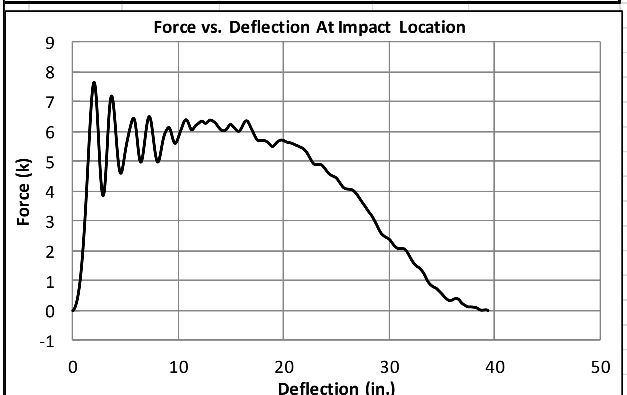

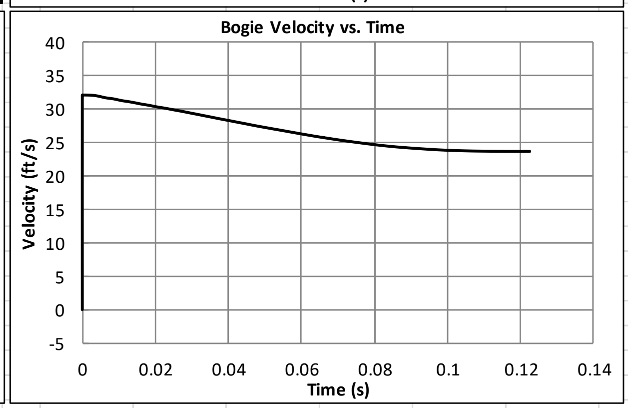

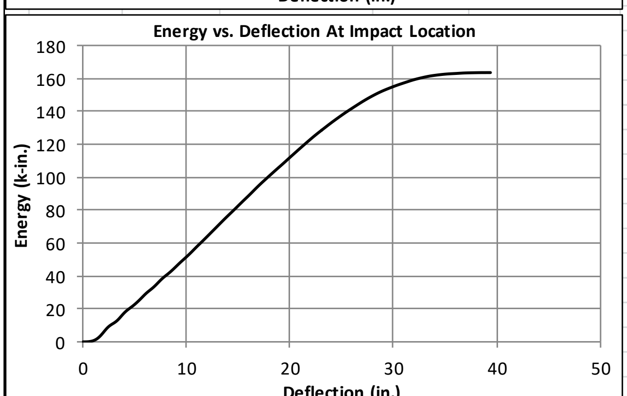

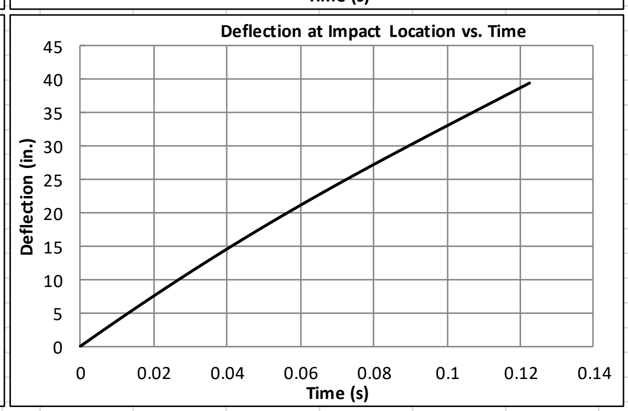

Figure B-2. Test No. LTCB-2 Results (SLICE-2)

MIDWEST ROADSIDE SAFETY FACILITY

Bogie Test Summary

Test Information		
Test Description:	S3x5.7 Low-Tension Cable Post 2 ft Offset from 1.8:	
Test Number:	LTCB-3	
Test Date:	5/28/2015	
Failure Type:	Post yielding with minor soil displacement	
Post Properties		
Post Type:	S3x5.7 with 8"x24"x1/4" Soil Plate (impact side of po	
Post Size:	S3x5.7	
Post Length:	63	
Embedment Depth:	30	
Orientation:	Strong Axis	
Soil Properties		
Gradation:	072014	
Moisture Content:	NA	
Compaction Method:	HE8	
Bogie Properties		
Impact Velocity:	20.85 mph	(30.58 ft/s)
Impact Height:	22	
Bogie Mass:	1868 lb	
Data Acquired		
Accelerometer:	SLICE-2	
Camera Data:	AOS-8	

Test Results Summary		
Event Duration:	0.1266	sec
Max. Deflection:	39.4	in.
Peak Force:	7.6	k
Initial Linear Stiffness:	4.2	k/in.
Total Energy:	131.6	k-in.

	@ 5"	@ 10"	@ 15"	@20"
Average Force (k)	4.91	5.50	5.65	5.20
Energy (k-in.)	24.6	55.0	84.7	104.1

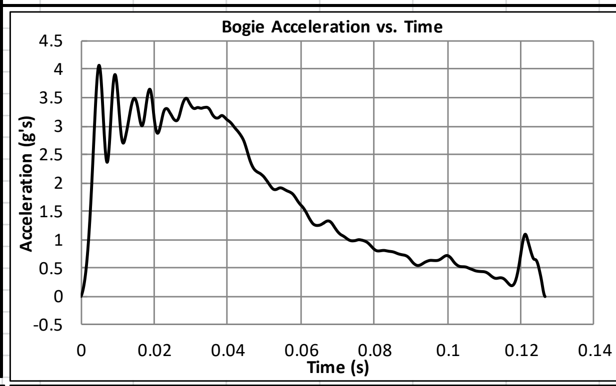

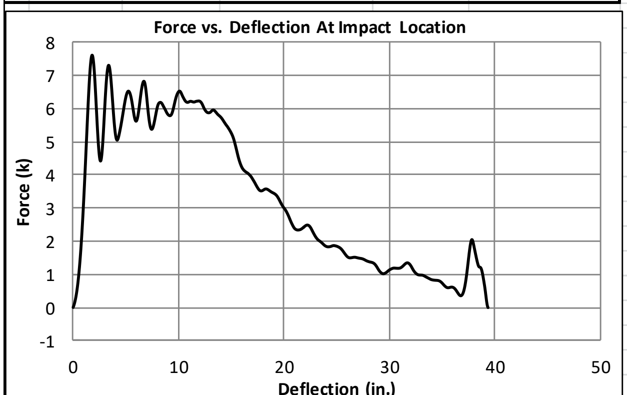

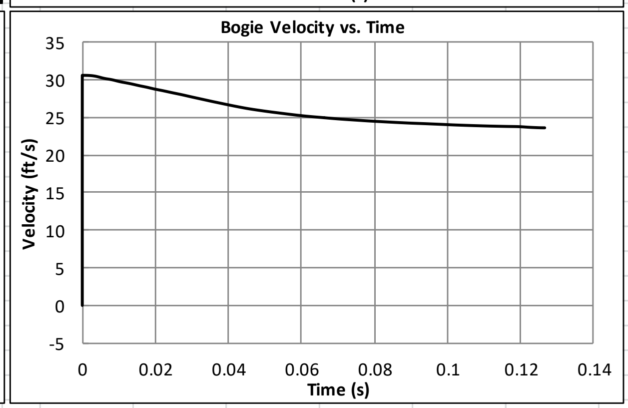

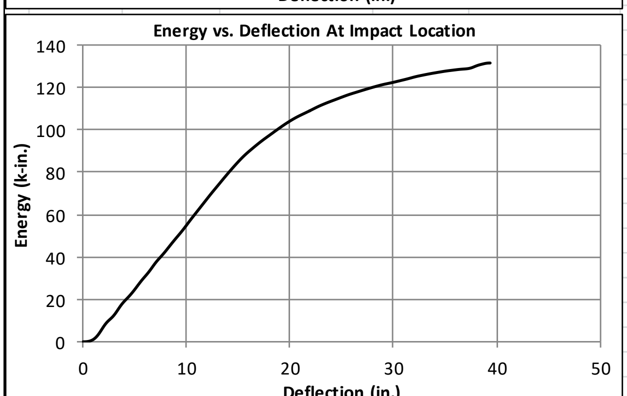

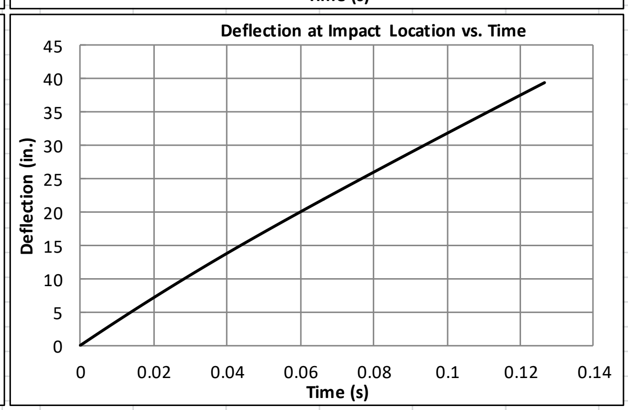

Figure B-3. Test No. LTCB-3 Results (SLICE-2)

MIDWEST ROADSIDE SAFETY FACILITY

Bogie Test Summary

Test Information		
Test Description:	S3x5.7 Low-Tension Cable Post 1 ft Offset from 1.8:	
Test Number:	LTCB-4	
Test Date:	6/1/2015	
Failure Type:	Post yielding with minor soil displacement	
Post Properties		
Post Type:	S3x5.7 with 8"x24"x1/4" Soil Plate (impact side of po	
Post Size:	S3x5.7	
Post Length:	63	
Embedment Depth:	30	
Orientation:	Strong Axis	
Soil Properties		
Gradation:	072014	
Moisture Content:	NA	
Compaction Method:	HE8	
Bogie Properties		
Impact Velocity:	20.35 mph	(29.85 ft/s)
Impact Height:	22	
Bogie Mass:	1868 lb	
Data Acquired		
Accelerometer:	SLICE-2	
Camera Data:	AOS-8	

Test Results Summary		
Event Duration:	0.1209	sec
Max. Deflection:	36.5	in.
Peak Force:	7.2	k
Initial Linear Stiffness:	4.9	k/in.
Total Energy:	127.4	k-in.

	@ 5"	@ 10"	@ 15"	@20"
Average Force (k)	5.07	5.69	5.80	5.31
Energy (k-in.)	25.4	56.9	87.0	106.1

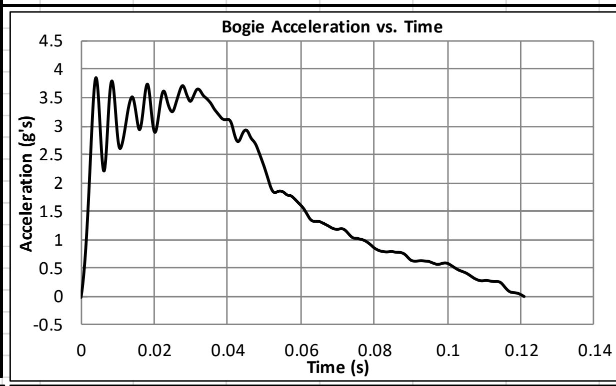

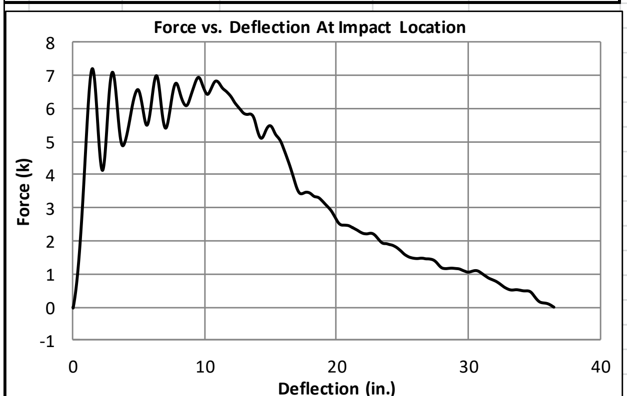

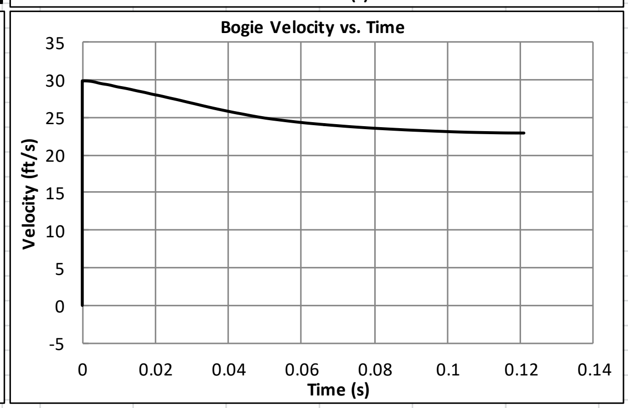

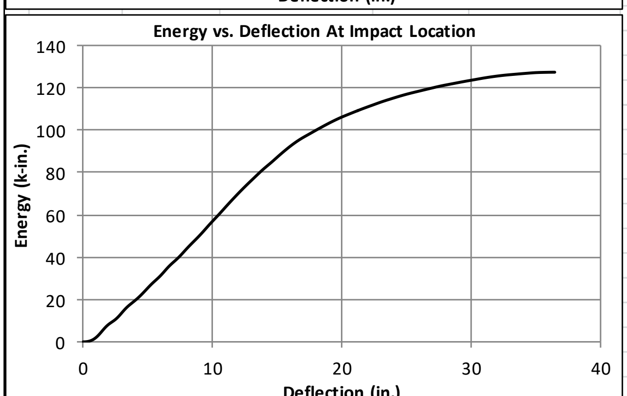

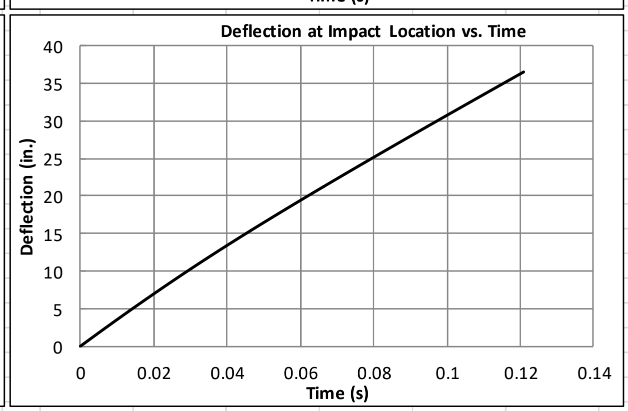

Figure B-4. Test No. LTCB-4 Results (SLICE-2)

MIDWEST ROADSIDE SAFETY FACILITY

Bogie Test Summary

Test Information	
Test Description:	S3x5.7 Low-Tension Cable Post 6 in. Offset from 1.8
Test Number:	LTCB-5
Test Date:	6/1/2015
Failure Type:	Post Rotation and Displacement of Slope Soil with
Post Properties	
Post Type:	S3x5.7 with 8"x24"x1/4" Soil Plate (impact side of po
Post Size:	S3x5.7
Post Length:	63
Embedment Depth:	30
Orientation:	Strong Axis
Soil Properties	
Gradation:	072014
Moisture Content:	NA
Compaction Method:	HE8
Bogie Properties	
Impact Velocity:	20.6 mph (30.21 ft/s)
Impact Height:	22
Bogie Mass:	1868 lb
Data Acquired	
Accelerometer:	SLICE-2
Camera Data:	AOS-8

Test Results Summary		
Event Duration:	0.1369	sec
Max. Deflection:	42.2	in.
Peak Force:	7.3	k
Initial Linear Stiffness:	4.7	k/in.
Total Energy:	127.4	k-in.

	@ 5"	@ 10"	@ 15"	@20"
Average Force (k)	4.67	5.04	5.05	4.73
Energy (k-in.)	23.3	50.4	75.8	94.5

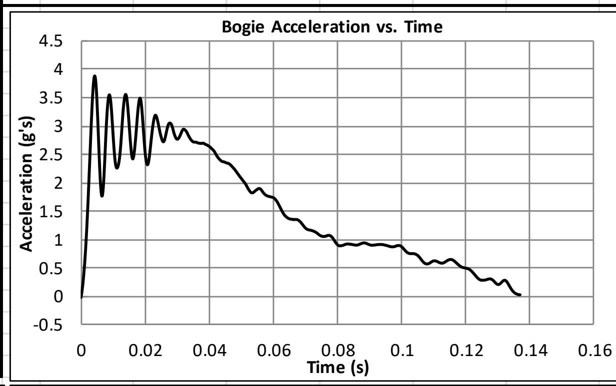

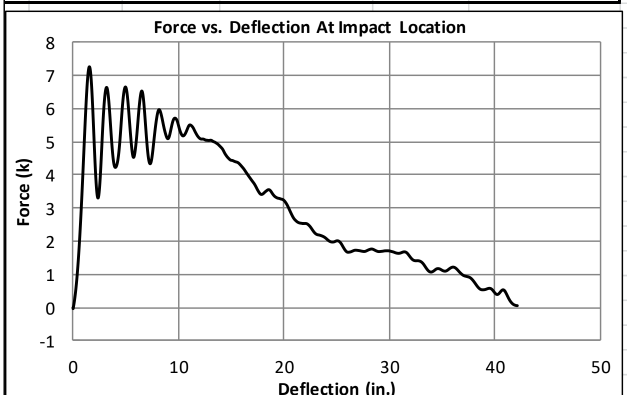

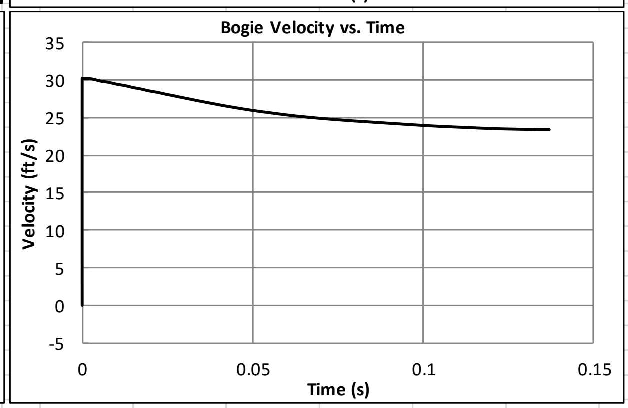

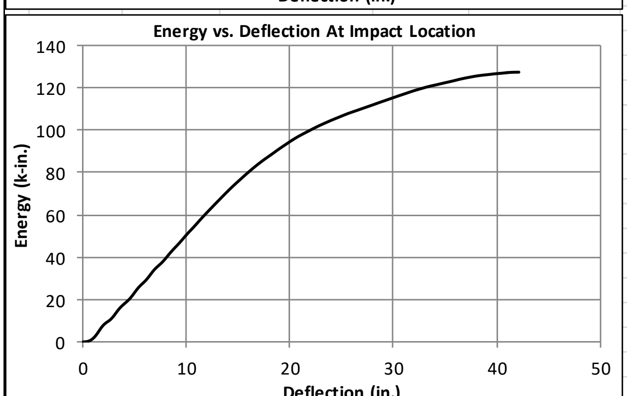

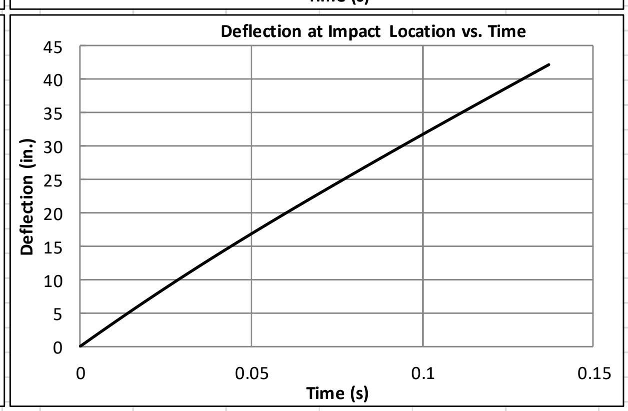

Figure B-5. Test No. LTCB-5 Results (SLICE-2)

MIDWEST ROADSIDE SAFETY FACILITY

Bogie Test Summary

Test Information

Test Description:	Dual S3x5.7 Low-Tension Cable Post @ 25 Degree
Test Number:	LTCB-6
Test Date:	6/9/2015
Failure Type:	Simulated floorpan tearing by both posts along floo

Post Properties

Post Type:	S3x5.7 with 8"x24"x1/4" Soil Plate (impact side of po
Post Size:	S3x5.7
Post Length:	63
Embedment Depth:	30
Orientation:	25 degrees

Soil Properties

Gradation:	072014
Moisture Content:	NA
Compaction Method:	HE8

Bogie Properties

Impact Velocity:	25.83 mph	(37.88 ft/s)
Impact Height:	22	
Bogie Mass:	2548 lb	

Data Acquired

Accelerometer:	SLICE-2
Camera Data:	AOS-8

Test Results Summary

Event Duration:	0.7000	sec
Max. Deflection:	287.1	in.
Peak Force:	6.9	k
Initial Linear Stiffness:	3.5	k/in.
Total Energy:	192.1	k-in.

	@ 5"	@ 10"	@ 15"	@20"
Average Force (k)	2.37	2.28	2.25	2.11
Energy (k-in.)	11.9	22.8	33.7	42.2

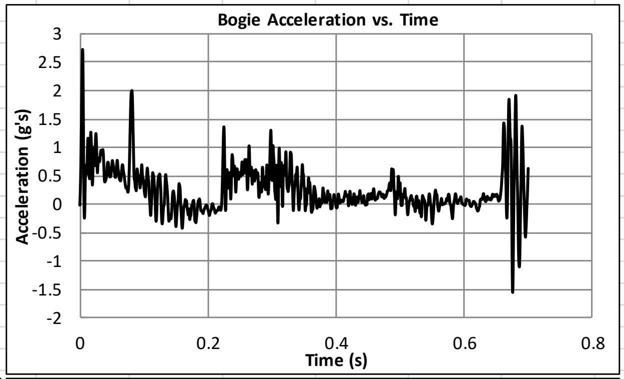

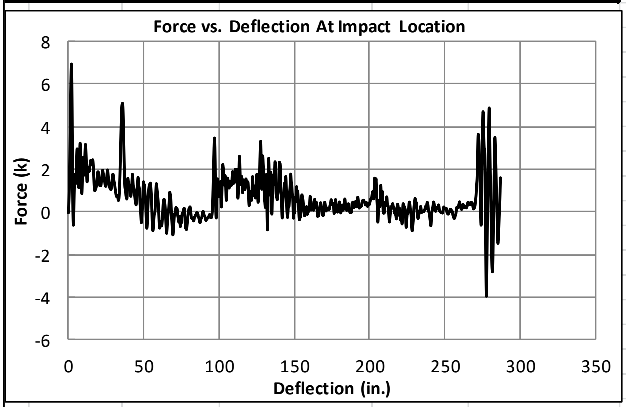

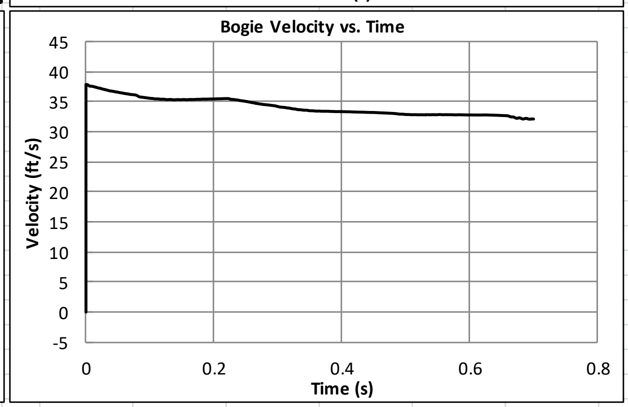

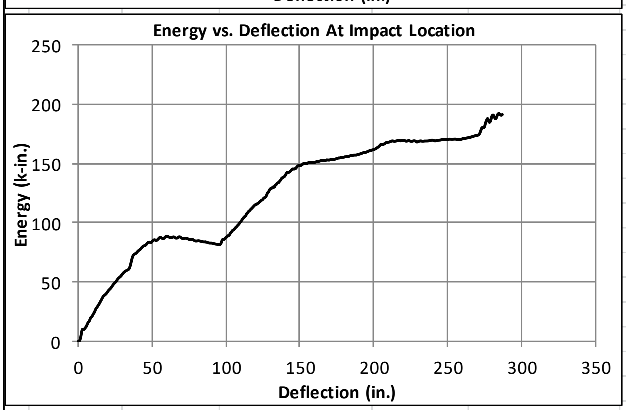

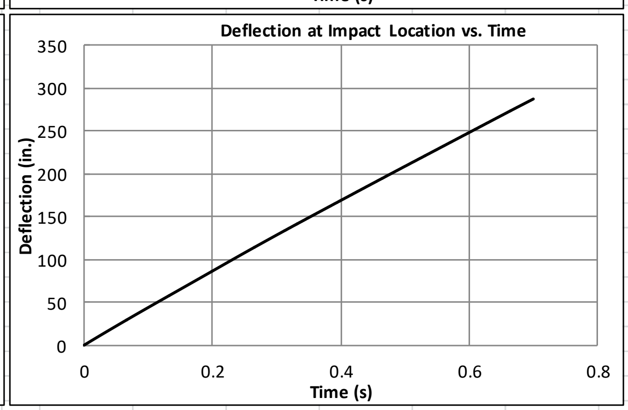

Figure B-6. Test No. LTCB-6 Results (SLICE-2)

Appendix C. Bogie Test Results, Test Nos. CTPS-1 and CTPS-2

The results of the recorded data from each accelerometer for every dynamic bogie test are provided in the summary sheets found in this appendix. Summary sheets include acceleration, velocity, and deflection vs. time plots as well, as force vs. deflection and energy vs. deflection plots.

MIDWEST ROADSIDE SAFETY FACILITY

Bogie Test Summary

Test Information

Test Description:	Bogie - Post
Test Number:	ctps-1
Test Date:	1/31/2018
Failure Type:	Post yield

Post Properties

Post Type:	Steel Tube
Post Size:	HSS 3"x2"x1/8"
Post Length:	78 in
Embedment Depth:	40 in
Orientation:	Strong

Soil Properties

Gradation:	level front 1.8:1 slope 12 in behind post
Moisture Content:	
Compaction Method:	HE8

Bogie Properties

Impact Velocity:	23.22 mph	(34.05 ft/s)
Impact Height:	22 in	
Bogie Mass:	1872 lb	

Data Acquired

Accelerometer:	SLICE1
Camera Data:	AOS9, GP15, GP16

Test Results Summary

Event Duration:	0.1040	sec
Max. Deflection:	39.9	in.
Peak Force:	7.3	k
Initial Linear Stiffness:	3.8	k/in.
Total Energy:	75.0	k-in.

	@ 5"	@ 10"	@ 15"	@20"
Average Force (k)	3.39	3.39	2.93	2.62
Energy (k-in.)	17.0	33.9	43.9	52.4

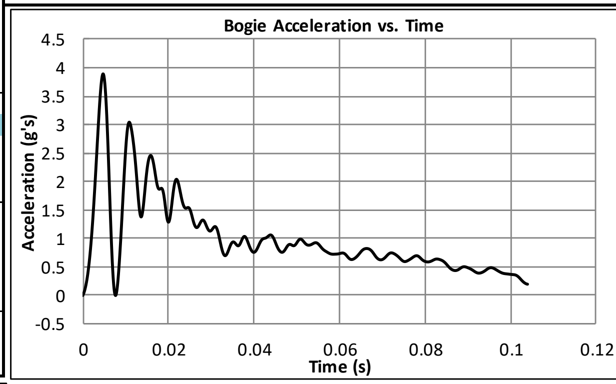

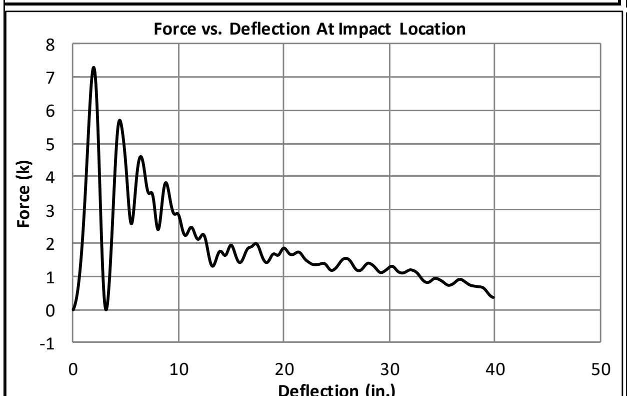

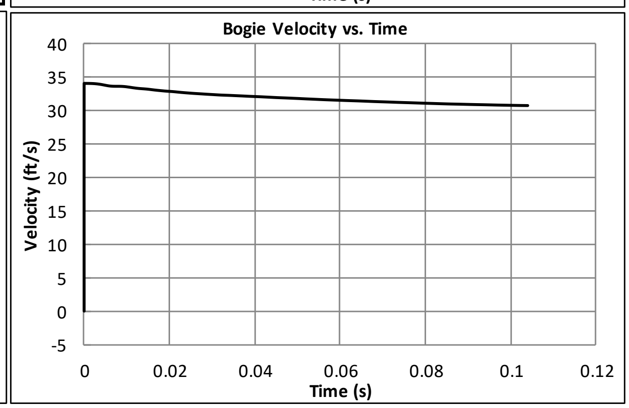

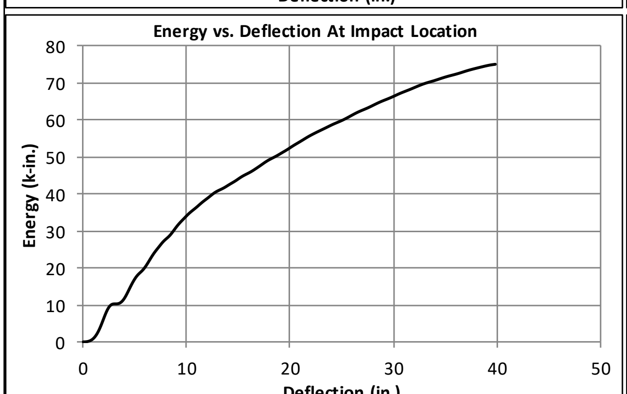

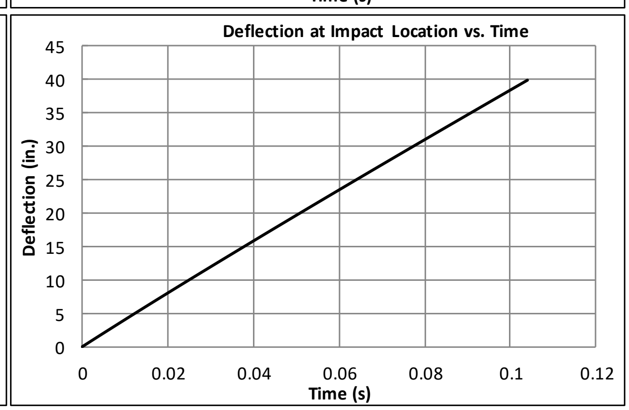

Figure C-1. Test No. CTPS-1 Results (SLICE-1)

MIDWEST ROADSIDE SAFETY FACILITY

Bogie Test Summary

Test Information

Test Description:	Bogie - Post
Test Number:	ctps-1
Test Date:	1/31/2018
Failure Type:	Post Yield

Post Properties

Post Type:	Steel Tube
Post Size:	HSS 3"x2"x1/8"
Post Length:	78 in
Embedment Depth:	40 in
Orientation:	Strong

Soil Properties

Gradation:	level front 1.8:1 slope 12 in behind post
Moisture Content:	
Compaction Method:	HE8

Bogie Properties

Impact Velocity:	23.22 mph	(34.05 ft/s)
Impact Height:	22 in	
Bogie Mass:	1872 lb	

Data Acquired

Accelerometer:	SLICE2
Camera Data:	AOS9, GP15, GP16

Test Results Summary

Event Duration:	0.1040	sec
Max. Deflection:	40.0	in.
Peak Force:	6.7	k
Initial Linear Stiffness:	3.4	k/in.
Total Energy:	70.9	k-in.

	@ 5"	@ 10"	@ 15"	@20"
Average Force (k)	3.13	3.25	2.82	2.51
Energy (k-in.)	15.7	32.5	42.3	50.2

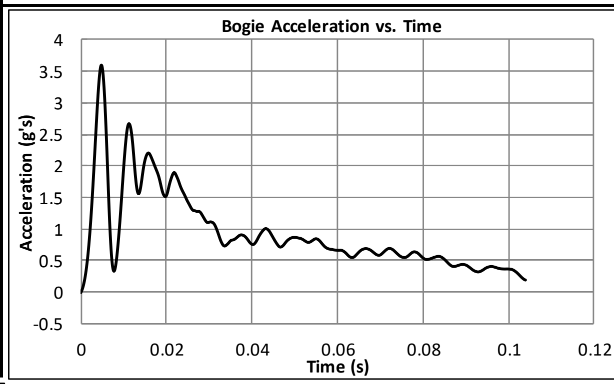

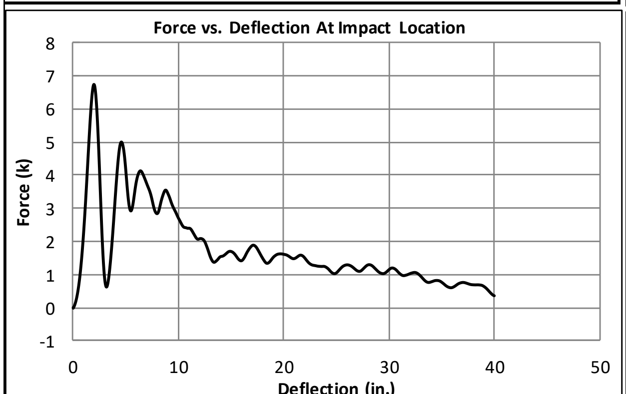

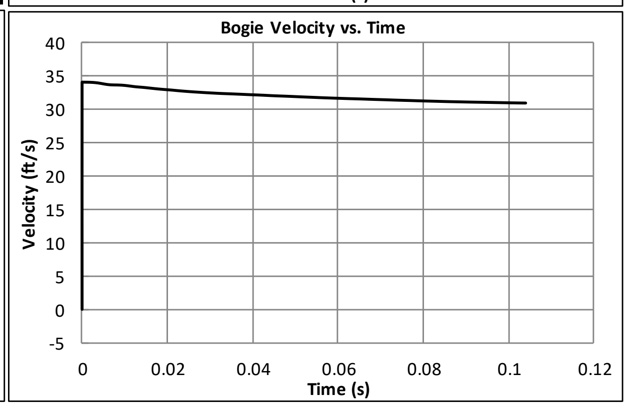

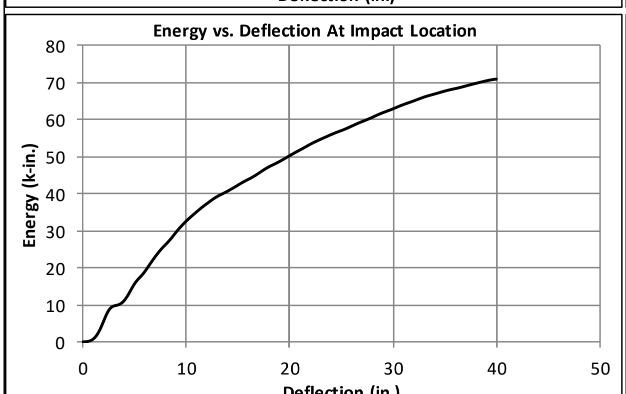

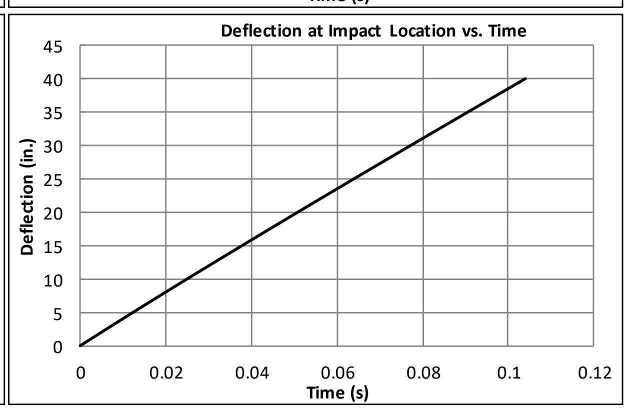

Figure C-2. Test No. CTPS-1 Results (SLICE-2)

MIDWEST ROADSIDE SAFETY FACILITY

Bogie Test Summary

Test Information

Test Description:	Bogie - Post
Test Number:	ctps-2
Test Date:	2/1/2018
Failure Type:	Post Yield below groundline

Post Properties

Post Type:	Steel Tube
Post Size:	HSS 3x2x1/8
Post Length:	78"
Embedment Depth:	40"
Orientation:	Strong

Soil Properties

Gradation:	level front 1.8:1 slope 6" behind post
Moisture Content:	
Compaction Method:	HE8

Bogie Properties

Impact Velocity:	22.08 mph	(32.38 ft/s)
Impact Height:	22"	
Bogie Mass:	1872 lb	

Data Acquired

Accelerometer:	SLICE1
Camera Data:	aos9, gp17, gp18

Test Results Summary

Event Duration:	0.1240	sec
Max. Deflection:	43.8	in.
Peak Force:	7.7	k
Initial Linear Stiffness:	3.3	k/in.
Total Energy:	96.5	k-in.

	@ 5"	@ 10"	@ 15"	@20"
Average Force (k)	3.07	3.51	3.57	3.23
Energy (k-in.)	15.4	35.1	53.5	64.7

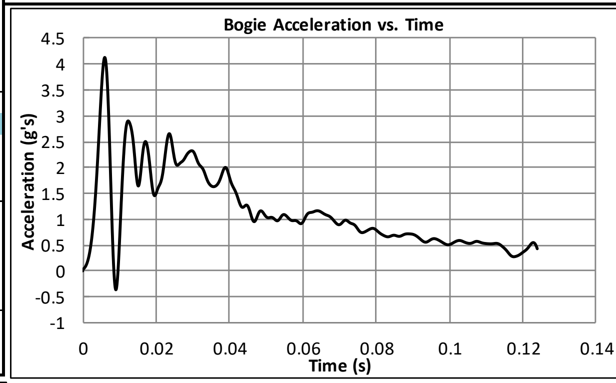

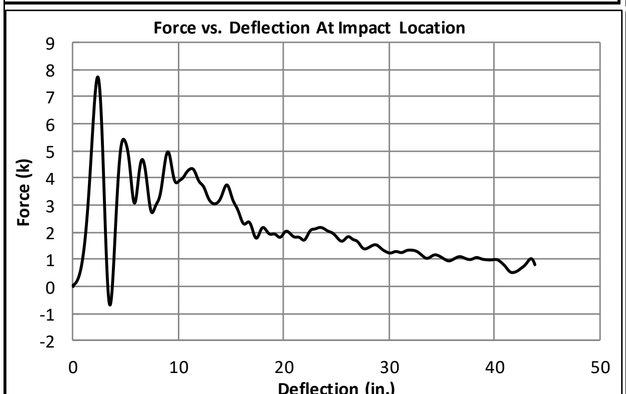

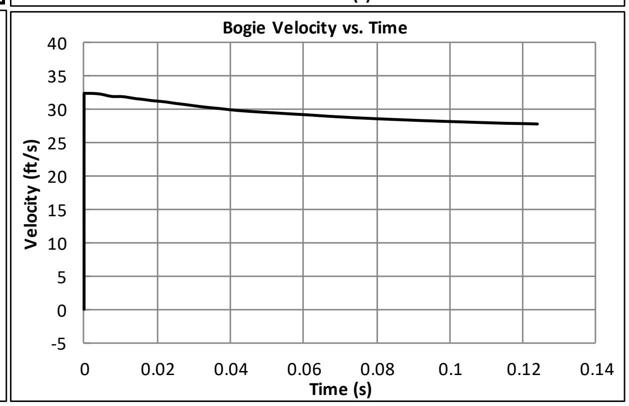

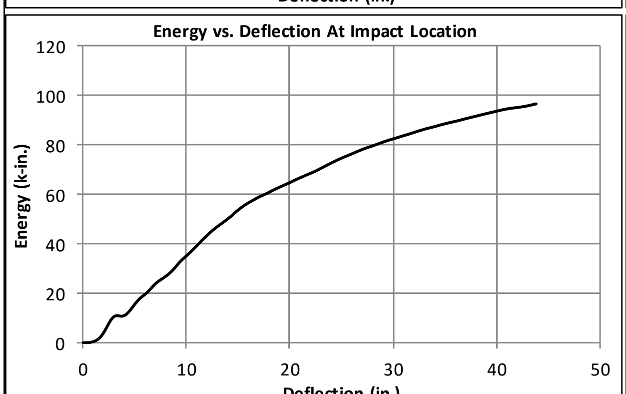

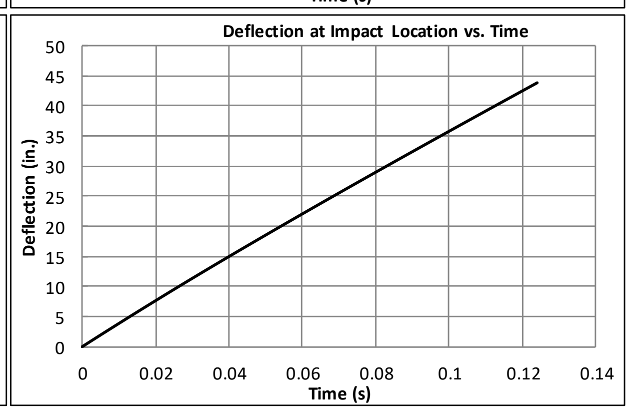

Figure C-3. Test No. CTPS-2 Results (SLICE-1)

MIDWEST ROADSIDE SAFETY FACILITY

Bogie Test Summary

Test Information

Test Description:	Bogie - Post
Test Number:	ctps-2
Test Date:	2/1/2018
Failure Type:	Post Yield below groundline

Post Properties

Post Type:	Steel Tube
Post Size:	HSS 3x2x1/8
Post Length:	78"
Embedment Depth:	40"
Orientation:	Strong

Soil Properties

Gradation:	level front 1.8:1 slope 6" behind post
Moisture Content:	
Compaction Method:	HE8

Bogie Properties

Impact Velocity:	22.08 mph	(32.38 ft/s)
Impact Height:	22"	
Bogie Mass:	1872 lb	

Data Acquired

Accelerometer:	SLICE2
Camera Data:	aos9, gp17, gp18

Test Results Summary

Event Duration:	0.1240	sec
Max. Deflection:	44.1	in.
Peak Force:	7.2	k
Initial Linear Stiffness:	3.1	k/in.
Total Energy:	91.1	k-in.

	@ 5"	@ 10"	@ 15"	@20"
Average Force (k)	2.96	3.42	3.46	3.10
Energy (k-in.)	14.8	34.2	51.9	62.0

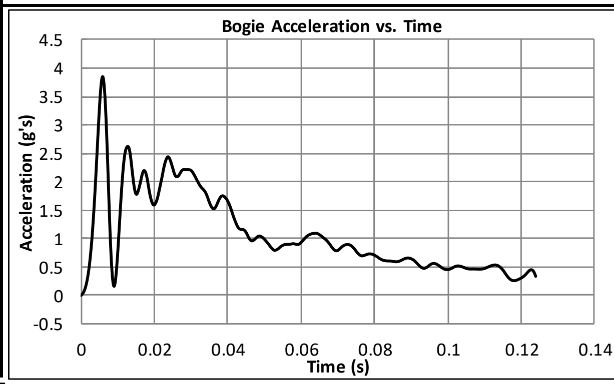

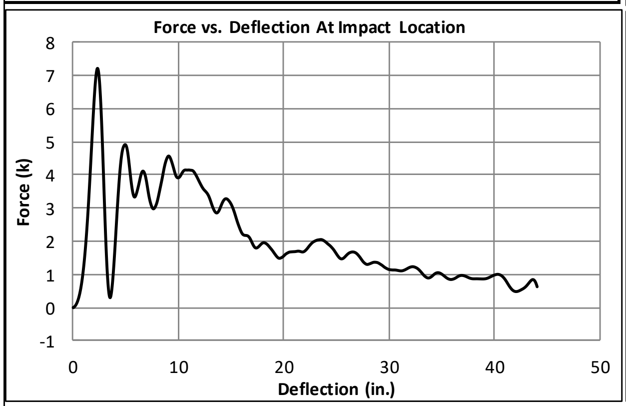

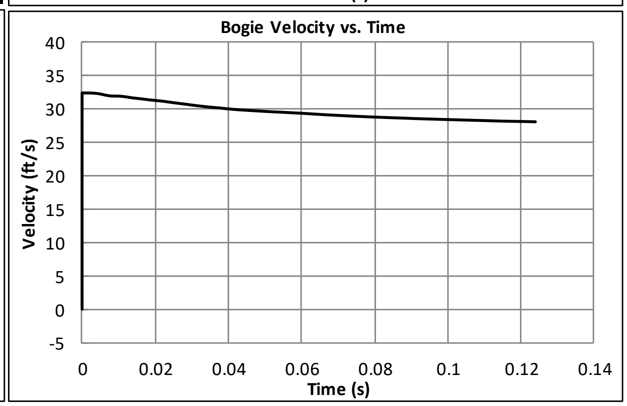

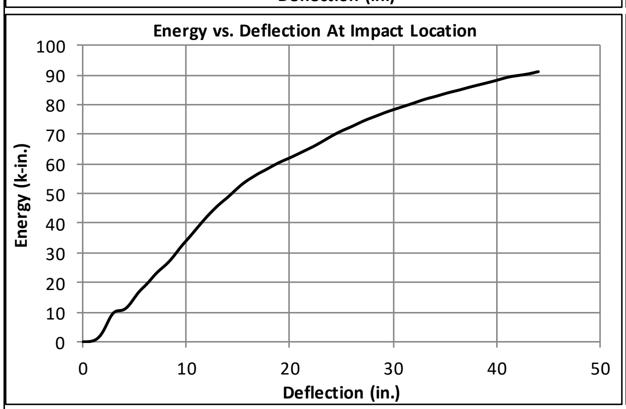

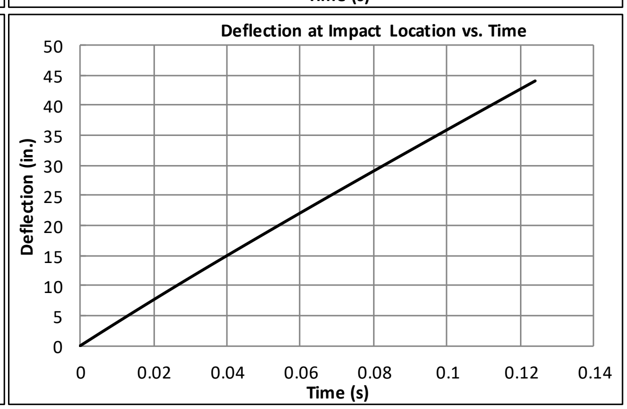

Figure C-4. Test No. CTPS-2 Results (SLICE-2)

END OF DOCUMENT